Charles University in Prague
Faculty of Science

Dual Role of CD9 Protein in Mast Cell Activation

Diploma thesis

Martin Machyna
Supervisor: RNDr. Petr Dráber, DrSc.

Prague 2009

On the first place, I would like to thank to my supervisor Petr Dráber for his guidance and useful comments throughout my thesis and also to Daniel Smrž, who was helpful in indentifying CD9 as target of our monoclonal antibody. Next my gratitude belongs to Lukáš Kocanda, Dana Lorenčíková and Hana Mrázová who under leadership of Ľuba Dráberová prepared 2H9 monoclonal antibody.

My personal thanks also go to other members of our laboratory for their advices, kindness and friendly working atmosphere. And last but not least to my family and Zuzka Varadínová for their patience and morale support.

I proclaim that results presented in this diploma thesis were obtained by me independently under the leadership of my supervisor RNDr. Petr Dráber, DrSc. and other before mentioned members of our laboratory and all literature used was cited accordingly.

Prague 30th of April 2009 …….

Abstract

Mast cells are well known effector cells in immune system. They have been implicated in such important processes as host defense against bacteria, toxins or parasites. However, in some cases they can develop improper reaction against harmless environmental antigens and thus causing allergies. It is therefore essential to understand signaling events that lead to activation of these cells in order to develop new treatment strategies.

Newly prepared rat monoclonal antibody of IgG_1 subtype raised against murine mast cells was characterized and found suitable for flow cytometry, immunoblotting and immunoprecipitation. Employing of optimized procedure for immunopurification in combination with mass spectrometry led to identification of its target cluster of differentiation (CD)9 protein. CD9 is a member of large protein family called tetraspanins. Functional studies showed that binding of this antibody to mast cells induced degranulation and early activation events such as increased tyrosine phosphorylation and enhanced levels of free cytoplasmic calcium. Interestingly, subsequent activation of these cells via antigen-mediated aggregation of the high-affinity IgE receptor (FcεRI) led to decreased degranulation, calcium response and tyrosine phosphorylation of several substrates. Importantly, anti-CD9 antibody did not inhibit these responses in cells activated by thapsigargin, an inhibitor of endoplasmic reticulum calcium ATPases, indicating that downstream signaling events were not affected. The observed effects of the antibody were not caused by blocking binding of the antigen to FcεRI, coupling of CD9 to FcεRI by antibody nor by engagement of Fcγ receptors.

Involvement of CD9 in FcεRI-mediated activation events was supported by experiments employing cells with enhanced or decreased expression of CD9 by transfection with CD9 cDNA or silencing RNA, respectively. Cells with enhanced expression of CD9 exhibited more, while cells with decreased expression exhibited less anti-CD9-mediated effects. Surprisingly, degranulation of cells with decreased CD9 expression was comparable to wild-type cells which probably reflects of compensation by other tetraspanin family member. The combined data suggest that CD9 acts as a regulator of FcεRI-mediated activation. Antibody-mediated aggregation of CD9 leads to cell activation events. This might also activate negative feed-back mechanism which dampens FcεRI-mediated activation resulting in impaired degranulation.

Key words: CD9, tetraspanins, mast cells, signal transduction, antibody

Abstrakt

Žírne bunky sú známe efektorové bunky imunitného systemu. Ich účasť bola preukázaná v takých dôležitých procesoch ako sú obrana hostiteľa pred baktériami, toxínmi alebo parazitmi. Niekedy však môžu vytvárať neprimeranú reakciu proti neškodným antigénom v našom prostredí a spôsobovať tak alergie. Je práve preto vrcholne dôležité pochopiť signálne deje, ktoré vedú k aktivácii týchto buniek, za účelom vyvýjania nových stratégii liečby.

Novovytvorená potkania monoklonálna protilátka izotypu IgG_1, špecifická proti myším žírnym bunkám, bola charakterizovaná ako vhodná pre použitie v prietokovej cytometrii, imunoznačení a imunoprecipitácii. Použitie optimalizovaného postupu imunoizolácie v spojení s hmotnostnou spektrometriou umožnilo identifikovať CD9 ako jej cieľový proteín. CD9 je členom rozsiahlej rodiny nazývanej „tetraspanins“. Funkčné štúdie ukázali, že väzba tejto protilátky na žírne bunky spôsobila degranuláciu a aktiváciu včasných dejov ako sú zvýšená tyrozínová fosforylácia a zvýšená hladina voľného cytoplazmatického vápnika. Prekvapivé bolo zistenie že, následná aktivácia týchto buniek cez agregáciu FcεRI receptoru pomocou antigénu viedla naopak ku zníženej degranulácii, vápnikovej odpovedi a tyrozínovej fosforylácii niekoľkých substrátov. Anti-CD9 protilátka však neinhibovala tieto bunkové odpovede, keď boli bunky aktivované thapsigarginom, inhibítorom vápnikových ATPáz v endoplazmatickom retikule, čo naznačuje, že neskoršie signálne deje neboli protilátkou ovplyvnené. Tieto efekty spôsobené protilátkou neboli spôsobené zabránením väzby antigénu na FcεRI, prepojením CD9 a FcεRI pomocou protilátky ani prekrýžením Fcγ receptorov.

Účasť proteínu CD9 v procese aktivácie žírnych buniek cez FcεRI bola tiež podporená experimentami za využitia buniek so zníženou a zvýšenou expresiou CD9 pomocou transfekcie CD9 cDNA alebo „silencing RNA“. Bunky so zvýšenou expresiou CD9 vykazovali viac, zatiaľ čo bunky so zníženou expresiou vykazovali menej účinkov spôsobených anti-CD9. Degranulácia buniek so zníženou expresiou CD9 však bola porovnateľná s bunkami divokého typu, čo pravdepodobne odráža možnú kompenzáciu iným členom rodiny „tetraspanins“. Zhrnutím výsledkov sa ukazuje možnosť, že CD9 vystupuje ako regulátor aktivácie cez FcεRI receptor. Agregácia CD9 pomocou protilátky vedie k aktivácii buniek. To však môže aktivovať negatívne spätnoväzobné mechanizmy, ktoré následne tlmia FcεRI receptorovú aktiváciu, čo vyúsťuje do zníženej degranulácie.

Kľúčové slová: CD9, tetraspanins, žírne bunky, signálna transdukcia, protilátka

Contents

List of abbreviations

ATCC	American Type Culture Collection
BMMC	Bone marrow-derived mast cell
BSA	Bovine serum albumin
BSS-BSA	Buffered salt saline containing 0.1% BSA
Btk	Burton's tyrosine kinase
CD	Cluster of differentiation
CD9KD	Cells with downregulated CD9 expression
CD9OE	Cells with upregulated CD9 expression
cDNA	Complementary DNA
CHAPS	3-[(3-chloamidopropyl)dimethyammonio]-1-propanesulfonate
CM/PBS	Complete medium diluted in PBS
CMV	Cytomegalovirus
Csk	C-terminal Src kinase
CTMC	Connective tissue mast cell
DAG	Diacylglycerol
DMP	Dimethyl pimelimidate
DMSO	Dimethyl sulfoxide
ECL	Enhanced chemiluminescence
EDTA	Ethylenediaminetetraacetic acid
ER	Endoplasmic reticulum
Erk	Extracellular signal-regulated protein kinase
EtBr	Ethidium bromide
FCS	Fetal calf serum
FcεRI	High-affinity IgE receptor
Gab2	Grb2-associated binding protein 2
GADS	Grb2-related adaptor protein
GEF	Guanine nucleotide exchange factor
GM-CSF	Granulocyte macrophage colony-stimulating factor
GPCR	G protein-coupled receptor
GPI	Glycosyl-phosphatidylinositol
Grb2	Growth factor receptor-bound protein 2
HB-EGF	Heparin-binding-epidermal growth factor

HRP	Horseradish peroxidase
IAA	Iodoacetamide
ICL	Intracellular loop
IL	Interleukin
IP_3	Inositol (1,4,5) trisphosphate
ITAM	Immunoreceptor tyrosine-based activation motif
JNK	Jun N-terminal kinase
kDa	Kilodalton
KO	Knock-out
LAT	Linker of activated T cells
LB	Luria-Bertani
LEL	Large extracellular loop
MALDI/FTMS	Matrix-assisted laser desorption/ionization Fourier transform mass spectrometry
ME	2-mercaptoethanol
MHC-II	Major histocompatibility complex II
microHPLC-ESI-MS/MS	Microcapillary liquid chromatography in combination with electrospray ionization tandem mass spectrometry
MMC	Mucosal mast cell
MMP-2	Matrix metalloproteinase 2
MRP-1	Motility-related protein 1
MS	Mass spectrometry
MUGlcU	4-Methylumbelliferyl β-D-Glucuronide
NFAT	Nuclear factor of activated T-cells
NF-κB	Nuclear factor-κB
NI	Non-infected
non-OE	Cells infected with empty pCDH vector
non-siRNA	Cells infected with non-silencing vector
NP-40	Nonidet P-40
NTAL	Non-T cell activation linker
PBS	Phosphate buffered saline
PI3K	Phosphatidylinositol 3-Kinase
PI4KII	Phosphatidylinositol 4-kinase type II
PIP_2	Phosphatidylinositol (4,5)-bisphosphate

PIP_3	Phosphatidylinositol (3,4,5)-trisphosphate
PI-PLC	Phosphatidylinositol-specific phospholipase C
PKC	Protein kinase C
PLA_2	Phospholipase A_2
PLCγ	Phospholipase Cγ
PMSF	Phenylmethylsulphonyl fluoride
RBL-2H3	2H3 subclone of RBL cell line
SCF	Stem cell factor
SDS	Sodium dodecyl sulfate
SDS-PAGE	Sodium dodecyl sulfate polyacrylamide gel electrophoresis
SEL	Small extracellular loop
SH2	Src homology 2 domain
Shc	SH2 domain-containing transforming protein C
shRNA	Short hairpin ribonucleic acid
SOC	Super optimal broth with catabolite repression
STIM1	Stromal interaction molecule 1
Syk	Spleen tyrosine kinase
TCEP	Tris(2-carboxyethyl)phosphine
TE buffer	Tris-EDTA buffer
TEM	Tetraspanin-enriched microdomain
TGF	Transforming growth factor
TM	Transmembrane domain
TNF	Tumor necrosis factor
TNP	2,4,6-trinitrophenyl
TNP-BSA	TNP conjugated to BSA
TNP-BSA-TRITC	TNP-BSA conjugated to TRITC
TNT	Tris-NaCl-Tween buffer
TRITC	Tetramethyl Rhodamine Isothiocyanate
VEGF	Vascular endothelial growth factor
WAVE	Wiskott-Aldrich syndrome protein family verprolin-homologous protein
WT	Wild-type

1 Introduction

Immune system is a complex cellular network whose main task is to establish integrity and homeostasis of host organism by mounting appropriate immune response. Many types of cells, both circulating in blood or residing in tissues, participate in this process and the efficiency of immune system is strictly dependent on their tight cooperation. Key feature is their ability to communicate either by direct cell-cell contact or remotely using cytokine network.

Mast cells play indispensable role in immune system. They are leukocytes of myeloid cell linage which originate in bone marrow and their progenitors then enter blood stream to finish their development in different connective tissues. There they serve as defenders against multicellular parasites, bacteria and toxins but in certain cases they may react to harmless environmental antigens and thus causing allergies. It is therefore essential to understand processes that lead to their activation and release of effector molecules.

Monoclonal antibodies turned out to be useful tools for identification of many new molecules and characterization of various protein functions. Even more, monoclonal antibodies are widely used as therapeutic agents to cure various severe diseases including cancer. Developing antibody which could negatively regulate mast cell activation and degranulation could have tremendous clinical impact.

One of possible targets for such antibodies could be members of tetraspanin family because previous research with monoclonal antibodies raised against these proteins showed multiple inhibitory and also activatory effects on cells of hematopoietic origin including mast cells.

Our laboratory has developed a panel of monoclonal antibodies which enabled us to clarify function of by then not well characterized proteins (e.g. Tec-21, PLSCR1). Recently, we generated a new panel of hybridomas producing monoclonal antibodies against bone marrow-derived mast cells (BMMCs) plasma membrane antigens. Next step was to select antibodies capable to modulate mast cell activation or recognizing proteins with yet unknown role in mast cell signaling.

2 Aims

Aims of this diploma thesis were:

- To characterize specificity of newly prepared monoclonal antibody recognizing an antigen on BMMCs (2H9).
- To characterize properties of the target antigen recognized by 2H9 antibody.
- To investigate effects of the antibody on mast cell degranulation.
- To examine functional alterations in selected components of mast cell signaling pathways.
- To generate cells with decreased or increased levels of the target antigen and compare their properties.

3 Literature review

3.1 Tetraspanins

3.1.1 Tetraspanin family

Tetraspanins are large superfamily (Boucheix et al., 1991) of membrane type II proteins of molecular weight approximately 24–50 kilodaltons (kDa) consisting of approximately total 250 amino acids (Hemler, 2001). They were discovered on preB and leukemic cells relatively long time ago (Kersey et al., 1981) but later they were described on other hematopoietic and non-hematopoietic cell types (Lanza et al., 1991; Mitamura et al., 1992). Genome sequences search revealed large number of tetraspanin members in other organisms from protozoan amoebae, plants (Huang et al., 2005), *C. elegans* (20 members) (Moribe et al., 2004), Drosophila (37 members) (Todres et al., 2000) to mammals (33 members) (Garcia-Espana et al., 2008). Recent attempt for phylogenetic analysis from 10 fully sequenced metazoan genomes divided tetraspanin superfamily into four major orthologous groups – the CD family, CD63 family, uroplakin family and RDS family (Garcia-Espana et al., 2008). It is now clear that this protein family is highly conserved and emerged early in the evolution. What more, tetraspanins are ubiquitously expressed in reasonably high numbers ranging from 30,000 to 100,000 molecules per cell (Hemler, 2005) and usually more than one tetraspanin gene is expressed in one cell type. Tarrant et al. estimate number of expressed tetraspanin genes in leukocytes to ≤ 20 (Tarrant et al., 2003).

3.1.2 Structure of tetraspanins

As can be deduced from their name tetraspanins cross plasma membrane four times facing both N-terminal and C-terminal ends to the cytosol. Four transmembrane domains (TM1-4) are linked by one very short intracellular loop (ICL) and two extracellular loops termed as small extracellular loop (SEL), joining TM1 and TM2, and large extracellular loop (LEL), joining TM3 with TM4. Although many other proteins contain four transmembrane domains, they are not members of tetraspanin family because they do not contain other tetraspanin-specific features. These are conserved cysteine residues in LEL and multiple conserved polar residues in transmembrane domains (Fig. 1).

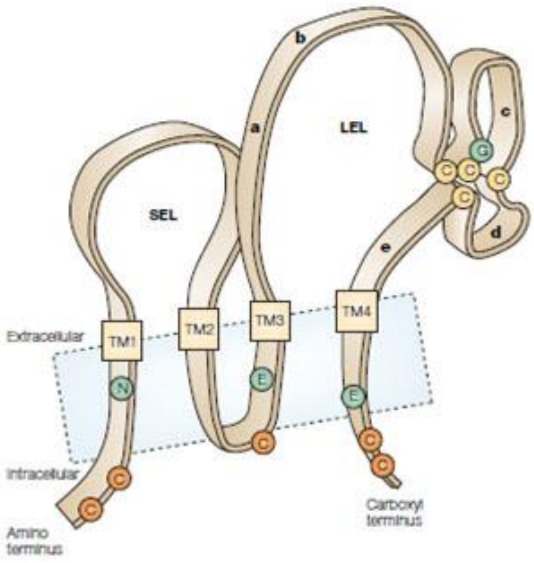

Fig. 1 – Schematic structure of tetraspanins.

Tetraspanins consist of four transmembrane domains (TM) containing conserved polar residues (green circles), short terminal ends, intracellular loop, small extracellular loop (SEL) and large extracellular loop (LEL). Relatively conserved and hydrophobic helices a, b and e are separated from hypervariable helices c and d by conserved cysteine residues (yellow circles). Juxtamembrane cysteines that can undergo palmitoylation are also shown (orange circles) (Levy and Shoham, 2005b).

Taken together, tetraspanin consist of five distinct functional regions (Stipp et al., 2003b). On the first place, it is LEL which is the most studied part of tetraspanins and also the only part whose structure was determined from crystal X-ray diffraction (Kitadokoro et al., 2001). Analysis of its structure revealed that it is formed by 5-helix bundle consisting of helixes A–E. Although LEL is not as conserved as TM parts, helices A, B and E possess a considerable amount of homology between tetraspanin members and their hydrophobic surface is believed to play role in homodimerization of tetraspanins. Helices C and D are hypervariable and contain more polar residues and mediate most of tetraspanin interactions with their protein partners. This is supported by localization of several specific interaction motifs – SFQ (173–175) in CD9 indispensable for sperm-egg fusion (Zhu et al., 2002), F186 in CD81 responsible for hepatitis virus C binding (Higginbottom et al., 2000a) and also QRD (194–196) motif in CD151 which is required for α3 and α6 integrins association (Kazarov et al., 2002). All these motifs overlap the same place in variable part of LEL. The most conserved part of LEL are cysteine residues organized to highly conserved motifs CCG and PXXC which are also one of the family specific markers. Totally four (CD9, CD81), six (CD151) or eight cysteine residues can be positioned within LEL capable of forming 2–

4 disulphide bridges which stabilize overall bundle structure and separate variable part from conserved (see Fig. 1). According to these parameters, tetraspanins can be divided into three topological groups. Variable domain of group 1 tetraspanins (CD9, CD81) represents minimal topology comprising of two peptide stretches of variable domain and two disulphide bridges. Group 2 has one of its peptide stretch divided into two by additional cysteine which forms third disulphide bridge. The most complex tetraspanins belong to group 3 and have inserted additional peptide stretches and pair of cysteines which forms another disulphide bridge. Therefore, it seems likely that more complex tetraspanins evolved from a basic topology by duplication of specific peptide stretches and disulphide insertions (Fig. 2) (Kitadokoro et al., 2002; Seigneuret et al., 2001).

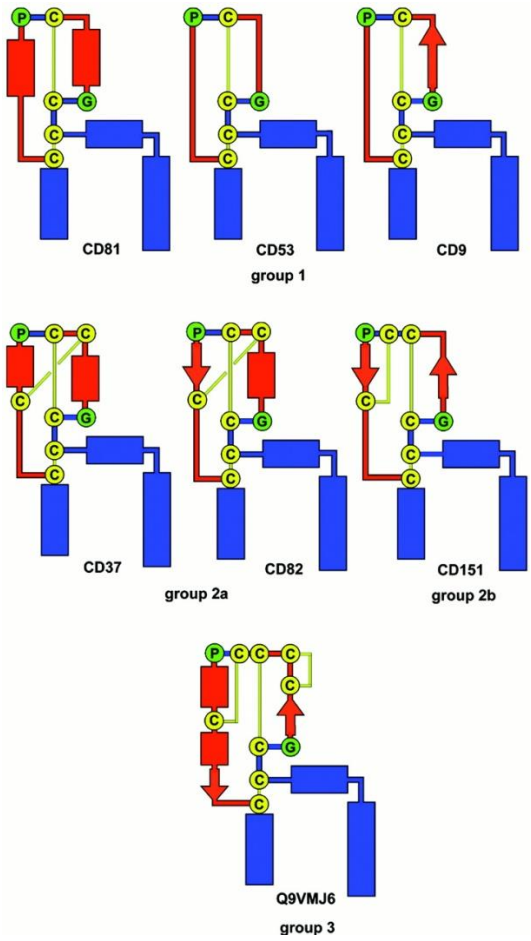

Fig. 2 – LEL topography of several tetraspanins

Tetraspanins can be divided into three groups according to their LEL chain topology. Rectangles, arrows, and thinner lines represent helices, strands, and coil, respectively. Conserved parts are indicated in blue while variable domain is red. Cysteines and disulfide bridges are indicated in yellow. Glycine and proline residues of CCG and PXXC motifs are shown in green (Seigneuret et al., 2001).

Knowledge about 13–30 amino acid long SEL is very limited. It was reported that deletion of SEL reduces surface expression of truncated form of CD151 and thus it is required for optimal LEL expression (Masciopinto et al., 2001). SEL also contains putative site for N-glycosylation in CD9 but it is currently unknown whether glycosylation in this position really occurs. However, one or more N-glycosylations of LEL is typical for almost all tetraspanins except CD9 and CD81.

Transmembrane domains are the most conserved part of tetraspanin proteins. They contain highly polar residues which are also conserved and help to stabilize closely packed tertiary structure of these domains while hydrophobic residues contribute to tetraspanin-tetraspanin and tetraspanin-non-tetraspanin partner interactions. Namely TM1-TM2 interface mediates interaction with other tetraspanins while second TM3-TM4 interface mediates heterotypic interaction with non-tetraspanin partner (Kovalenko et al., 2005; Min et al., 2006). However presence of LEL is probably also important for homotypic tetraspanin-tetraspanin interactions because deletion of LEL disrupted homotypic interactions while interaction with other tetraspanins remained unchanged (Berditchevski et al., 2001). CD82 lacking TM1 was retained in endoplasmic reticulum (ER). However when mutant CD82 was co-expressed with TM1 peptide it was again able to reach PM. This suggests that transmembrane domains are also necessary for correct folding and transport of tetraspanins from ER to their destination (Cannon and Cresswell, 2001).

Intracellular part of tetraspanins contains highly conserved cysteines which are palmitoylated in the process of protein maturation in Golgi. Tetraspanins first associate with their specific non-tetraspanin partner in ER and later promoted by palmitoylation they tend to interact in tetraspanin-tetraspanin fashion creating thus higher order structures (Tu et al., 2002). When cysteine residues are mutated in CD9 and CD151 proteins, intertetraspanin interactions are lost while association with non-tetraspanin partners remains untouched (Berditchevski et al., 2002; Charrin et al., 2002; Yang et al., 2002). Presence of excessive palmitoylation in tetraspanins may raise a question about localization of these proteins in lipid raft structures. Results suggest that palmitoylation is not sufficient signal for lipid rafts residency although certain fraction of tetraspanins is present in these structures. However similarly large fraction is not included and is independent of lipid rafts (Claas et al., 2001; Yashiro-Ohtani et al., 2000).

Intracellular parts of tetraspanins, including ICL and terminal ends, are relatively conserved among species but are divergent between tetraspanin members. The most variable is C-terminal cytosolic tail which is believed to be related to specific function of each tetraspanin member. Indeed, specific motif GYEVM was discovered in CD63 C-terminal tail which localizes it to lysosomes (Rous et al., 2002). Other potential targeting motifs were predicted in various

tetraspanins but their significance was not tested. In addition it was proposed that tetraspanins that do not contain any targeting motif can be localized to various cellular compartments by interaction with tetraspanin that does contain one of these motifs (Stipp et al., 2003b).

3.1.3 Tetraspanin interactions and tetraspanin-enriched microdomains (TEMs)

As described in previous chapter, members of tetraspanin superfamily possess variety of interaction surfaces. Some of them serve for interaction with another tetraspanin molecule while others serve as specific site for non-tetraspanin partner molecule. Extensive research in the past decade produced huge amount of evidence of interactions between tetraspanins and their partners. Mentioning all of these results exceeds limits of this review and thus we refer to recent review articles which summarize most of the data (Hemler, 2008; Levy and Shoham, 2005a; Tarrant et al., 2003).

The most characteristic feature of the tetraspanin family members is their ability to interact with other partner molecules. From the result of the immunoprecipitation experiments, which were most frequently used to determine interaction partners, tetraspanin-partner interactions can be divided into three levels.

Primary interaction is between tetraspanin and its specific non-tetraspanin partner. This interaction is direct and robust and is maintained even in harsh non-ionic detergents like Triton X-100 or nonidet P-40 (NP-40). Typical feature of these interactions is that single tetraspanin can form different partnerships in different cell types and their interaction is always stoichiometric.

Secondary interactions take place between two molecules of tetraspanins and are mediated by hydrophobic surfaces of their TM domains. Therefore this might explain their low resistance to non-polar detergents such as Triton X-100. However they are no disrupted in milder detergents like Brij 96 or Brij 97 especially when divalent cations are present. As mentioned before these interactions are formed in Golgi and require functional palmitoylation of juxtamembrane cytosines to be formed. These interactions are also less robust and non-stoichiometric.

Tertiary interactions are very weak and are retained only in mild detergents like 3-[(3-chloamidopropyl)dimethyammonio]-1-propanesulfonate (CHAPS). They are indirect and link tetraspanins with partner of another tetraspanin by combined interaction (Boucheix and Rubinstein, 2001; Levy and Shoham, 2005a; Tarrant et al., 2003). Taking into account this types of interactions and the fact that tetraspanins often co-immunoprecipitate with more than one tetraspanin led to creation of a concept of the tetraspanin web or later termed as TEMs (Rubinstein et al., 1996).

TEMs are believed to be highly dynamic structures the integrity of which is dependent on palmitoylation but are distinct and independent of lipid rafts. With respect to their function three models were proposed. First one suggests that TEMs act as transmembrane linkers bringing membrane protein partners laterally interacting with LEL and cytosolic signaling molecules associated with cytosolic tails to close proximity. This might cause extension of signal (Lammerding et al., 2003). Second proposes that TEMs help to cluster partner molecules and thereby increasing overall avidity for their ligand (Kropshofer et al., 2002). Finally, the last one proposes that TEMs might sequester their partner molecules from signaling machinery and thus dampen signal and prevent inappropriate response (Odintsova et al., 2003).

3.1.4 CD9 is a member of tetraspanin family

CD9, also known as motility-related protein 1 (MRP-1), DRAP27 or Tspan29, is one of the most studied tetraspanin members. This 24–25 kDa protein contains two disulphide bridges in LEL and putative glycosylation site in SEL. Its expression is extended but not ubiquitous. It comprises presence in skin, connective tissues, lungs, liver, gut, kidney, muscles, nervous system but also lymphoid tissues and cells – spleen, lymphnodes, lymphocytes, monocytes, platelets and megakaryocytes (Sincock et al., 1997).

The most sever phenotype observed was reduced fertility of CD9 knock-out (KO) mice. This resulted from inability of CD9 KO mouse oocyte to fuse with a wild-type (WT) sperm, however binding of sperm and fusion of CD9 KO sperm with WT oocytes were unaffected (Kaji et al., 2000; Le Naour et al., 2000; Miyado et al., 2000). Reduced sperm-egg fusion was also observed in CD81 KO mouse, but it is completely diminished in CD9 CD81 double-KO mouse (Rubinstein et al., 2006). It was found that CD9 associates with EWI-2 and EWI-F (members of Ig superfamily) in oocyte membrane (Runge et al., 2007) and that EWI-2 membrane expression is significantly reduced in CD9 KO mouse (He et al., 2008). It is known that EWI proteins interact with ezrin-radixin-moesin proteins and thereby linking CD9, as a part of TEMs, to actin cytoskeleton (Sala-Valdes et al., 2006). EWI proteins also drive CD9 and CD81 localization to filopodia (Stipp et al., 2003a) which might explain localization of CD9 in oocyte microvillar structures and how it regulates their length, thickness and density. Because microvilli morphology is altered in CD9 KO oocytes, one might suggest that microvilli could serve as docking site for close sperm-egg membrane contact facilitating their fusion (Runge et al., 2007).

CD9 also plays a role in fusion of another cell types. Overexpression of CD9 caused increase in myoblast fusion (Tachibana and Hemler, 1999) and pretreatment with anti-CD9 antibody impaired osteoclast formation by inhibiting macrophages fusion (Tanio et al., 1999). Even more, CD9 is

responsible for canine distemper virus-induced cell-cell fusion but not cell-virus fusion (Singethan et al., 2006). In contrast, fusion of macrophages into multinucleated giant cells was increased in both CD9 and CD81 single-KO mice and even more CD9 and CD81 double-KO mouse spontaneously developed multinucleated giant cells and showed enhanced osteoclastogenesis. This resulted in kyphosis and osteopenia at later age (Takeda et al., 2008; Takeda et al., 2003). Taken this together, CD9 is implicated in regulation of various cell fusion events.

Thanks to extensive study of tetraspanins many interacting partners of CD9 were discovered. They include membrane structural proteins like EWI-2 and EWI-F, adhesion molecules like Claudin-1 (Kovalenko et al., 2007) and various subsets of integrins (α1β1, α2β1, α3β1, α4β1, α5β1, α6β1, α7β1, α6β4, αIIbβ3) (Berditchevski, 2001), signaling receptors and molecules c-kit (Anzai et al., 2002), G protein-coupled receptor (GPCR) (Little et al., 2004), membrane form of heparin-binding-epidermal growth factor (HB-EGF) and transforming growth factor (TGF)-α (Nakamura et al., 1995; Shi et al., 2000) and major histocompatibility complex II (MHC-II) (Unternaehrer et al., 2007). Even more, besides membrane protein partners, various intracellular signaling molecules were found to interact with CD9. These include phosphatidylinositol 4-Kinase type II (PI4KII) (Yauch and Hemler, 2000) and multiple forms of protein kinase C (PKC) (Zhang et al., 2001). However, CD9 can associate with other protein partners through indirect interactions in TEMs. These interactions confer CD9 ability to contribute to various cellular activities.

CD9 was found downregulated in many tumors and surprisingly its expression inversely correlated with metastasis promotion. Low level of CD9 in cancer cells is maintained by promoter hypermethylation (Drucker et al., 2006) and this leads to activation of phosphatidylinositol 3-Kinase (PI3K) and Akt and thus increased integrin-mediated adhesion, higher motility, cell proliferation, survival and matrix metalloproteinase 2 (MMP-2) expression. All these effects are reversed by ectopic expression of CD9 or anti-CD9 antibody treatment (Ovalle et al., 2007; Saito et al., 2006). CD9 also plays a role in metastasis and transendotelial invasion, where its expression is locally restored at site of migration and even more CD9 on epithelial cells localizes to cell-cell contact area to facilitate migration (Longo et al., 2001; Sauer et al., 2003). This implicates that CD9 may play a role of tumor suppressor. This is supported by trials of adenoviral CD9 gene delivery into tumors. These *in vivo* experiments showed that mice injected with CD9 gene lived longer and developed less metastasis (Miyake et al., 2000; Takeda et al., 2007). However, this is not always the case because overexpression of CD9 in human melanoma cells resulted in p38 and Jun N-terminal kinase (JNK) activation which led to phosphorylation of c-Jun and expression of MMP-2 (Hong et

al., 2005). Furthermore, CD9 CD81 double-KO mouse showed impaired macrophages motility leading to pulmonary emphysema (Takeda et al., 2008).

Precise mechanism by which CD9 regulates cell migration, motility or adhesion is not clear but few possibilities emerge (Zoller, 2009). First is regulation of actin cytoskeleton by Wiskott-Aldrich syndrome protein family verprolin-homologous protein (WAVE) 2 which was shown to be downregulated in cells ectopically expressing CD9. WAVE2 is known to link upstream signals to ARP proteins which nucleates actin polymerization. However, way how CD9 regulates WAVE2 expression is not clear (Huang et al., 2006). Second could be downregulation of Wnt1, Wnt2b and Wnt5a genes induced by CD9 expression. Although mechanism of this action is unknown, Wnt5a acts through Wnt-Ca^{2+} pathway which leads to actin reorganization and might modulate cell adhesion and motility (Huang et al., 2004). Third might be through interaction of CD9 with ganglioside GM3 which enables to associate with α3β1 integrin and translocates C-terminal Src kinase (Csk) to TEMs. This causes inhibition of Scr and Rac but activation of PI3K and Akt (Mitsuzuka et al., 2005). And finally as mentioned before, CD9 associates with members of EWI family which link CD9 to actin cytoskeleton and drives it to filopodia (Stipp et al., 2003a).

Taking this together, CD9 plays important role in cell fusion, motility, adhesion, survival and possibly acts as tumor suppressor.

3.2 Mast cells

3.2.1 Mast cells overview

Mast cells are leukocytes of myeloid origin initially identified by Ehrilich in 19th century. As a part of innate immunity, they play role in host defense against bacterial infections, viruses, venom toxins and multicellular parasites. However the major focus of current research still remains on their IgE-mediated hyperreativity to allergens. This is coupled with exhibiting allergic rhinitis, asthma, atopic dermatitis and several food allergies. It is therefore crucial to understand mast cell physiology and signaling events leading to their effector functions.

3.2.2 Function and development

Mast cells are derived from a hematopoietic stem cell. In contrast to related basophils, their committed precursors, characterized by c-$kit^{+}CD34^{+}CD13^{+}Fc\varepsilon RI^{-}$ surface markers, leave bone marrow and finish their development in peripheral tissues such as skin, mucosa and airways (Kirshenbaum et al., 1999). Depending on local environment, they can maturate to different subsets like mucosal mast cells (MMCs) and connective tissue mast cells (CTMCs) which differ in their

granules content (Stevens et al., 1994). MMCs are T cell-dependent and do not maturate in the absence of inflammation while CTMCs are T cell-independent (Irani et al., 1987). However, both subtypes require interleukin (IL)-3 and stem cell factor (SCF) for their successful development as inferred from phenotype of mice carrying mutation in c-kit gene (Grimbaldeston et al., 2005). Mast cells with their lifespan ranging from weeks to months belong to long-lived cells and are also able to proliferate after finishing their maturation.

Before being able to be activated by antigen, mast cells must bind antigen-specific IgE antibody to the high-affinity receptor FcεRI on their surface. This process called sensitization is not just a passive event but sensitized cells increase their adhesion to extracellular matrix (Lam et al., 2003), cell proliferation and survival (Asai et al., 2001) and, importantly, expression of surface FcεRI (Yamaguchi et al., 1997) enabling further IgE binding. On encountering of specific multivalent antigen, mast cells became activated and release three types of effector molecules. Within first few minutes, which is called immediate reaction, they release prestored content of their cytosolic secretory granules such as biologically active amines (histamin and serotonin), proteoglycans, proteases, exoglycosidases and in some cases also tumor necrosis factor (TNF)-α. In late reaction which starts within 30 min, several arachidonic acids derivates (leukotrien C_4 and prostaglandin D_2) are synthesized followed by *de novo* protesynthesis of various cytokines, such as TNF-α, TGF-β, vascular endothelial growth factor (VEGF), interleukin IL-1, IL-3, IL-4, IL-5, IL-6, IL-9, IL-10, IL-13 and various chemokines (Marshall, 2004; Metcalfe et al., 1997). IL-4 was discovered as potent factor promoting antibody isotype switch to IgE and its increased production. This suggests possible positive feedback loop by which mast cells might enhance and maintain IgE-associated reaction driven by T_H2 response (Yamaguchi et al., 1997).

3.2.3 Structure of FcεRI receptor

Selected effector functions of mast cells are mediated by FcεRI localized on their surface. FcεRI, together with T-cell receptor, B-cell receptor and other Fc receptors, belongs to immunoreceptor family which is characterized by absence of intrinsic kinase activity and presence of at least one immunoreceptor tyrosine-based activation motif (ITAM). This multimeric receptor comprises of one α subunit, one β subunit, which passes plasma membrane four times, and two single-spanning γ subunits linked by disulphide bridge. However, trimeric receptor $\alpha\gamma_2$ was described to be present on human monocytes, Langerhans cells, eosinophils and dendritic cells. All subunits are maintained in complex through electrostatic and hydrophobic non-covalent interactions (Kinet, 1999).

The FcεRI α chain consists of short cytoplasmic tail, transmembrane region and two immunoglobulin-related domains which are N-glycosylated at seven sites. Glycosylation is required

for proper folding in ER but not for IgE binding (Letourneur et al., 1995). Extracellular part contains two binding sites for Cε3 domains of IgE and thus α subunit binds IgE in 1:1 stoichiometry (Garman et al., 2000). While cytoplasmic part does not confer any signaling activity and α subunit thus serves only for binding IgE, β and γ_2 subunits play role in sensing of bound antigen and transduction of signal. They both contain ITAM motifs which are phosphorylated upon antigen-mediated crosslinking of the receptor and then serve as binding sites for signaling molecules containing Src homology 2 (SH2) domains. Subunit β spans plasma membrane four times and serves as signal amplifier (Dombrowicz et al., 1998; Lin et al., 1996). However, homodimer consisting of two disulphide linked γ subunits is the main signaling unit of Fc receptor. Each γ subunit consists of transmembrane domain and cytosolic part containing single ITAM motif (Kinet, 1999).

3.2.4 Signaling pathways involved in mast cell activation

After crosslinking of IgE-bound FcεRI receptor, cytosolic parts of β and γ_2 chains containing ITAM motifs that have consensus sequence Y-x-x-(L/I/V)-x_{6-8}-Y-x-x-(L/I/V) become phosphorylated. This is mediated by activity of Scr family kinase Lyn. The precise mechanism of these early steps remains elusive, however two hypotheses were proposed. First one suggests translocation of the receptor complex to lipid rafts upon antigen-mediated FcεRI aggregation where it is phosphorylated by resident Lyn kinase (Field et al., 1999). Another one is based on constitutive association of Lyn kinase minor fraction with Fc receptor and thus antigen-mediated aggregation leads to trans-phosphorylation of close receptors (Vonakis et al., 2001). Two phosphorylated tyrosines in β chain then serve as new docking sites for Lyn kinase while phosphorylated γ subunits harbor spleen tyrosine kinase (Syk) which is then activated by conformational change, autophosphorylation and/or phosphorylation by Lyn (Kimura et al., 1996). In addition to this signal-initiating activity, Lyn also negatively regulates mast cell activation by inhibiting second Src family kinase Fyn. Fyn has positive role in mast cell signaling and it also associates with β chain and helps to active Syk kinase (Parravicini et al., 2002). Third Src family kinase is Hck is proposed to inhibit negative activity of Lyn kinase. Hck thus negatively regulates Lyn which negative regulates Fyn (Hong et al., 2007). Lyn also activates phosphatases and in this way also inhibits FcεRI signaling.

Activated Syk and Src kinases then affect other downstream signaling proteins. First step in downstream signal transduction is phosphorylation of transmembrane adaptor proteins linker of activated T cells (LAT) and non-T cell activation linker (NTAL). BMMCs from NTAL KO mouse show augmented response to antigen challenge which led to conclusion that NTAL, in contrast to

LAT, is mainly negative regulator of mast cell signaling (Volná et al., 2004). Transmembrane adaptor proteins are special group of signaling molecules which lack intrinsic kinase or other enzymatic activities. Instead, they are bound to plasma membrane through their TM region and act as a meeting place for other signaling molecules by providing docking point for their interaction domains. Both LAT and NTAL contain docking site for growth factor receptor-bound protein 2 (Grb2) which serves as cytosolic adaptor protein for SH2 domain-containing transforming protein C (Shc) and son of sevenless (SOS). SOS is a guanine nucleotide exchange factor (GEF) and facilitates exchange of GDP towards GTP in small G protein Ras. Ras-GTP then triggers cascade of phosphorylation events which lead to activation of extracellular signal-regulated protein kinase (Erk) (Jabril-Cuenod et al., 1996). This is followed by activation of phospholipase A_2 (PLA_2), which leads to eicosanoids production (Miura et al., 1999), and activation of activator protein 1 (AP1) transcription factor which turns on transcription of cytokine genes (Gilfillan and Tkaczyk, 2006).

However, LAT but not NTAL holds binding sites for Grb2-related adaptor protein (GADS) and Phospholipase Cγ (PLCγ). GADS also interacts with SH2-domain-containig leukocyte protein of 65 kDa (SLP76) which is phosphorylated by Lyn and Syk and is along with VAV protein necessary for full activation of PLCγ (Pivniouk et al., 1999). In addition to this main Lyn-LAT- PLCγ pathway, alternative Fyn-Gab2-PI3K axis was described which is believed to be associated with NTAL adaptor protein (Rivera, 2005). Grb2-associated binding protein 2 (Gab2) is phosphorylated by Src kinase Fyn and this leads to activation of PI3K which then phosphorylates phosphatidylinositol (4,5)-bisphosphate (PIP_2) to phosphatidylinositol (3,4,5)-trisphosphate (PIP_3). Accumulation of PIP_3 in the plasma membrane provides docking sites for proteins containing pleckstrin-homology (PH) domains such as PLCγ, Akt and TEC-family kinase Burton's tyrosine kinase (Btk). Akt is known to stimulate transcription of prosurvival genes and through activation of nuclear factor-κB (NF-κB) induces generation of cytokines. Recently, it was discovered that IκB kinase 2 phosphorylates SNAP-23 which then facilitates fusion of secretory granules with plasma membrane and thus promotes degranulation (Suzuki and Verma, 2008). Btk was shown to phosphorylate and therefore activate PLCγ (Hata et al., 1998). It is therefore obvious that both Lyn- and Fyn-mediated pathways converge to the same effector, although it seems that latter is responsible for maintenance, but not the initiation of the signal (Tkaczyk et al., 2004).

Active PLCγ then cleaves plasma membrane PIP_2 into two molecular messengers diacylglycerol (DAG) and inositol (1,4,5) trisphosphate (IP_3). While membrane-bound DAG serves as activator of PKC, soluble IP_3 diffuses to ER membrane and opens calcium channels which leads to release of

Ca^{2+} from ER lumen to cytosol. After depleting ER calcium store, calcium sensor stromal interaction molecule 1 (STIM1) triggers calcium influx by opening Orai channels in plasma membrane. This prolonged calcium signal is necessary for proper activation of nuclear factor of activated T-cells (NFAT) which again turns on various cytokine genes. Moreover, calcium together with DAG activates PKC which also regulate transcription but more importantly stimulates degranulation (Vig and Kinet, 2009).

Mast cells also express other receptors on their surface such as Fcγ receptors which can be either stimulatory or inhibitory, receptor tyrosine kinase c-kit and several G protein-coupled receptors for different ligands. Signal from all of these receptor converge at different points with above-mentioned cascades and modifies threshold for mast cell activation (Gilfillan et al., 2009; Kuehn et al., 2008).

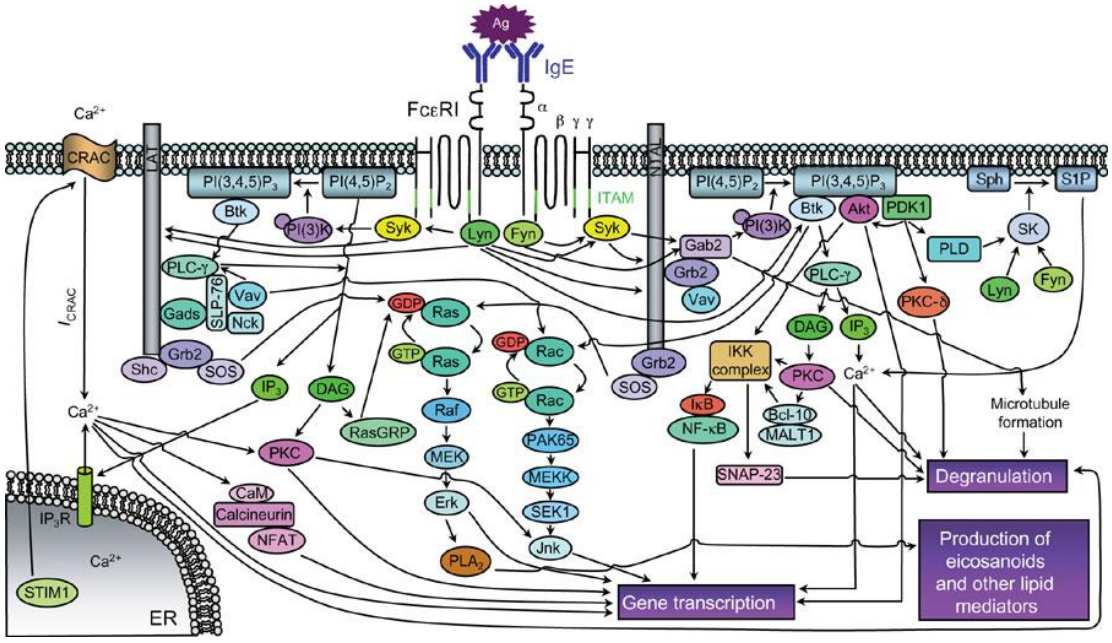

Fig. 3 – Overview of mast cell signaling

When the tetrameric FcεRI receptor (consisting of α,β and γ_2 chains) with bound IgE antibody is crosslinked with multivalent antigen (Ag), Src-family kinases Fyn and Lyn phosphorylate ITAM motifs and associated Syk kinase. Lyn and Syk then phosphorylate transmembrane adaptor proteins LAT and NTAL which harbor Grb2-SOS-Shc complexes that activate Ras-Raf-MEK-Erk cascade. Erk can either activate gene transcription or PLA_2 activity which leads to eicosanoids production. LAT also binds GADS-SLP-76-Vav complex which helps to activate PLCγ. Alternatively Fyn can activate PLCγ through Gab2-PI(3)K-$PI(3,4,6)P_3$-Btk pathway. PLCγ then cleaves $PI(4,5)P_2$ into DAG and IP_3 which releases Ca^{2+} from ER by opening IP_3R channels. Decrease in calcium content in ER is sensed by STIM1 which then opens calcium-release-activated-calcium (CRAC) channels consisting of Orai1 subunits in plasma membrane. Elevated calcium level activates NFAT transcription factor and together with DAG also PKC, which activate gene transcription and also degranulation. Akt kinase stimulate gene transcription alone and also through NFκB pathway. IKK also activate SNAP-23 which mediates fusion of granules with plasma membrane (Kalesnikoff and Galli, 2008).

3.3 CD9 and other tetraspanins in the context of mast cells signaling

Despite extensive study of CD9 and other tetraspanin members, our current knowledge of their implication in mast cells remains limited to a few reports. First of all, direct interaction between CD9 and FcεRI receptor was confirmed in human CD9-transfected RBL cells. Monoclonal antibody against CD9 activated these cells in concentration dependent manner, but addition of IgE

suppressed this effect which suggests that activation is mediated by colligation of CD9 with FcεRI (Higginbottom et al., 2000b). Another study showed that anti-CD81 antibody inhibited FcεRI-mediated degranulation in both *in vitro* and *in vivo*. Surprisingly, no detectable effect on global phospho-tyrosine pattern, calcium release or leukotrien synthesis was observed (Fleming et al., 1997). Similar results were obtained with anti-CD63 antibody. However, inhibition of degranulation was present only in adherent cells and in addition anti-CD63 antibody inhibited also adhesion to fibronectin and vitronectin. Using specific inhibitors revealed that these effects were caused by impairment of Gab2-PI3K pathway (Kraft et al., 2005). Another indication of possible IP3K involvement in CD9 effects is report that CD9 works as an alternative IL-16 receptor in mast cells. When CD9 expression level is downregulated by antisense oligonucleotides, IL-16 binding and chemotactic response to this cytokine are inhibited. Furthermore, anti-CD9 antibody blocks IL-16-mediated activation and associated calcium response (Qi et al., 2006). All three tetraspanins CD9, CD63 and CD81 were found physically associated with receptor tyrosine kinase c-kit. It was proposed that tetraspanins negatively modulate c-kit function and thus its sensitivity to SCF. This is because tetraspanin-associated fraction of c-kit has lower kinase activity in basal state and also after SCF stimulation (Anzai et al., 2002).

Eosinophills are minor fraction of blood-circulating granulocytes related to mast cells. It was shown that immobilized anti-CD9 antibody activated these cells and this was reversed by anti-β_2 integrin antibody. Antibody against CD9 also stimulated cell survival by autocrine production of granulocyte macrophage colony-stimulating factor (GM-CSF) (Kim et al., 1997).

4 Materials and methods

4.1 Cell cultures

4.1.1 BMMCs

Bone marrow cells were isolated from femurs and tibias of 6–10 weeks old mice. The cells were then kept in suspension culture for 4–8 weeks in complete medium IMDM supplemented with 10% fetal calf serum (FCS), 41μM 2-mercaptoethanol, 100 U/ml penicillin, 100 μg/ml streptomycin, murine recombinant IL-3 (36 ng/ml; PeproTech EC) and murine recombinant SCF (36 ng/ml; PeproTech EC) at 37°C in an atmosphere of 10% CO_2. Before conducting the experiments, the cells were assayed for high level of FcεRI expression using flow cytometry analysis and tested for their ability to degranulate in response to antigen – TNP conjugated to BSA (TNP-BSA) using β-glucuronidase assay.

4.1.2 Immortalized BMMCs

Immortalized BMMCs were kindly provided by M. Hibbs (Ludwig Institute for Cancer Research, Melbourne, Australia). Suspension cultures were grown in IMDM medium supplemented with 10% FCS, 41μM 2-mercaptoethanol, 100 U/ml penicillin, 100 μg/ml streptomycin and 10% WEHI supernatant as a source of IL-3 at 37°C in a humidified atmosphere of 10% CO_2. Immortalized BMMCs were used for experiments from chapter 5.7 to chapter 5.12.

4.1.3 Rat basophilic leukemia cell line

Subclone 2H3 of RBL cell line (RBL-2H3) originally acquired from H. Metzger (NIH, Bethesda, MD) was maintained in RPMI-1640 medium supplemented with 100 U/ml penicillin, 100 μg/ml streptomycin and 10% FCS. Monolayer cultures were passaged every 2–3 days and kept in humidified and 5% CO_2 atmosphere at 37°C.

4.1.4 293 T/17 cell line

Human embryonic kidney 293 T/17 cells were purchased from American Type Culture Collection (ATCC) (Manassas, VA, USA). The cells were grown as an adherent monolayer culture in DMEM medium containing 10% FCS, 100 U/ml penicillin and 100 μg/ml streptomycin. Cultures were passaged regularly every 4–5 days and kept at 37°C at an atmosphere of 5% CO_2.

4.2 β-glucuronidase assay

BMMCs were incubated at concentration 6.66 × 10^6/ml in cytokine-free medium (IMDM containing 10% FCS, 41 μM 2-mercaptoethanol, 100 U/ml penicillin and 100 μg/ml streptomycin) with 1000× diluted 2,4,6-trinitrophenyl (TNP)-specific IgE ascites (IGEL) for 4 hours or overnight at 37°C. Subsequently, cells were 3× centrifuged at 290 × g for 5min at room temperature and washed with balanced salt saline containing 0.1% bovine serum albumin (BSS-BSA). They were then transferred into 30 μl U-bottom 96-well plate (P-lab, Prague, Czech Republic) at a concentration 7 × 10^6/ml, mixed with 30 μl of TNP-BSA (1 μg/ml) and incubated at 37°C for indicated time. As positive control 30 μl of 0.1% Triton X-100 instead of TNP-BSA was added. Activation was stopped by placing plate on ice and adding 60 μl of cold BSS-BSA. After centrifugation (290 × g, 5min, 4°C) 30 μl of supernatant was transferred to flat-bottom white FluoroNunc plate (Nunc, Roskilde, DK) and 30 μl of 60 μM 4-Methylumbelliferyl β-D-Glucuronide (MUGlcU) substrate in acetate buffer (pH 4.4) was added and incubated at 37°C for 30 min. Reaction was terminated by addition of 200 μl cold glycine buffer (pH 10), and amount of fluorescent product was assessed by reading the plate with Infinite 200M (Tecan Group Ltd., Männedorf, CH) plate reader instrument at excitation and emission wavelength, 355 nm and 460 nm respectively. Alternatively, in some experiments thapsigargin instead of TNP-BSA was added.

4.3 Calcium assay

BMMCs were washed 2× with BSS-BSA and resuspended in BSS-BSA supplemented with 2.5mM probenecid and 1 μg/ml Fura-2 AM at a concentration 6 × 10^6/ml. After 30 min incubation in water bath at 37°C, the cells were washed and resuspended in BSS-BSA containing probenecid and incubated for another 15 min at 37°C to fully hydrolyze Fura-2 dye. Subsequently, the cells were washed with BSS-BSA supplemented with probenecid , resuspended at a concentration 4 × 10^6/ml in BSS-BSA and 50 μl of this suspension was transferred to flat-bottom white FluoroNunc plate (Nunc, Roskilde, DK) and measured on Infinite 200M plate reader (Tecan Group Ltd., Männedorf, CH). Calcium response was triggered by injection of an equal amount of 2× concentrated activator. Alternatively, same amount of 3× concentrated second activator was injected at specified times after first injection. Fluorescence was recorded from dual excitation (340 nm, 380 nm) and single emission 510 nm wavelength. Final Ca^{2+} curve was calculated as ratio of emission with excitation at 340 nm and 380 nm in same cycle.

4.4 Preparation of tissue lysates and protein quantification assay

Mouse was sacrificed and extracted organs were kept on ice. Approximately equal-weight piece of each organ (where applicable) was transferred to 1 ml of ice-cold organ-lysis-solution. All samples were homogenized for 5 min by electric homogenizer and incubated on ice for 30 min. In order to break down DNA aggregates, samples were repeatedly aspirated through medical needle (Ø 1.20 × 40 mm) and then centrifuged (14,000 × g, 10 min, 4°C). Protein content in samples was then quantified using DC Protein Assay (Bio-Rad Laboratories, Hercules, CA) according to manufacturer's protocol. Absorbance of samples was read at 750 nm on Infinite 200M plate reader and protein concentrations were calculated from bovine serum albumin (BSA) standard curves. All samples were then diluted with organ-lysis-solution to obtain final protein concentration 1.66 mg/ml. Subsequently, 30 µl was mixed with 2× concentrated sample buffer and resolved on sodium dodecyl sulfate polyacrylamide gel electrophoresis (SDS-PAGE).

4.5 Immunoprecipitation and covalent coupling of antibody to protein G

All steps were performed on ice or at temperature 4°C unless otherwise stated. Protein G Ultralink resin (Pierce, Rockford, IL, USA) was incubated with antibody diluted in phosphate buffered saline (PBS) for 1.5 h with continual agitation. Resin was then washed 2× with PBS and 2× with 10 volumes of borate buffer. Finally, resin was resuspended in 10 volumes of borate buffer supplemented with dimethyl pimelimidate (DMP) (20mM) and incubated for 30 min at room temperature with constant agitation. Reaction was quenched by 2× washing and then incubating the resin with Tris-HCl (1M, pH 8.0) for 2 h at room temperature. Non-cross-linked proteins were eluted by washing 2× with glycine buffer (pH 2.5) and then neutralized with lysis buffer.

BMMCs were lysed in lysis buffer A supplemented with 1% Triton X-100 for 30 min. Lysate was centrifuged (14,000 × g, 10 min, 4°C) and cleared supernatant was added to Protein G Ultralink resin (6.6×10^6 cells/10 µl of resin). After 2 h incubation with continual agitation, the resin was 3× washed with lysis buffer A supplemented with 1% Triton X-100 and 1× with lysis buffer A alone to remove unbound proteins. Antigen was eluted by boiling with 1× concentrated sample buffer (non-reducing) for 5 min and then separated on SDS-PAGE.

4.6 Protein analysis

4.6.1 SDS-PAGE

Cells were lysed in cold lysis buffer B containing 1% NP-40 and 1% Lauryl maltoside for 30 min and then centrifuged (10 min, 14,000 × g, 4°C). Supernatant was diluted with 2× concentrated sample buffer (reducing or non-reducing). In case of immunoprecipitation with antibody bound to protein G immobilized on agarose beads, 1× concentrated sample buffer was used for antigen elution. Before loading, the samples were boiled for 5 min and then resolved by 10% or 15% separating gel with 4% stacking gel. Electrophoretic separation was performed using Mini-protean II (Bio-Rad Laboratories, Hercules, CA) with constant voltage setting 100 V for 15 min and then 120 V for 75 min.

4.6.2 Western blotting and protein immunodetection on nitrocellulose membrane

Gel was rinsed in transfer buffer and then used for transferring size-fractioned proteins onto nitrocellulose membrane (Schleicher a Schuell BioScience, Inc., Keene, NH) with dimensions 8.5 cm × 6 cm. Western blotting was performed using Mini Trans-Blot (Bio-Rad Laboratories, Hercules, CA) system at constant current 200 mA for 90 min.

Nitrocellulose membrane was first washed for 15 min in Tris-NaCl-Tween (TNT) buffer and then blocked by incubation in TNT supplemented with 2% BSA for 1 h. Subsequently, the membrane was probed with primary antibody diluted in TNT containing 2% BSA for 1 h, followed by 3× 5 min wash with TNT. Membrane was then incubated with secondary antibody conjugated with horseradish peroxidase (HRP), diluted in TNT supplemented with 0.5% nonfat dry milk for 1 h. In case of anti-phosphotyrosine primary antibody (PY-20) conjugated with HRP, probing was performed in TNT supplemented with 0.5% nonfat dry milk. Membrane was then washed as previous, incubated in enhanced chemiluminiscence (ECL) for 1 min, placed on plastic pad and covered with Saran foil (Dow Chemical Company). Luminescent signal was detected by LAS-3000 imaging instrument (Fuji Photo Film Co.).

4.6.3 Protein staining in the gel by Coomassie Brilliant Blue R-250

Polyacrylamide gel was fixed and stained overnight in staining solution. After that, the gel was destained by rinsing with destining solution. For long-term storage, the gel was kept in 1% acetic acid.

4.6.4 Sample preparation for mass spectrometry (MS) analysis

Spot of our interest was excised from the gel, cut into small pieces and washed several times with 0.1M 4-ethylmorpholine acetate (pH 8.1) in 50% acetonitrile. After complete destaining, 50 mM tris(2-carboxyethyl)phosphine (TCEP) was added to the gel pieces and incubated for 15 min at 80°C. Then the gel pieces were washed in water and 100mM iodoacetamide (IAA) solution was added for 40 min in the dark. The gel was washed with deionized water, shrunk by dehydration in acetonitrile. The supernatant was removed, and the gel was partly dried in SpeedVac concentrator. Gel pieces were then reconstituted in cleavage buffer containing 50 mM 4-ethylmorpholine acetate, 10% acetonitrile and sequencing grade trypsin (50 ng/ml, Promega; Madison, WI).

After overnight digestion at 37°C, the resulting tryptic peptides were extracted with acetonitrile in final concentration of 10% and 1% acetic acid. Five microliters of the peptide mixture were applied on a reverse phase column (Magic C18, 0.2 × 150 mm, 200Å, 5 μm; Michrom Bioresources) and separated using a gradient elution (0–12% B for 10 min and 12–45% B for 90min at a flow rate of 2 μl/min). Solvent A was 5% acetonitrile, 0.5% acetic acid and solvent B 95% acetonitrile, 0.4% acetic acid. The column was interfaced with an ion trap mass spectrometer (LCQDECA ThermoFinnigen) equipped with nanoelectrospray ion source.

4.7 Generation of CD9 knockdown and overexpressing BMMCs

4.7.1 Competent cells

For propagation of plasmid DNA, competent DH5α E. coli cells were used. The cells were inoculated into 6 ml of Luria-Bertani (LB) medium and cultivated overnight in orbital shaker (Sanyo; 150rpm, 37°C). Next day 1 l of LB medium was inoculated with prepared bacterial culture and cultivated under the same conditions till optical density at 600 nm reached interval 0.5–0.7. Bacterial cells were then centrifuged (4 000 × g, 4°C, 10 min), supernatant was discarded and pellet was resuspended in 500ml of cold 10% glycerol. The cells were washed two more times in 250 ml and 125 ml of 10% glycerol respectively. Finally, they were resuspended in 3 ml of cold 10% glycerol and stored at −70°C in aliquots.

4.7.2 Vector construction

Plasmid pYX-Asc containing full-length CD9 complementary DNA (cDNA) (Open Biosystems, Huntsville, AL) and lentiviral expression plasmid pCDH-CMV-MCS-EF1-Puro (System Biosciences, Mountain View, CA) were propagated in bacteria and isolated using Lego kit (Top-Bio s.r.o., Praha, CZ) according to manufacturer protocol. Both vectors were cut by EcoRI

(Fermentas, Burlington, Ontario, CA) and NotI (Fermentas) restriction enzymes, separated on agarose gel and bands corresponding to cDNA (1314 bp) and linearized pCDH-CMV-MCS-EF1-Puro (7355 bp) were isolated using TaKaRa RECOCHIP (TAKARA BIO INC., Shiga, Japan) according to manufacturers protocol. DNA was precipitated overnight (200 µl of DNA, 50 µl of 3M sodium acetate pH 5.2, 1ml of 96% ethanol) at −20°C, washed 3× with 75% ethanol, dryed and dissolved in deionized water at 65°C. Purified cDNA fragment was then ligated with linearized expression plasmid using T4 DNA ligase (Fermentas)and thus creating plasmid construct termed pCDH/CD9.

4.7.3 Bacterial transformation

Transformation of E. coli bacterial strain DH5α was carried out by electroporation when 1 µl of ligation product was mixed with 40 µl of competent cells and transferred to cold electroporation cuvette. The cells were then subjected to electrical pulse of 1.8 kV in Pulser Transformation Apparatus (BioRad Laboratories) and immediately supplemented with 1 ml of super optimal broth with catabolite repression (SOC) medium. After 60 min incubation on shaker at 37°C, cells were seeded on LB agar plate with ampicillin (100 µg/ml) and grown bottom up at 37°C overnight.

Six colonies were used for inoculation of 3 ml of LB media containing ampicillin (100 µg/ml). Plasmid was isolated using Lego kit, all clones were verified by restriction digest by PvuII (New England Biolabs, Ipswich, MA; generates 4 fragments, one with increased molecular weight in case of successful insertion) and ApaI (New England Biolabs; cleaves only inside cDNA sequence) and one clone was then verified by sequencing from cytomegalovirus (CMV) promoter.

4.7.4 Generation of lentiviral particles and cells infection

To generate lentiviral particles for stable and effective BMMCs transformation, production cell line 293 T/17 cells were transfected with desired lentiviral vector and vectors essential for viral particles production. At first, 82µl of Lipofectamine was mixed with 1 ml of OPTI-MEM medium and incubated for 5 min at room temperature. Then 500 µl of OPTI-MEM containing 21 µl (1 µg/ml) of packaging vectors equimolar mixture (pPL1, pPL2, VSVG) and 14 µg of desired lentiviral vector (maxiprep isolated) was added. After gentle agitation, the mixture was left to react at room temperature for 20 min. 293 T/17 cells were grown in 150 cm^2 plastic culture bottles to subconfluency and old medium was removed and changed for 10 ml of fresh DMEM medium without antibiotics. The tranfection mixture was then mixed with 10 ml of DMEM medium without antibiotics and added to the cells. After brief swirling, the culture bottles were placed into incubator (37°C, 10% CO_2) and incubated for at least 6 h. The medium used for transfection was then

replaced with 25 ml of new DMEM medium with antibiotics. The cells were then cultivated for another 3 days. Supernatant was then subjected to brief centrifugation (290 × g, 10 min) to remove dead cells and debris and then centrifuged at higher speed (75,600 × g, 2h, 4°C) to collect viral particles. Supernatant was then discarded and pelleted viral particles were resuspended to 1 ml of complete media by repetitive aspiration with insulin needle. Viral suspension was then added to required amount of BMMCs (1×10^6/ml) in complete medium without antibiotics and cells were incubated for 2 days. Medium was then replaced with complete medium supplemented with puromycin (5 μg/ml) and infected cells were selected for 4 days. The cells were regularly passaged and kept in complete medium containing puromycin (2 μg/ml).

4.7.5 Plasmid miniprep

Minipreparative plasmid isolation from bacteria was performed using commercial DNA Lego kit according to manufacturer's protocol. Briefly, 3 ml of LB medium supplemented with ampicillin (100 μg/ml) was inoculated with bacteria carrying plasmid of interest and incubated in orbital shaker overnight at 37°C. Then 1.5 ml of bacterial suspension was centrifuged (14,000 × g, 30 s) and pellet was resuspended in 200 μl of suspension solution. The cells were lysed by addition of 200 μl of Lysis solution, mixed by inversion and incubated for 5 min. Lysis was terminated by 200 μl of neutralization solution, mixed by slow inversion and centrifuged (14,000 × g, 7 min). Meanwhile minicolumns were attached to Vac-Man Laboratory vacuum manifold (Promega, Madison, WI) and 100 μl of DNA bind particle suspension was loaded. Cleared supernatant was then mixed with 600 μl of DNA binding buffer and loaded onto column with DNA bind particles. Solution was then sucked through the column by applying vacuum and washed by 2 ml of Wash buffer. DNA was eluted by centrifugation (14,000 × g, 1min) with deionized water preheated to 50°C. DNA purity and concentration was measured using Nanodrop instrument (Thermo Scientific, Wilmington, DE).

4.7.6 Plasmid maxiprep

Bacterial cells were inoculated into 3 ml of LB medium supplemented with ampicillin (100 μg/ml) and cultivated in orbital shaker at 37°C overnight. Bacterial suspension was then used to inoculate 1 l of LB medium with ampicillin (100 μg/ml) and cultivated as previously. Next day, the bacterial suspension was cooled on ice and centrifuged (4,620 × g, 12min, 4°C). Pelleted cells were resuspended in 64 ml of GTE solution and lysed for 10 min on ice by adding 128 ml of NaOH/SDS solution and mixed by slow inversion. Lysis was stopped with 64 ml of KAc/Ac solution and intensive shaking. Lysate was centrifuged (4000 × g, 20 min, 4°C), supernatant was filtered

through sterile gauze and precipitated in 74 ml of ice-cold isopropanol for 30 min on ice. After centrifugation (4000 × g, 20 min, 4°C), supernatant was discarded, pelleted DNA was dried and then dissolved in 8 ml of Tris-EDTA (TE) buffer for 10 min at 65°C. Into fully dissolved DNA solution, 9.2 g of CsCl and 0.25ml of ethidium bromide (EtBr) (10 mg/ml) was added. The solution was then transferred into two 5 ml centrifugal tubes (Beckman Instruments,Inc., Palo Alto, CA) and ultracentrifuged (65,000 rpm, 16 h, 18°C, NVT 90 rotor, Ultracentrifuge L-70, Beckman Instruments,Inc., Palo Alto, CA) till equilibrium. Tubes were carefully pierced with needle and approximately 1–2 ml of solution (containing lower EtBr band consisting of plasmid) was aspirated. Recovered solution was then mixed with 100 µl of EtBr (10 mg/ml), 9 g of CsCl and 8 ml of TE buffer and loaded into new centrifugal tubes. Plasmid was again separated on CsCl gradient by ultracentrifugation (70,000 rpm, 6 h, 18°C, NVT 90 rotor, Ultracentifuge L-70) and extracted as before. To remove remaining EtBr from plasmid sample, the solution was 5× mixed with 8 ml of butanol, briefly centrifuged and upper butanol phase was discarded. For each ml of cleared plasmid solution, 1ml of TE buffer, 100 µl of 3M sodium acetate and 2 ml of 96% ethanol cooled to −20°C were added and mixture was precipitated for at least 2 h at −20°C. The precipitate was then centrifuged (27,216 × g, 20 min), pellet was mixed with 10 ml of 70% ethanol by wortexing and centrifuged again (20min, 7,000 rpm). Purified and pelleted plasmid was then dried in vacuum and dissolved in 1 ml of TE buffer. Small aliquots were stored at −70°C.

4.8 Labeling of TNP-BSA with tetramethyl rhodamine isothiocyanate (TRITC)

TNP-BSA (2.5 mg/ml) was first dialyzed overnight against carbonate/bicarbonate buffer (100mM, pH 9.6). Then, 35 µl of TRITC (1mg/ml) dissolved in non-aqueous dimethyl sulfoxide (DMSO) was slowly added to 0.5 ml of dialyzed TNP-BSA while stirring. Mixture was incubated for 2 h at room temperature in the dark. Excess of TRITC was removed by overnight dialysis against PBS. TNP-BSA-TRITC was immediately used for experiments or stored at −20°C in aliquots.

4.9 Flow cytometry

Flow cytometry was used for detection of surface antigens on BMMCs. Non-sensitized cells were probed by incubation for 30 min at 4°C with primary antibody diluted in 20% complete medium in PBS (CM/PBS). In case of Fc receptor was being detected, the cells were sensitized with IgE as described previously. Cells were then washed 2× with CM/PBS followed by incubation with anti-rat IgG secondary antibody conjugated to fluorescein isothiocyanate (anti-rat-IgG-FITC)

diluted in CM/PBS (1:300) for 30min at 4°C. After 2× wash with CM/PBS, the cells were resuspended in cold PBS and analyzed on FACSCalibur or LSR II flow cytometer (BD Biosciences, San Jose, CA, USA) in FL1 channel.

When level of antigen binding to IgE-loaded Fc receptor was being assessed, cells were sensitized as usual and then incubated with TNP-BSA-TRITC (1 μg/ml) in BSS/BSA for 30 min at 37°C. Excess of unbound TNP-BSA-TRITC was removed by 2× wash with cold BSS/BSA and cells were then resuspended in cold PBS. Fluorescence of bound antigen was measured on flow cytometer in FL2 channel.

4.10 Phosphatidylinositol-specific phospholipase C (PI-PLC) assay

Cells were washed 2 × in BSS-BSA, centrifuged and supernatant was removed. Pellet was resuspended in complete medium supplemented with PBS and PI-PLC (1×10^6 cells per 50 μl of medium containing 2 μl of PI-PLC) and incubated 40 min at 37°C. Cells were then washed 2×, labeled with appropriate antibodies and decrease in surface content of examined proteins were analyzed by flow cytometry.

4.11 Preparation of rat monoclonal antibodies against BMMCs membrane antigens

Murine BMMCs were permeabilized in PBS supplemented with Saponin (final concentration 0.1%) and $MgCl_2$ (10mM), centrifuged and sedimented membrane fraction was used for immunization of rat (strain Wistar). Interspecies hybridomas were created by fusion of rat spleen cells with murine myeloma cell line (SP2/0). Hybridomas were then cloned and supernatants from individual clones were subjected to testing for the presence of antibodies capable of binding to surface antigens of BMMCs as detected by flow cytometry analysis. Clones with the best binding ability were picked and also tested for their reactivity to BMMCs lysate on western blot.

4.12 Purification of 2H9 antibody and normal rat serum IgG

For 2H9 antibody purification, hybridoma cells (prepared as described in 4.11) were cultivated in RPMI-1640 medium supplemented with 10% FCS until color of the medium became pale yellow. Cells were then centrifuged and supernatant was either immediately used for purification of IgG antibodies or stored for further use at −20°C.

In case of IgG antibodies isolation from normal serum, non-immunized rat was sacrificed and collected blood was clotted at room temperature. Clot was then centrifuged at 290 × g for 5 min.

Serum supernatant was collected, diluted 1:1 with PBS containing 0.5 M NaCl and immediately used for purification.

Purification of IgG faction of antibodies was performed by immunoaffine chromatography using anti-rat IgG-Agarose (Sigma-Aldrich, St. Louis, MO). Column was first equilibrated by wash with PBS supplemented with 0.5 M NaCl and then either hybridoma supernatant or rat serum was slowly applied. Column was then again washed with PBS containing 0.5 M NaCl and bound antibodies were eluted with elution buffer. Each fraction was neutralized by addition of 1 M Tris pH 8.0. Fractions were assayed for protein content on NanoDrop ND-1000 spectrophotometer (NanoDrop products, Wilmington, DE, USA) using Protein A280 program. Those with highest concentration were combined and dialyzed against PBS overnight using 25,000 molecular weight cut off dialyzing Spectra/Por membrane (Spectrum Laboratories, Inc., Rancho Dominguez, CA, USA). Product was then concentrated to desired concentration with NANOSEP 30K OMEGA (Pall Life Sciences, MI, USA) with 30,000 molecular weight cut off value.

4.13 Antibody isotyping

Isotyping was performed with IsoStrip Isotyping kit (Cat.No. 1 493 027, Roche Diagnostics, Indianapolis, IN, USA) following the manufacturer's protocol. Antibody of interest was first diluted in PBS and bound to blue latex beads coated with antibodies specific for light chain. Isotyping strip was then dipped into latex bead solution. After leading edge reached the control position, strip was removed and results were read as blue bands on strip in areas with immobilized antibody specific for given isotype.

4.14 Statistical analysis

Statistical significance was determined using an unpaired Student's t test: *, $P<0.05$.

4.15 List of chemicals and material

2-mercaptoethanol	MERCK-Schuchardt, Hohenbrunn, SRN
Acetic acid	Lachema a. s., Neratovice, CZ
Acrylamide	Fluka Chemie GmbH, Buchs, Switzerland
Agarose	Top-Bio s.r.o., Praha
Ammonium persulfate	Sigma-Aldrich, St. Louis, MO
anti-actin	Santa Cruz Biotechnology, Inc., Santa Cruz, CA, USA
anti-CD48	Developed in our laboratory
anti-CD9 (KMC8.8)	Santa Cruz Biotechnology, Inc., Santa Cruz, CA, USA
anti-CD9 (N-19)	Santa Cruz Biotechnology, Inc., Santa Cruz, CA, USA
anti-goat-IgG-Cy3	Jackson ImmunoResearch Laboratories, Inc., West Grove, PA, USA
anti-mouse-IgG-FITC	Sigma-Aldrich, St. Louis, MO
anti-mouse-IgG-HRP	Santa Cruz Biotechnology, Inc., Santa Cruz, CA, USA
anti-phosphoPLCγ1	Santa Cruz Biotechnology, Inc., Santa Cruz, CA, USA
anti-phosphotyrosine (PY20)	BD, Franklin Lakes, NJ, USA
anti-rabbit-IgG-HRP	Santa Cruz Biotechnology, Inc., Santa Cruz, CA, USA
anti-rat-IgG	Jackson ImmunoResearch Laboratories, Inc., West Grove, PA, USA
anti-rat-IgG-FITC	Sigma-Aldrich, St. Louis, MO
anti-rat-IgG-HRP	A5795, Sigma-Aldrich, St. Louis, MO
anti-Thy1.1 (OX-7)	Developed in our laboratory
Aprotinin	Carl Roth GmbH, Karlsruhe, D
Calcein AM	Molecular Probes, Eugene, Oregon, USA
Calcium chloride	Sigma-Aldrich, St. Louis, MO
Coomassie Brilliant Blue R-250	Serva, Heidelberg, D
Dimethyl pimelimidate	Fluka Chemie GmbH, Buchs, Switzerland
DMSO	Fluka Chemie GmbH, Buchs, Switzerland
EcoRI	Fermentas International Inc., Ontario, Canada
EDTA	Carl Roth GmbH, Karlsruhe, D
Ethanol	Lachema a. s., Neratovice, CZ
Fura-2 AM	Molecular Probes, Eugene, Oregon, USA
Glucose	Sigma-Aldrich, St. Louis, MO

Glycerol	Sigma-Aldrich, St. Louis, MO
Glycin	Sigma-Aldrich, St. Louis, MO
HEPES	Sigma-Aldrich, St. Louis, MO
IL-3	PeproTech Inc., Rocky Hill, NJ, USA
Lauryl maltoside	Apollo scientific Ltd., Cheshire, UK
Lipofectamine	Invirtogen, Carlsbad, CA, USA
Luminol	Sigma-Aldrich, St. Louis, MO
Magnesium chloride	Fluka Chemie GmbH, Buchs, Switzerland
Methanol	Lachema a. s., Neratovice, CZ
MUGlcU	Molecular Probes, Eugene, Oregon, USA
Nonfat dry milk	Super G, Inc., Landover, MD, USA
NP-40	USB, Cleveland, Ohio, USA
OPTI-MEM	Gibco, Carlsbad, CA, USA
p-coumaric acid	Sigma-Aldrich, St. Louis, MO
Penicilin	Biotika a.s., Slovenská Ľupča, SR
PI-PLC	Boehringer Mannheim GmbH, Germany
PMSF	Sigma-Aldrich, St. Louis, MO
Ponceau S	Sigma-Aldrich, St. Louis, MO
Potassium chloride	Carl Roth GmbH, Karlsruhe, D
Probenecid	Sigma-Aldrich, St. Louis, MO
Puromycin	InvivoGen, San Diego, California, USA
Saponin	Sigma-Aldrich, St. Louis, MO
SCF	PeproTech Inc., Rocky Hill, NJ, USA
SDS	Carl Roth GmbH, Karlsruhe, D
Sodium acetate	Lachema a. s., Neratovice, CZ
Sodium orthovanadate	Sigma-Aldrich, St. Louis, MO
Streptomycin	Sigma-Aldrich, St. Louis, MO
Thapsigargin	Sigma-Aldrich, St. Louis, MO
Tris	Sigma-Aldrich, St. Louis, MO
TRITC	Fluka Chemie GmbH, Buchs, Switzerland
Triton X-100	USB, Cleveland, Ohio, USA
TWEEN 20	USB, Cleveland, Ohio, USA

4.16 Buffers, Solutions and Media

Acetate buffer

0.1 M	Sodium acetate
0.5 M	NaOH
pH 4.4	with HCl

Glycine buffer

0.35 M	Glycine
0.44 M	Na_2CO_3
pH 10.0	with NaOH

BSS-BSA

0.1 %	BSA
135 mM	NaCl
5 mM	KCl
1.8 mM	$CaCl_2.H_2O$
5.6 mM	Glucose
20 mM	HEPES
pH 7.4	

PBS

137 mM	NaCl
2.7 mM	KCl
8 mM	Na_2HPO_4
2 mM	KH_2PO_4
pH 7.4	

LB medium

1%	Bacto-tryptone
0.5%	Bacto-yeast extract
86 mM	NaCl
pH 7.0	with NaOH

LB agar

1%	Bacto-tryptone
0.5%	Bacto-yeast extract
86 mM	NaCl
1.6%	Bacto agar
pH 7.0	with NaOH

SOC medium

2%	Bacto-tryptone
0.5%	Bacto-yeast extract
10 mM	NaCl
2.5 mM	KCl
10 mM	$MgCl_2$
10 mM	$MgSO_4$
20 mM	Glucose

GTE solution

50 mM	Glucose
25 mM	Tris
10 mM	EDTA

NaOH/SDS solution

0.2 M	NaOH
1%	SDS

KAc/Ac solution

3 M	Potassium Acetate
11.5%	Acetic acid

TE buffer

10 mM	Tris
1 mM	EDTA
pH 8.0	

Sample buffer

125 mM	Tris
20%	Glycerol
(10%	2-mercaptoethanol)
4%	SDS
5%	Bromophenol blue
pH 6.75	with HCl

Lysis buffer A

20 mM	Tris
100 mM	NaCl
2 mM	EDTA
0.02 µg/ml	Aprotinin
0.1 mg/ml	PMSF
pH 8.0	

Lysis buffer B

20 mM	Tris
135 mM	NaCl
2 mM	EDTA
(1mM	Na_3VO_4)
0.02 µg/ml	Aprotinin
0.1 mg/ml	PMSF
pH 7.5	

Transfer buffer

27 mM	Tris
0.2 M	Glycine
10%	Methanol
pH 8.3	

TNT

10 mM	Tris
0.1 M	NaCl
0.1%	Tween-20
pH 7.5	

ECL

100 mM	Tris
1.25 mM	Luminol
0.2 mM	p-coumaric acid
0.006%	H_2O_2
pH 8.8	

Carbonate/bicarbonate buffer

32 mM	Na_2CO_3
68 mM	$NaHCO_3$
pH 9.6	

Borate buffer

0.2 mM	$Na_2B_4O_7 \cdot 10H_2O$
pH 9.0	with H_3BO_3

Glycine buffer (pH 2.5)

0.1 mM	Glycine
pH 2.5	with HCl

Elution Buffer

0.1 mM	Glycine
150 mM	NaCl
pH 2.4	with HCl

Staining solution

0.05%	Coomassie Brilliant Blue R-250
45%	Methanol
10%	Acetic acid

Destaining solution

25%	Methanol
10%	Acetic acid

Ponceau S staining solution

0.1%	Ponceau S
5%	Acetic acid

5 Results

5.1 Generation of rat monoclonal antibodies against BMMCs membrane antigens

Monoclonal antibodies proved themselves in past as a useful and unique tool in biological research and particularly in case where they enabled identification of new important signaling molecules or unravel their unknown function (Williams et al., 1977). In our laboratory we have prepared and extensively used several monoclonal antibodies specific for membrane antigens of rat RBL cells (Hálová et al., 2002; Smrž et al., 2007; Smrž et al., 2008). Because monoclonal antibodies against membrane antigens of murine BMMCs were limited, we decided to generate new antibodies against such antigens with the aim to use them as unique tools which could potentially harbor yet unidentified role of membrane structure in mast cell activation and degranulation processes.

My contribution in this part of work was limited to selection of antibodies and thus I refer to Materials and methods section (4.11) for description of monoclonal antibodies preparation. From the palette of preselected antibodies one clone with full name 1/2H9/3D3/1A1 (later on termed as 2H9) was chosen as a potential candidate for target protein identification.

At first, binding ability of the antibody to its cell-surface target was necessary to be verified. For this purpose alive BMMCs were incubated with 30 μg/ml of 2H9 antibody isolated from cell culture media (see below) or 1000× diluted serum from BMMCs-immunized rat as a positive control. After washing the cells were probed with anti-rat-IgG-FITC secondary antibody and then analyzed by flow cytometry. Shift in fluorescence intensity in FL1 channel compared to cells probed with secondary antibody alone indicated that 2H9 antibody efficiently binds to its membrane target (Fig. 4).

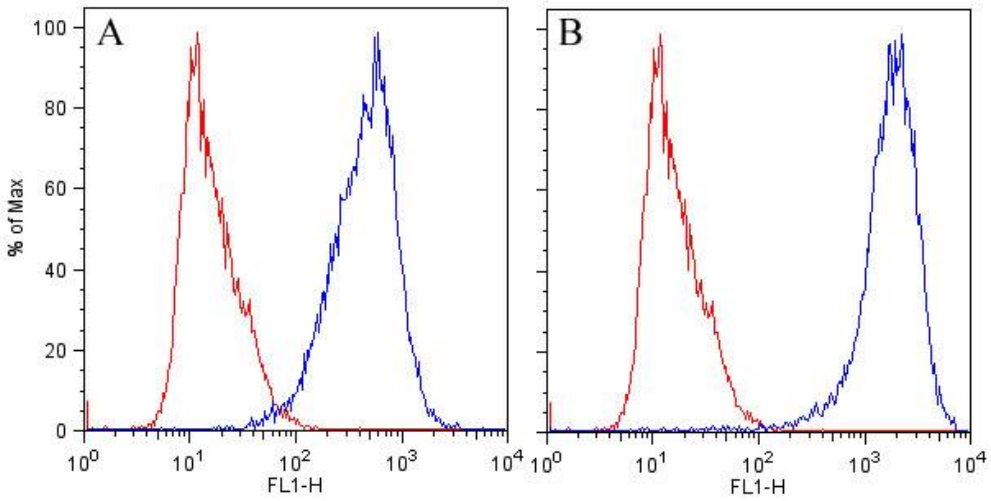

Fig. 4 – Binding of 2H9 antibody to its target protein on the surface of BMMCs analyzed by flow cytometry.

Binding efficiency of 2H9 antibody was analyzed by flow cytometry in FL1 channel. Red line represents background fluorescence of BMMCs treated only by secondary anti-rat-IgG-FITC. Blue line represents BMMCs first probed with serum from BMMC-immunized rat (A) or 2H9 antibody (B) and then stained with anti-rat-IgG-FITC secondary antibody.

Antibody was then tested for its ability to detect specific antigen on western blot. BMMCs were lysed in lysis buffer B supplemented with 1% Triton X-100 and the lysate was diluted with sample buffer (reducing or non-reducing). Amount of lysate corresponding to 6×10^5 cells per line was resolved on 12% gel by SDS-PAGE. After western blotting, membrane was probed with 1 μg/ml of 2H9 antibody and 8000× diluted anti-rat-IgG-HRP. Results in Fig. 5 show that 2H9 antibody detects single protein band of approximate molecular weight 24–25 kDa. Furthermore, detection with 2H9 antibody is less sensitive under reducing conditions, where it detects faster migrating band, compared to non-reducing conditions. This suggests that the antibody binds to a conformational epitope stabilized by one or more disulphide bonds. Based on this finding, only non-reducing sample buffer was used for SDS-PAGE in later experiments.

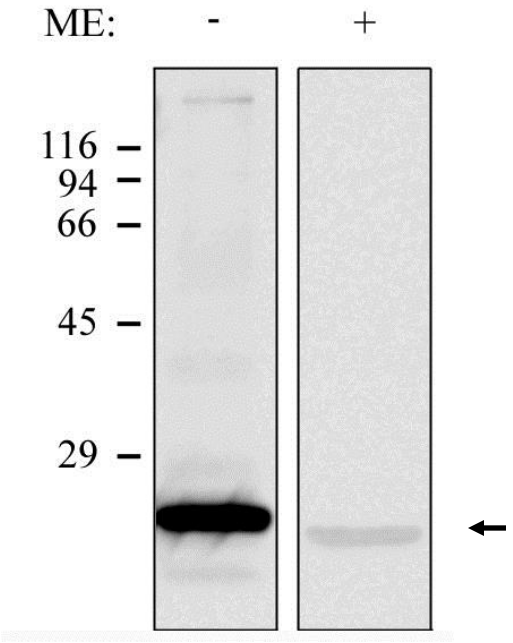

Fig. 5 – Detection of 2H9-target protein in lysate from BMMCs using SDS-PAGE and immunoblotting.

Lysates from BMMCs were diluted with sample buffer either containing(+) or not (-) 2-mercaptoethanol (ME), resolved on 12% SDS-PAGE gel and blotted onto nitrocellulose membrane. Target protein of 2H9 antibody was detected by probing the membrane with 2H9 antibody and anti-rat-IgG-HRP secondary antibody. Arrow indicates band corresponding to detected protein and numbers on the left represent position of molecular weight markers in kDa.

5.2 Tissue distribution of antibody binding partner

Information about expression profile in different tissues might be in some cases helpful in determination of antigen identity. For this purpose we prepared lysates from various organs of BALB/c strain mouse by their homogenization in organ lysis solution. Lysates from BMMCs and RBL cells were also included. According to the results from previous experiments, proteins were separated on 12% SDS-PAGE gels under non-reducing conditions and target protein was again detected as described above. Results of this experiment show that target protein is broadly expressed in various types of tissues. Inability to detect 24–25 kDa band in lysate from RBL cells implies that antibody probably recognizes epitope, which is mouse specific or target protein expression is not present in this cell line (Fig. 6).

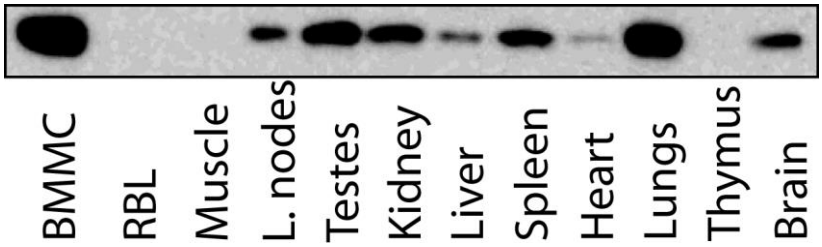

Fig. 6 – Distribution of 2H9 antibody-target protein among different tissues.

After lysing organs and cells in organ lysis solution, protein content was determined by DC protein assay and lysates containing 50 μg of proteins/line were resolved on 12% SDS-PAGE gel and transferred onto membrane by western blotting. Target protein was detected by 2H9 antibody and anti-rat-IgG-HRP secondary antibody. Comparable amount of proteins was verified by Ponceau S staining (not shown).

5.3 PI-PLC assay

Mode of anchor to the plasma membrane is another useful aspect of protein identity. Membrane proteins can exist either as integral transmembrane proteins or can be tethered to plasma membrane bilayer through glycosyl-phosphatidylinositol (GPI) anchor. To determine whether protein recognized by 2H9 antibody is transmembrane or GPI-anchored, phosphatidylinositol-specific phospholipase C (PI-PLC), which cleaves phosphoester bond between DAG and PI group, was used to cut off all proteins linked to GPI anchor.

BMMCs were incubated with PI-PLC at 37°C and then probed with 2H9 antibody and anti-rat-IgG-FITC. As a control, RBL cells were incubated under the same conditions and labeled with anti-Thy1.1 (OX7) and anti-mouse-IgG-FITC antibodies; Thy-1.1 was selected because it is known GPI-anchored protein expressed in RBL cells (Dráberová and Dráber, 1993). Cells were then analyzed by flow cytometer in FL1 channel.

Fig. 7 clearly demonstrates that in contrast to control RBL cells, BMMCs did not show decrease in overall fluorescence after PI-PLC treatment which suggests that target protein has a transmembrane domain.

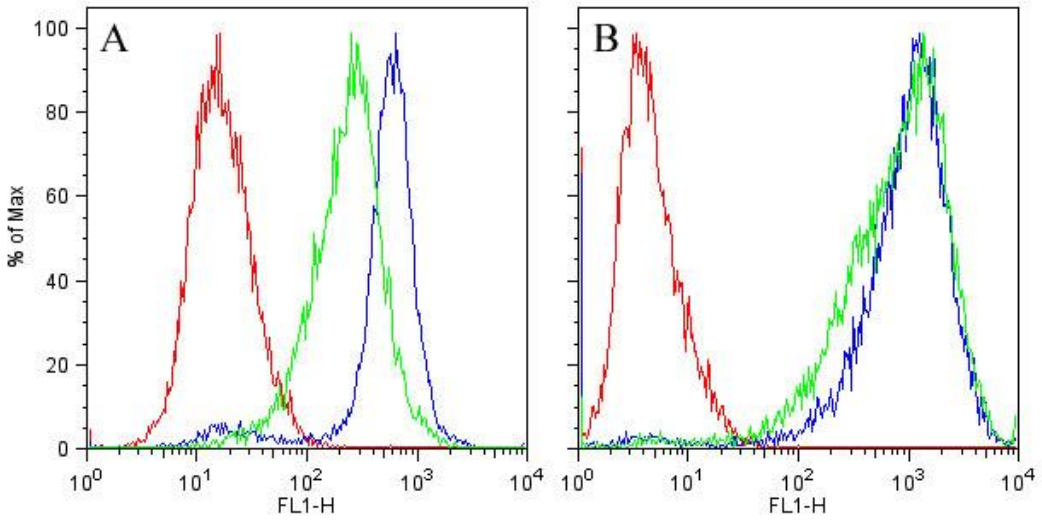

Fig. 7 – Determination of anchor mode of 2H9 antibody-target protein.

Content of GPI-anchored Thy1.1 (OX-7) protein in RBL cells (A) and 2H9 target protein in BMMCs (B) in plasma membrane after PI-PLC treatment was determined by fluorescent labeling and analysis by flow cytometry. Red line represents background fluorescence of cells with FITC-conjugated secondary antibody only. Blue line represents fluorescence of PI-PLC-non-treated and green line fluorescence of PI-PLC-treated cells probed by appropriate primary (OX-7, 2H9) and secondary FITC-conjugated antibody.

5.4 Isotype determination

Isotype of 2H9 antibody was determined with IsoStrip kit (Roche Diagnostics, IN, USA) according to manufacturer protocol. Hybridoma supernatant containing the antibody was 20× diluted in PBS and then mixed with latex beads. Isotyping strip was dipped into suspension and results were read after 10 min incubation from position of blue bands on strip. As documented in Fig. 8, 2H9 antibody is IgG_1 subtype with κ (kappa) light chain.

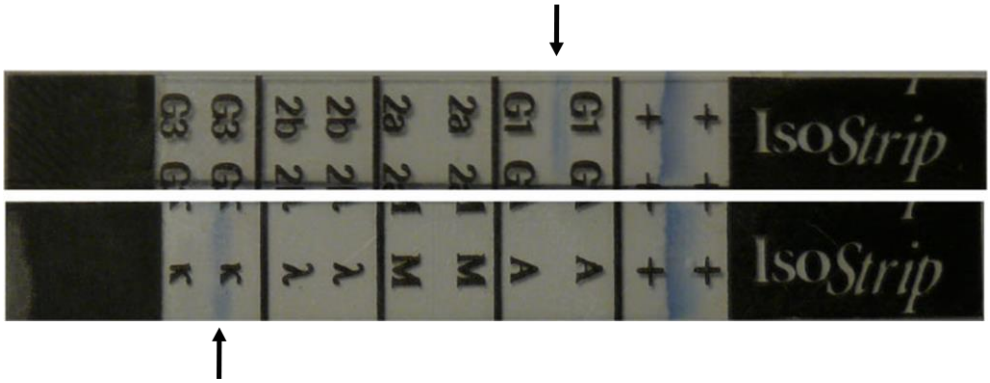

Fig. 8 – Identification of 2H9 antibody isotype.

After blue latex beads reached control area (+), strip was evaluated for 2H9 antibody isotype from position of blue bands (indicated by arrows) on strip.

5.5 Immunoprecipitation and MS analysis

Mass spectrometry provides good possibility to identify unknown protein, especially in combination with searches in peptide mass databases. However, major complication is requirement of relatively pure and concentrated protein sample. For this purpose we decided to immunoaffine purify target protein from BMMCs lysate with 2H9 antibody bound to protein G resin. To eliminate contamination of 24–25 kDa protein with similar mass immunoglobulin light-chain, antibody was covalently crosslinked to protein G using DMP. As a control for light-chain contamination, protein G resin was incubated with same amount of 2H9 antibody but not with BMMC lysate. Eluted sample was resolved on 12% SDS-PAGE and gel was stained with Coomassie Brilliant Blue R-250. Band corresponding to previously determined molecular weight was excised (Fig. 9, arrow) and analyzed with microcapillary liquid chromatography in combination with electrospray ionization tandem mass spectrometry (microHPLC-ESI-MS/MS) and matrix-assisted laser desorption/ionization Fourier transform mass spectrometry (MALDI/FTMS) by P. Pompach from the Institute of Microbiology AS CR. List of identified peptides are shown in Tab. 1 and Fig. 10. Results reveal that unknown antigen is murine CD9 protein.

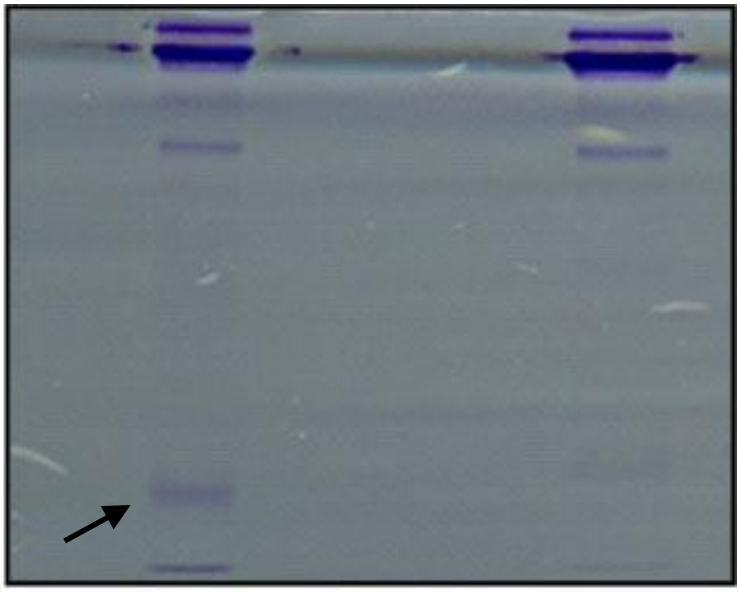

Antibody	+	+
Lysate	+	-

Fig. 9 – Isolated target protein from BMMCs lysate for MS analysis.

Two samples of protein G resin with covalently bound 2H9 antibody were either incubated or not with BMMCs lysate. After elution by heating the resin with sample buffer, samples were resolved on 12% SDS-PAGE gel and then stained with Coomassie Brilliant Blue R-250. Protein band indicated with arrow was excised and analyzed by mass spectrometry.

Identified peptides	MH+
microHPLC-ESI-MS/MS	
K.QLLESFQVK.P	1092.2
K.ELQEFYKDTYQK.L	1592.7
K.QLLESFQVKPC(+57)PEAISEVFNNK.F	2578.8
MALDI/FTMS	
ELQEFYK	956.4762
QLLESFQVK	1091.6137
ELQEFYKDTYQK	1591.7736

```
  1 MPVKGGSKCI KYLLFGFNFI FWLAGIAVLA IGLWLRFDSQ TKSIFEQENN HSSFYTGVYI
 61 LIGAGALMML VGFLGCCGAV QESQCMLGLF FGFLLVIFAI EIAAAVWGYT HKDEVIKELQ
121 EFYKDTYQKL RSKDEPQRET LKAIHMALDC CGIAGPLEQF ISDTCPKKQL LESFQVKPCP
181 EAISEVFNNK FHIIGAVGIG IAVVMIFGMI FSMILCCAIR RSREMV
```

Tab. 1 – List of successfully identified peptides by microHPLC-ESI-MS/MS and MALDI/FTMS.

Table shows sequences identified by MS analysis with mass of their appropriate MH+ ions. Their position in whole CD9 protein sequence (NCBI Reference Sequence: NP_031683.1) is marked with red letters.

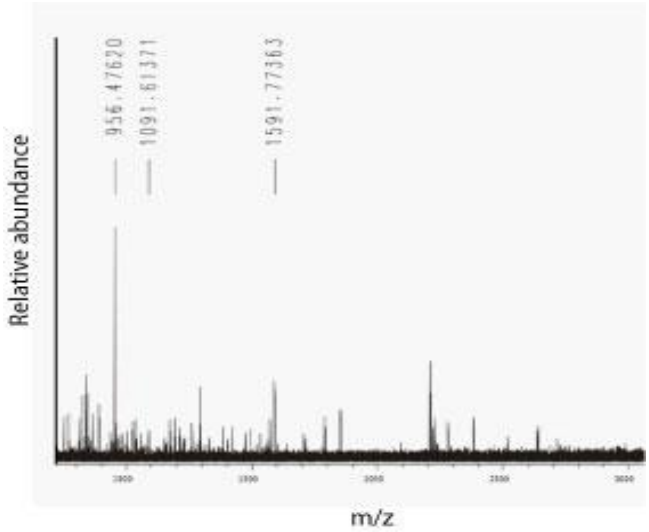

Fig. 10 – Peptide spectrum of target protein from MALDI/FTMS analysis.

Chart represents spectrum of detected peptides from trypsin digested target protein. Mass of identified peptides (MH+) and their corresponding peaks are indicated.

5.6 Cross-immunoprecipitation of CD9 protein

Previous results showed that 2H9 antibody binds to murine CD9 protein. To verify these results, CD9 protein was immunoprecipitated by both 2H9 and KMC8.8 (commercial anti-CD9 monoclonal antibody). Samples were electrophoretically separated on 12% SDS-PAGE and after western blotting, the CD9 protein was detected by either 2H9 (1000×) or KMC8.8 (1000×) and anti-rat-IgG-HRP (8000×) secondary antibodies.

Results in the Fig. 11 show that both antibodies immunoprecipitate single band of the same weight which can be detected on western blot by both antibodies. Therefore we conclude that our monoclonal antibody 2H9 indeed binds to extracellular part of CD9 protein.

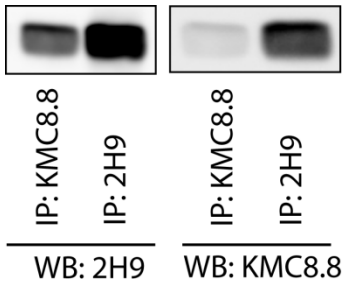

Fig. 11 – Cross-immunoprecipitation of CD9 protein by 2H9 and KMC8.8 antibodies.
BMMCs were lysed in lysis buffer A supplemented with 1% Triton X-100 and used for immunoprecipitation of CD9 by 2H9 and KMC8.8 antibodies bound to protein G resin. Samples were separated on 12% SDS-PAGE gel, western blotted onto nitrocellulose membrane and detected by either 2H9 or KMC8.8 antibody.

5.7 Degranulation of anti-CD9 treated BMMCs

5.7.1 Concentration dependence and time course

Tetraspanin proteins have been studied for considerably long time. Many experiments, in which antibodies against various tetraspanin members were used, showed effects on various aspects of cellular physiology and behavior (Higginbottom et al., 2000b; Qi et al., 1996; Tanio et al., 1999). We therefore decided to use our new monoclonal anti-CD9 antibody (2H9) for studies on possible roles of CD9 protein in mast cell physiology.

IgE sensitized BMMCs were first incubated in BSS-BSA supplemented with various concentrations of anti-CD9 antibody (2H9) for 15 min. Unbound antibody was washed out and the cells were activated with antigen (TNP-BSA; 0.5 μg/ml) for the indicated time. In case of time zero

of activation, no antigen was added. Activation of the cells was determined by amount of β-glucuronidase released from intracellular granules using β-glucuronidase assay.

Data from Fig. 12 show that binding of anti-CD9 antibody to BMMCs surface caused significant inhibition of antigen-mediated degranulation at all time points and this inhibition was antibody-concentration dependent. Moreover, binding of anti-CD9 antibody itself (0 min) triggered BMMCs degranulation in the absence of antigen.

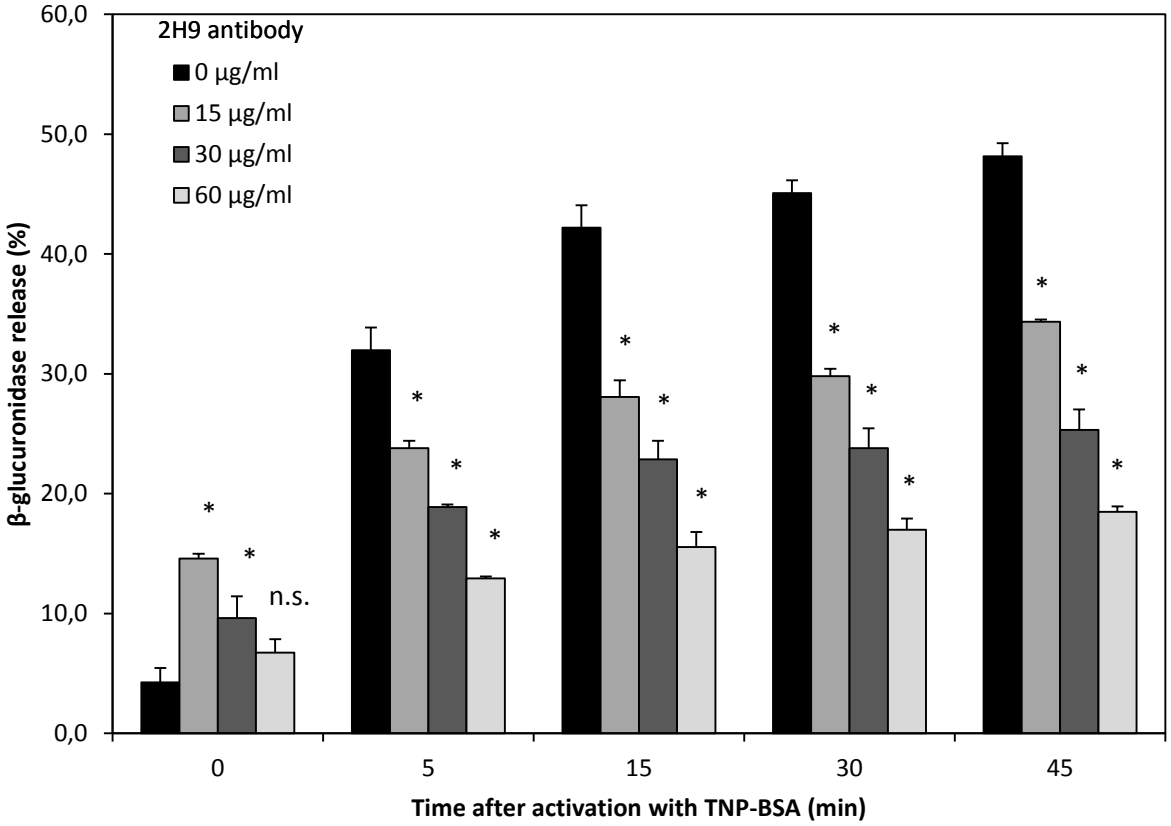

Fig. 12 – Comparison of BMMCs degranulation pretreated with different 2H9 concentration at different time-points after activation.

BMMCs sensitized with TNP-specific IgE were incubated for 15 min with the indicated 2H9 concentrations of antibody and then activated for specified time with 0.5 µg/ml of TNP-BSA. Extent of degranulation was estimated by amount of β-glucuronidase released to supernatant. Data are presented as mean ± SD of one experiment performed in triplicate of three similar experiments. Statistical significance of differences between antibody treated (15–16 µg/ml) and non-treated (0 µg/ml). (, P<0.05)*

5.7.2 Influence of other monoclonal antibodies

Previous experiment showed that our monoclonal anti-CD9 antibody causes inhibition of antigen-mediated BMMCs degranulation when bound to CD9 on cell surface. Next we analyzed whether this effect is restricted to 2H9 antibody or is a broader phenomena shared among other available antibodies and reflecting CD9 aggregation.

For this purpose we preincubated BMMCs as previous with 2H9 antibody or one of two commercially available antibodies against CD9 – KMC8.8 and N-19. As a control, cells were preincubated with antibody (anti-CD48) of the same isotype as 2H9 antibody. Cells were then activated with TNP-BSA (0.5 μg/ml) for 30 min and extent of degranulation was assessed by β-glucuronidase assay.

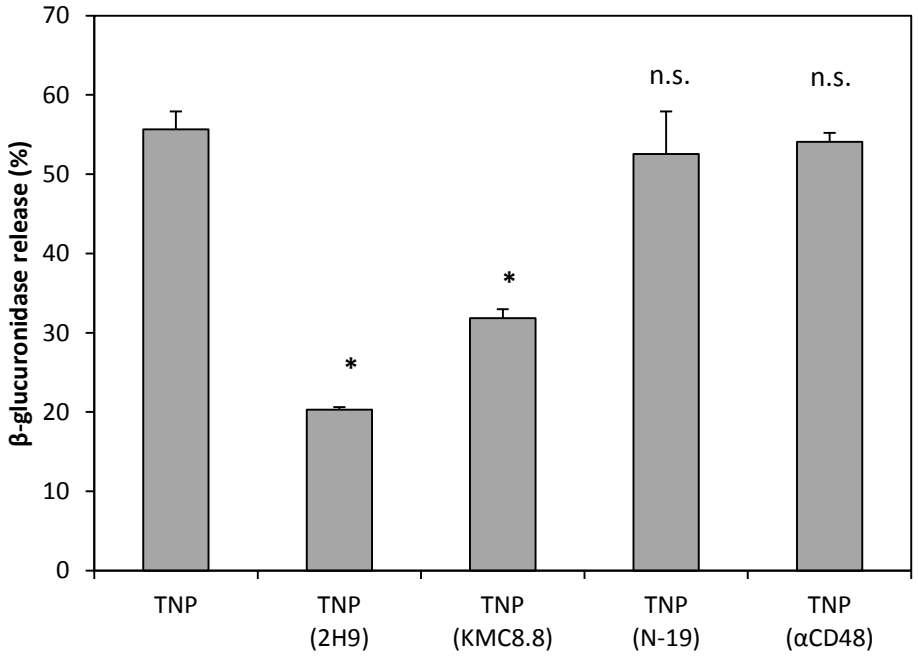

Fig. 13 – Degranulation of BMMCs preincubated with different antibodies.
BMMCs were preincubated with 30 μg/ml of anti-CD9 antibodies (2H9, KMC8.8, N-19) and anti-CD48 (αCD48) antibody. Cells were then activated with 0.5 μg/ml of TNP-BSA (TNP). Extent of degranulation was estimated by amount of β-glucuronidase released to supernatant. Data are presented as mean ± SD of one experiment performed in triplicate of two similar experiments. Statistical significance was determined between non-treated control (TNP) and antibody-treated samples. (, P<0.05)*

Results in Fig. 13 clearly demonstrate that inhibition of degranulation is present even in case when other commercially available antibody KMC8.8 is used. As expected, antibody used as

isotype control (anti-CD48) did not cause any significant change in extent of degranulation. Surprisingly, another commercially available anti-CD9 antibody N-19 did not inflict impairment of degranulation response. Therefore we next verified ability of each antibody to bind to their appropriate ligand on BMMC surface by flow cytometry analysis. BMMCs were probed with the tested antibodies (30 μg/ml), then labeled with 300× diluted secondary anti-rat-IgG-FITC or anti-goat-IgG-Cy3 and analyzed in FL1 and FL2 channel respectively.

As it is shown in Fig. 14, all antibodies except N-19 bind to their target protein on surface of BMMCs.

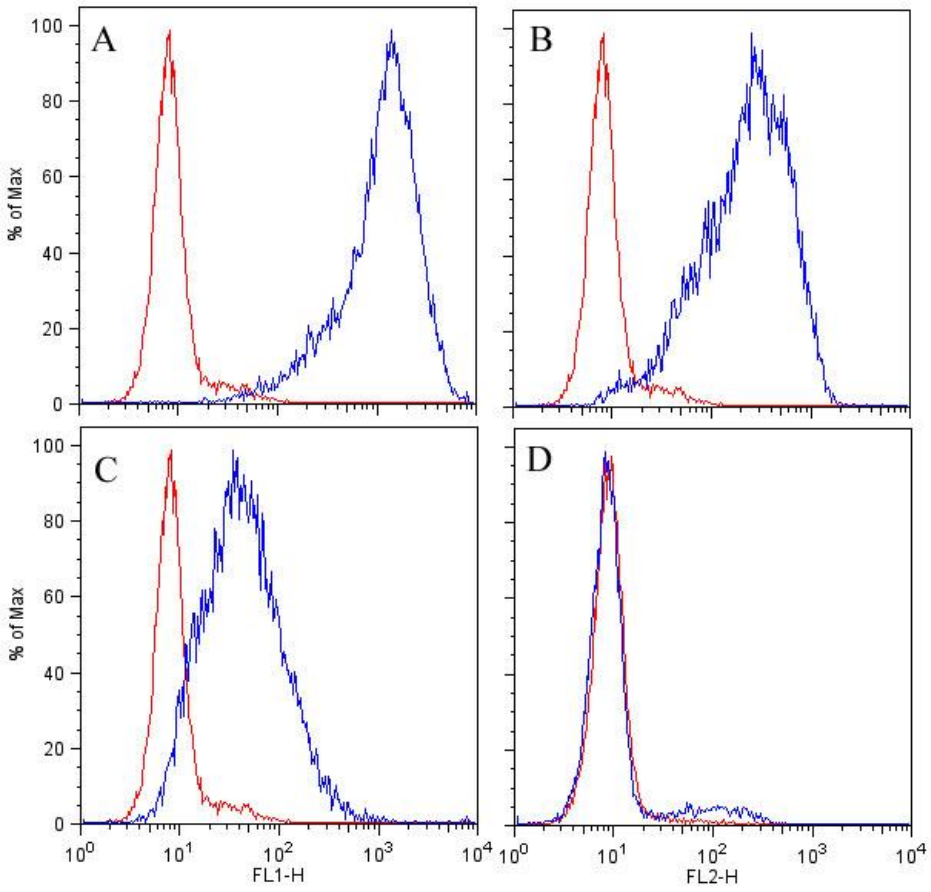

Fig. 14 – Verification of ability of antibodies to bind their target structures on BMMCs surface.

Ability of antibodies to bind their target proteins was determined after staining with appropriate fluorescent secondary antibody by flow cytometry analysis. Red line represents background fluorescence of cells incubated with secondary antibody only. Blue line represents fluorescence of cells probed with 2H9 (A), KMC8.8 (B), anti-CD48 (C) and N-19 (D) antibody and stained with anti-rat-IgG-FITC (A, B, C) or anti-goat-IgG-Cy3 (D) secondary antibody.

5.7.3 Effect of secondary antibody

Effect of anti-CD9 antibody on antigen-mediated degranulation might be inflicted by different mechanisms. One of them may be forced aggregation of otherwise distinctly located CD9 molecules by molecule of immunoglobulin. We therefore wanted to verify if this effect can be further strengthened by additional clustering with polyclonal antibody against rat IgG immunoglobulins. For this purpose BMMCs were first incubated with anti-CD9 antibody (30 μg/ml) for 20 min, washed with BSS-BSA and then incubated with anti-rat polyclonal antibody (10 μl/ml) for another 20 min. Cells were then activated as previous.

Results of this experiment show that additional aggregation of CD9 by anti-rat polyclonal antibody doesn't have any further effect on extent of BMMCs degranulation.

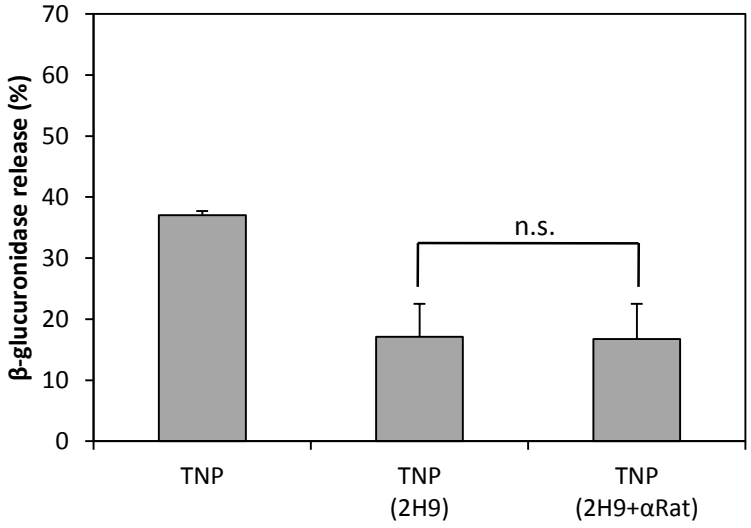

Fig. 15 – Effect of secondary antibody on 2H9-mediated BMMCs degranulation.
Cells were preincubated with anti-CD9 antibody (2H9) alone or with anti-CD9 followed by anti-rat-IgG incubation (2H9+αRat). Cells were then challenged with antigen (TNP-BSA, TNP) and amount β-glucuronidase in supernatant was estimated. Data are presented as mean ± SD of one experiment performed in triplicate of two similar experiments. (n.s., P>0.05)

5.7.4 Effect of IgE sensitization

Previous study concerning effects of anti-CD9 antibody on RBL cells transfected with human CD9 reported that these effects originated mainly from binding of anti-CD9 antibody to FcεRI receptor and thus cross-linking it to CD9 proteins (Higginbottom et al., 2000b). To exclude this possibility, we conducted experiment in which BMMCs were sensitized with different

concentrations of IgE and then incubated in mixture of anti-CD9 antibody (30 μg/ml) with appropriate concentration of IgE. Cells were then washed to remove unbound IgE and activated by TNP-BSA.

Result of this experiment suggests that co-clustering of CD9 with FcεRI does not play role in anti-CD9-mediated inhibition of degranulation in BMMCs because extent of inhibition was the same throughout all IgE concentrations as it may be seen in Fig. 16.

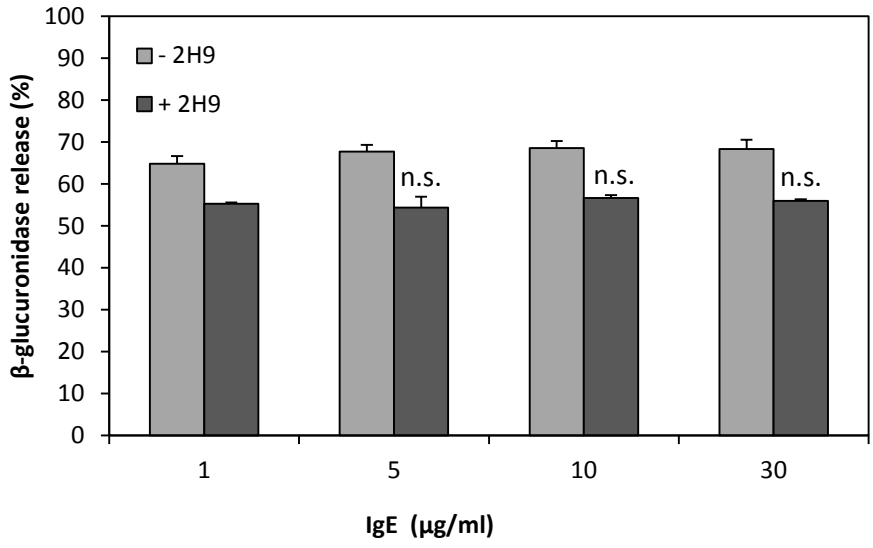

Fig. 16 – Degranulation of BMMCs preincubated with anti-CD9 antibody in the presence of various concentrations of IgE.

Sensitized BMMCs were incubated with mixture of 30 μg/ml 2H9 antibody and the indicated concentration of IgE. After brief wash, cells were activated with 0.5 μg/ml of TNP-BSA and extent of degranulation was measured by β-glucuronidase assay. Data are presented as mean ± SD of one experiment performed in triplicate of two similar experiments. Statistical significance was determined between control amount of IgE (1 μg/ml) and increased concentration of IgE (5, 10, 30 μg/ml) in presence of 2H9 antibody. (n.s., P>0.05)

5.8 BMMC degranulation induced by CD9 aggregation

5.8.1 Comparison with other monoclonal antibodies

Next we decided to look closer on degranulation elicited by antibody itself (see Fig. 12 at 0 min). Again, we tested whether this effect is restricted to our 2H9 antibody or it is induced also by other anti-CD9 antibodies. The cells were subjected to 30 μg/ml of 2H9, KMC8.8 or anti-CD48

antibody as isotype control for 30 min and then assayed for a degranulation. N-19 antibody was excluded from this experiment due to its inability to bind CD9 on BMMCs (see Fig. 14).

Fig. 17 shows that BMMCs degranulated in response to KMC8.8 antibody treatment, although to lesser extent than in case when 2H9 antibody was used. Degranulation caused by isotype control was almost on same level as in non-activated control.

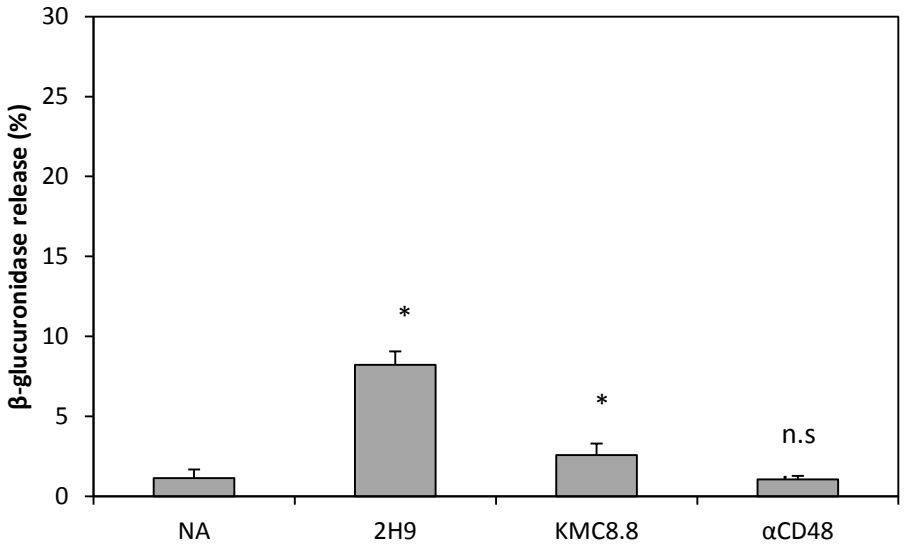

Fig. 17 – Degranulation triggered by anti-CD9 antibodies.

Non-sensitized cells were incubated for 15 min with 30 μg/ml of various anti-CD9 antibodies (2H9, KMC8.8) or anti-CD48 antibody (αCD48) and supernatant was examined for β-glucuronidase content. Data are presented as mean ± SD of one experiment performed in triplicate of three similar experiments. Statistical significance was determined between non-activated control (NA) and antibody-treated samples. (, P<0.05)*

5.8.2 Concentration dependence

To estimate relationship between concentration of antibody and rate of degranulation inflicted by its binding to CD9, non-sensitized BMMCs were exposed to different concentrations of 2H9 antibody for 15 min. Supernatant was then immediately assayed using β-glucuronidase assay.

Data in Fig. 18 show that antibody triggers degranulation at relatively low concentrations (100 ng/ml) and its maximal effect is at concentration 1 μg/ml after which BMMCs degranulation slowly declines.

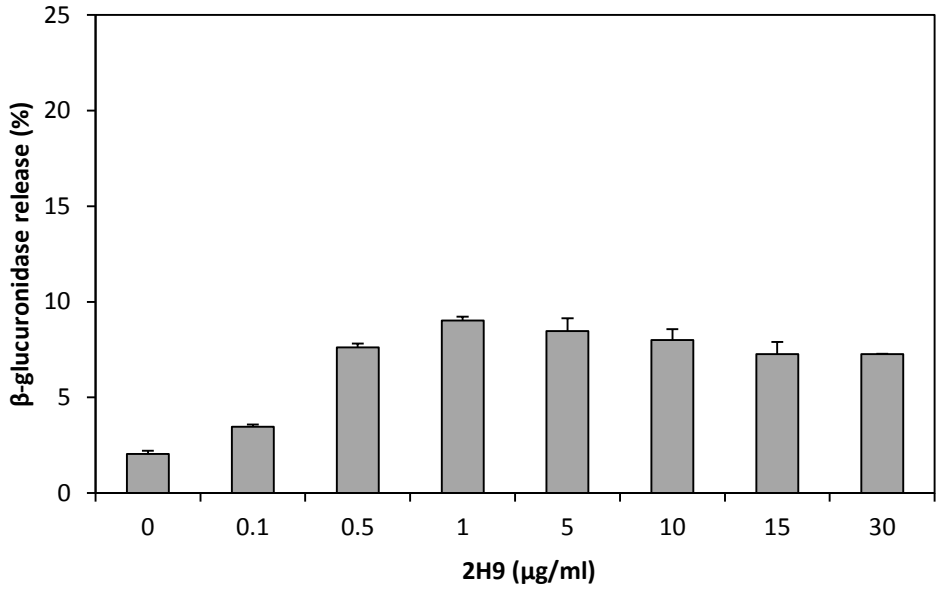

Fig. 18 – Degranulation of BMMCs in response to different concentrations of 2H9.
Non-sensitized cells were incubated for 15 min with the indicated concentration of 2H9 antibody. Extent of degranulation was estimated by amount of β-glucuronidase released to supernatant. Data are presented as mean ± SD of one experiment performed in triplicate.

5.8.3 CD9 and FcεRI co-clustering

Next, we wanted to know whether this direct effect of anti-CD9 antibody is caused by co-clustering of FcεRI receptor with CD9. Both sensitized and non-sensitized cells were subjected to 30 µg/ml of 2H9 antibody for different time intervals. Extent of degranulation was determined by presence of β-glucuronidase in supernatant.

No difference between sensitized and non-sensitized cells was observed as seen in Fig. 19 suggesting that cross-linking of FcεRI receptor with CD9 does not play role in this process. Moreover, kinetics of antibody-mediated degranulation is fast as determined from Fig. 19, since at 30 s after treatment degranulation almost reaches maximal response.

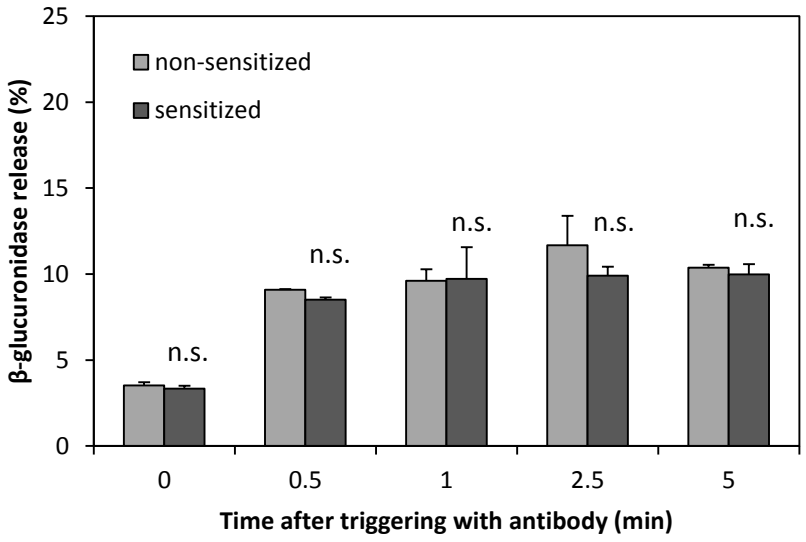

Fig. 19 – Comparison of 2H9-mediated degranulation between sensitized and non-sensitized cells.

Both sensitized and non-sensitized cells were challenged with 30 µg/ml of 2H9 antibody for indicated time. At 0 min, no 2H9 antibody was added. Data are presented as mean ± SD of one experiment performed in triplicate of two similar experiments. Statistical significance was determined between non-sensitized and sensitized cells at each time point. (n.s., P>0.05)

5.9 Binding of fluorescently labeled TNP-BSA to FcεRI receptor

One can think of another possibility which could explain inhibition of antigen-mediated degranulation by anti-CD9 antibodies. Because CD9 is relatively high abundant on cell surface (Hemler, 2005), extensive binding of anti-CD9 antibodies might physically interfere with TNP binding to IgE-loaded FcεRI receptor. This could lead to less receptor cross-linking, resulting in lesser degree of activation and degranulation.

In order to exclude this possibility, we decided to determine extent to which TNP-BSA binds to sensitized BMMCs when probed with anti-CD9 antibodies. TNP-BSA was fluorescently labeled with TRITC (see 4.8) which enabled us to detect its presence on cell surface. Sensitized cells were probed with increasing concentration of 2H9 antibody followed by addition of TNP-BSA-TRITC (0.5 µg/ml). After washing away unbound TNP-BSA-TRITC, cells were analyzed on LSRII flow cytometer using 561 nm excitation, 575/15 filter and 565 low-pass dichroic mirror configuration.

Results of this experiment show that TNP-TRITC binds to IgE-loaded FcεRI receptor to the same extent regardless of 2H9 concentration used. Furthermore this binding is always identical to binding to cells non-treated with 2H9 antibody (Fig. 20).

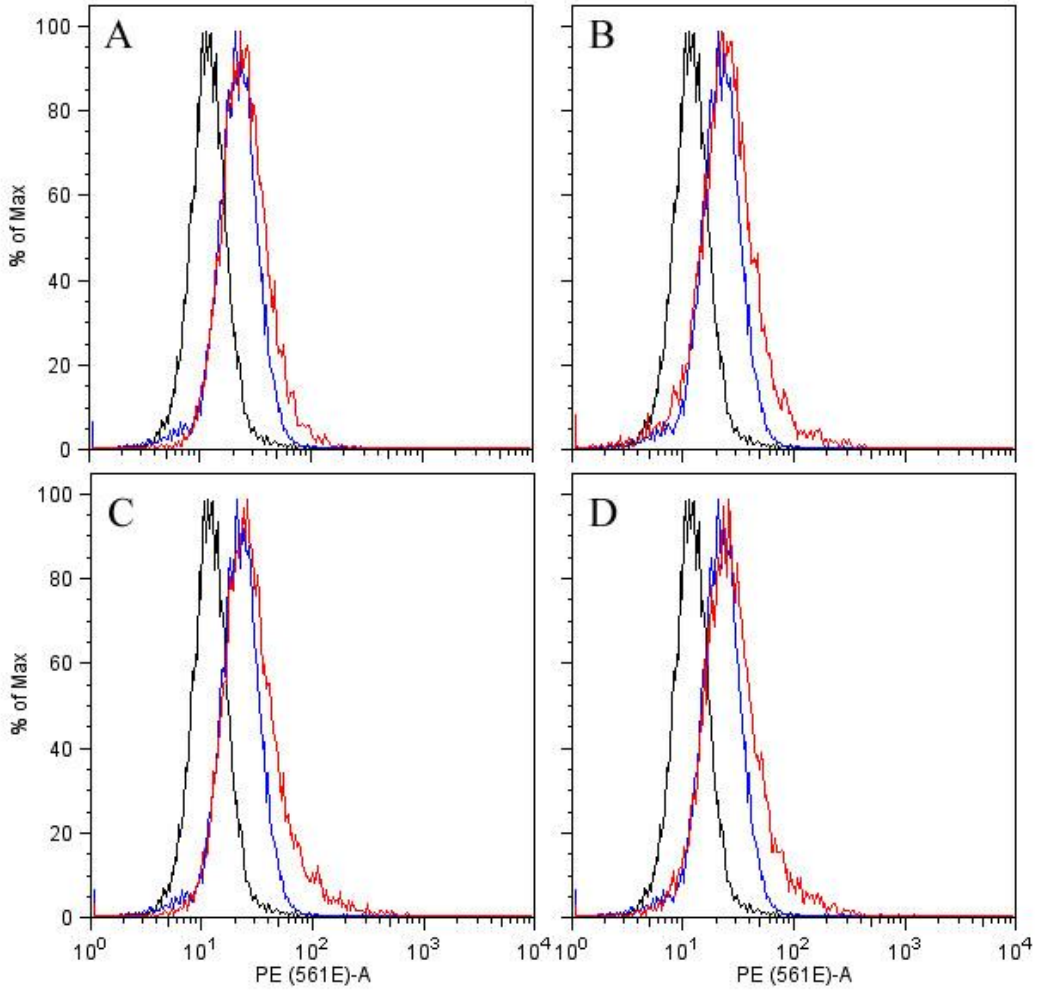

Fig. 20 – Level of TNP-BSA-TRITC binding to surface of BMMCs pretreated with different 2H9 concentrations.

Black line represents background fluorescence of non-sensitized BMMCs incubated with TNP-BSA-TRITC. In all charts, binding of TNP-BSA-TRITC to sensitized BMMCs is compared between cells preincubated with 0 µg/ml of 2H9 antibody (blue line) and cells preincubated with increasing concentration of 2H9 antibody (red line) – 1 µg/ml (A), 10 µg/ml (B), 30 µg/ml (C), 60 µg/ml (D).

5.10 Calcium release of cells treated with anti-CD9 antibody

5.10.1 Response induced by TNP and aggregation of CD9

Results from our experiments revealed that binding of anti-CD9 antibodies to CD9 on BMMCs surface causes low-level degranulation. Moreover, if subsequently these cells are activated via FcεRI receptor their degranulation response is lower compared to cells non-treated with anti-CD9 antibodies. One of the key steps in mast cell activation is release of calcium stored in ER to cytosol followed by influx of extracellular calcium ions. This rise of intracellular calcium in combination with other signaling events then leads to release of secretory granules content (Gilfillan and Tkaczyk, 2006). It is therefore essential to examine whether calcium response is also altered in cells exposed to anti-CD9 antibodies.

Sensitized BMMCs were first loaded with Fura-2 which is widely used fluorescent calcium reporter dye. After washing the cells, their calcium response was measured with or without pretreatment with 2H9 antibody followed by TNP-BSA. Fig. 21 shows that addition of 2H9 antibody by itself triggers calcium release which corresponds to previously observed effect on degranulation (Fig. 12 at 0 min). After subsequent TNP-BSA addition, calcium response of these cells is impaired compared to control cells without earlier 2H9 stimulation which again corresponds to previously observed results (Fig. 12 later time points).

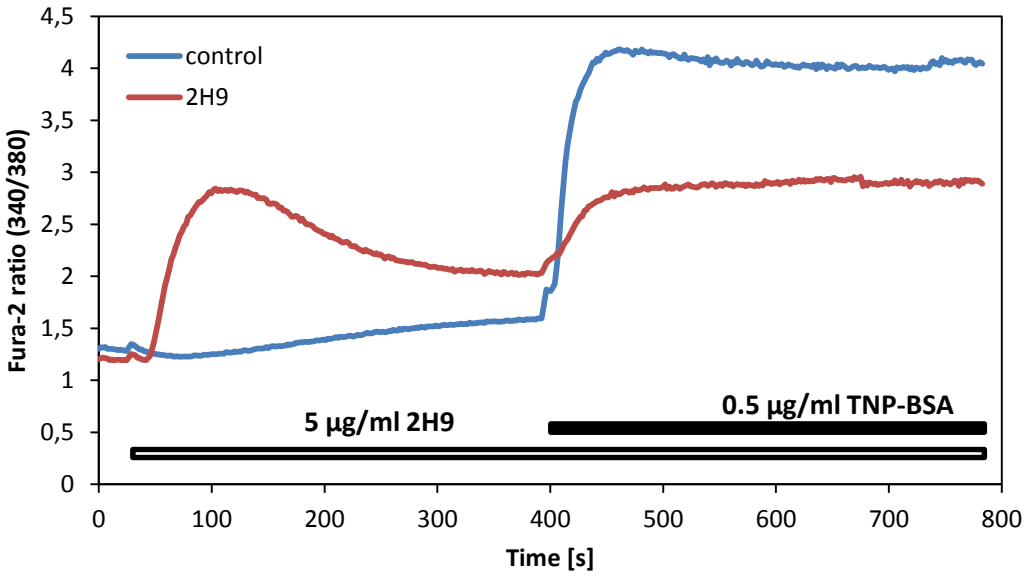

Fig. 21 – Calcium response after consequent 2H9 and TNP-BSA addition.

Calcium mobilization of Fura-2 loaded cells was measured on Infinite 200M plate reader. Cells were first triggered by 2H9 antibody followed by TNP-BSA triggering. Calcium level is expressed as ratio of emission with excitation at 340 nm and 380 nm. Curves represent mean of three experiments.

5.10.2 Effect of antibodies and serum pretreatment on TNP-induced calcium response

Mast cells along with FcεRI receptor express also several types of Fcγ receptors which contains activation ITAM or inhibitory ITIM motifs in their cytosolic part and thus can influence mast cell activation in either positive or negative way (Tkaczyk et al., 2004). To rule out involvement of these receptors in anti-CD9 antibody-mediated effects, BMMCs loaded with Fura-2 were incubated with IgG antibodies isolated from normal rat serum to block all Fcγ receptors. Cells were then probed with anti-CD9 antibodies or anti-CD48 antibody as isotype control and their calcium levels after triggering were measured by TNP-BSA.

Fig. 22 demonstrates that both 2H9 and KMC8.8 antibodies inhibit antigen-mediated calcium response compared to non-treated and isotype controls. These results also suggest that anti-CD9-mediated inhibition of degranulation and calcium release is not dependent on Fcγ receptors.

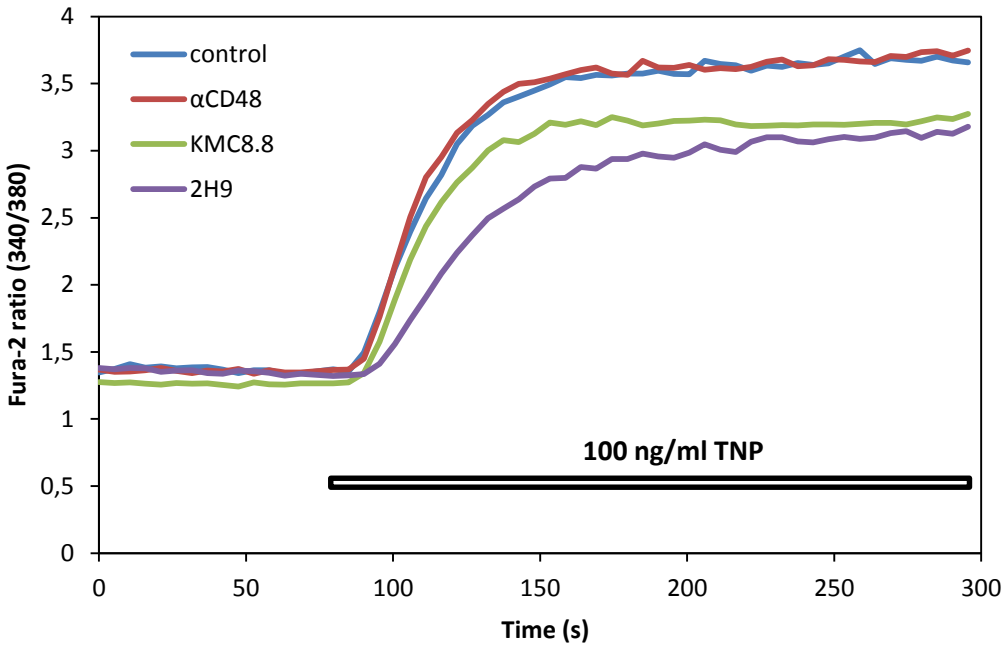

Fig. 22 – Effect of BMMCs co-incubation with serum IgGs and different antibodies on antigen-mediated calcium response.

Calcium mobilization of Fura-2 loaded cells was measured on Infinite 200M plate reader. Cells were first coincubated with normal rat serum IgGs together with anti-CD9 antibodies (2H9, KMC8.8) or anti-CD48 antibody (αCD48) and then triggered by TNP-BSA. Calcium level is expressed as ratio of emission with excitation at 340 nm and 380 nm. Curves represent mean of three experiments.

5.10.3 Role of CD9 aggregation in ER calcium release and influx of calcium

To investigate detailed features of intracellular calcium signal in the context of anti-CD9 antibodies effect, it is necessary to distinguish between initial release of calcium from ER and consequent influx of calcium ions from extracellular space. This is possible by activating cells in calcium-free environment which prevents entry of extracellular calcium and therefore only ions from ER are released to the cytosol. When are ER stores depleted, calcium channels in the plasma membrane consisting of Orai subunits became opened due to action of ER calcium sensor STIM 1 (Vig and Kinet, 2009). Restoring levels of extracellular calcium then leads to immediate influx of calcium to cytosol from extracellular space.

Firstly, we examined antibody-mediated inhibition of calcium response after triggering by TNP-BSA. Sensitized and Fura-2 loaded cells were either incubated or not with 2H9 antibody for 15 min

and then triggered by TNP-BSA in the absence of extracellular calcium. This was followed by addition of calcium to restore its level.

Results reveal that 2H9 antibody-treated cells release calcium from their ER in slightly lower extent and, interestingly, this release lags behind one present in non-treated cells. Subsequent calcium influx measured after calcium addition was also lower in 2H9-treated cells (Fig. 23).

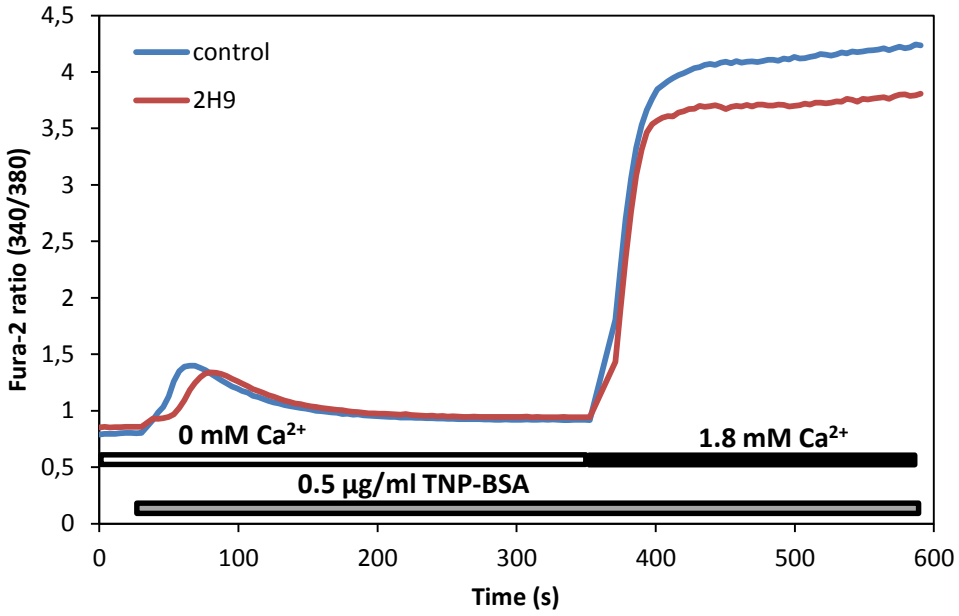

Fig. 23 – Effect of 2H9 on antigen-mediated calcium release from ER and calcium influx. *Calcium mobilization of Fura-2 loaded cells was measured on Infinite 200M plate reader. Cells were first preincubated with 2H9 antibody and then triggered by TNP-BSA in calcium-free environment. Calcium content was then restored to 1.8 mM. Calcium level is expressed as ratio of emission with excitation at 340 nm and 380 nm. Curves represent mean of three experiments.*

Next we analyzed activation of the cells mediated by antibody itself. For this purpose, Fura-2 loaded cells were challenged or not with 2H9 antibody in the absence of extracellular calcium, followed by its addition. Fig. 24 shows that binding of 2H9 antibody to cell surface causes release of calcium from intracellular stores with subsequent influx from extracellular space compared to background level of control cells.

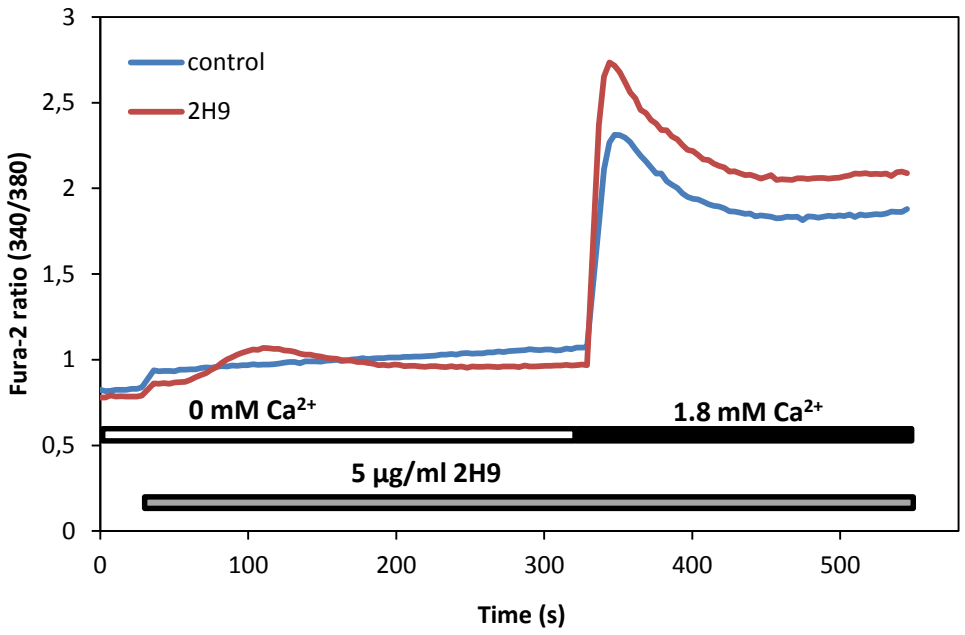

Fig. 24 – 2H9-mediated calcium influx and calcium release from ER.

Calcium mobilization of Fura-2 loaded cells was measured on Infinite 200M plate reader. Cells were first triggered by 2H9 antibody in calcium-free environment followed by calcium addition. Calcium level is expressed as ratio of emission with excitation at 340 nm and 380 nm. Curves represent mean of three experiments.

5.10.4 Thapsigargin-induced calcium release

Results in Fig. 23 demonstrate that 2H9 antibody alters both phases of calcium mobilization. To finally distinguish whether antibodies against CD9 modulate first or second part of calcium response, we decided to use thapsigargin. Thapsigargin is a drug produced by plant *Thapsia garganica* and acts as a potent inhibitor of Ca^{2+} ATPase in ER membrane and thus preventing them from refueling ER calcium stores. This leads to triggering of calcium influx even when cells are not being activated through membrane receptors, which means that all proximal signaling events are skipped.

In this experiment cells were again loaded with Fura-2 and incubated with 2H9 antibody for 15 min. Intracellular calcium levels were measured after addition of thapsigargin (0.5 µM) in the absence of extracellular calcium. Levels of extracellular calcium were restored by its addition.

Data shown in Fig. 25 demonstrate that both 2H9-treated and non-treated cells release calcium after thapsigargin administration to the same extent. This suggests that anti-CD9 antibody act upstream or at level of calcium release from ER.

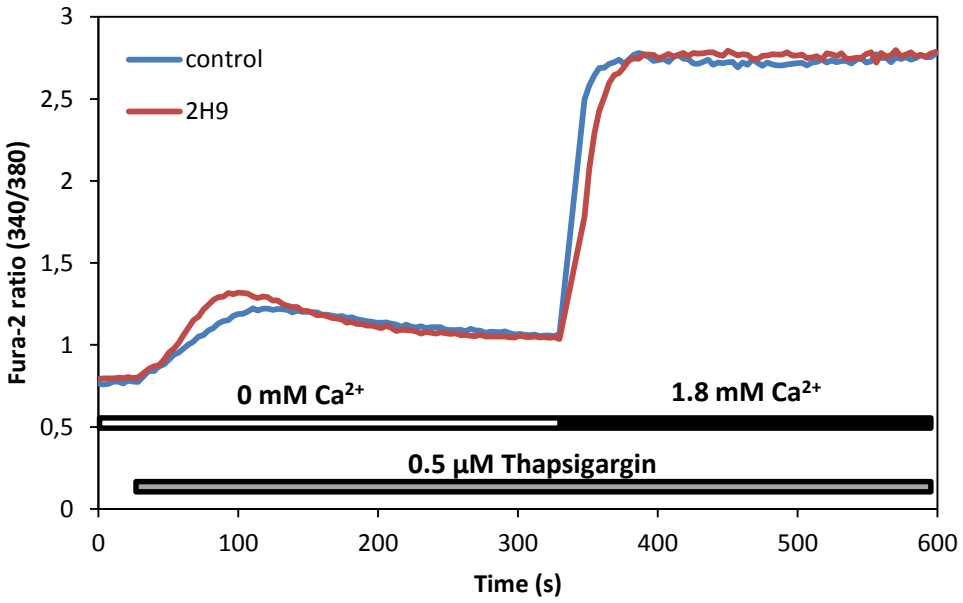

Fig. 25 – Effect of 2H9 on thapsigargin-mediated calcium release from ER and calcium influx. *Calcium mobilization of Fura-2 loaded cells was measured on Infinite 200M plate reader. Cells were first preincubated with 2H9 antibody and then triggered by thapsigargin in calcium-free environment. Calcium content was then restored to 1.8 mM. Calcium level is expressed as ratio of emission with excitation at 340 nm and 380 nm. Curves represent mean of three experiments.*

Effects of 2H9 antibody on BMMCs degranulation induced by thapsigargin were also tested. Cells preincubated with 2H9 antibody were subjected to 0.5 µM thapsigargin for 30 min and the extent of degranulation was assessed by β-glucuronidase assay.

Results of this experiment confirm the results of previous experiment that 2H9 antibody does not have effect on activation via thapsigargin route and thus it has to act upstream of calcium response (Fig. 26).

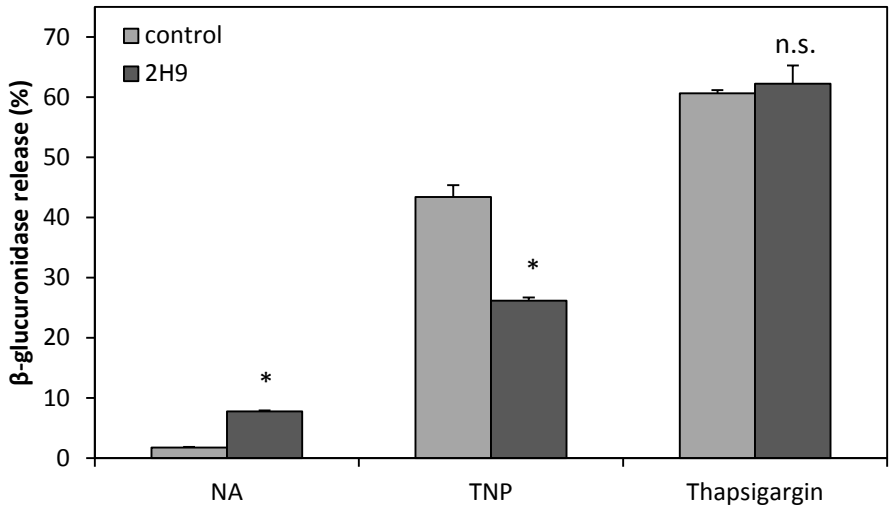

Fig. 26 – Effect of 2H9 antibody on thapsigargin-induced degranulation of BMMCs.
BMMCs were preincubated with 30 μg/ml of anti-CD9 antibody (2H9). Cells were then activated with 0.5 μg/ml of TNP-BSA (TNP) or 0.5 μM thapsigargin or were left non-activated (NA). Extent of degranulation was estimated by amount of β-glucuronidase released to supernatant. Data are presented as mean ± SD of one experiment performed in triplicate of three similar experiments. Statistical significance was determined between non-treated controls and 2H9-treated samples. (, P<0.05)*

5.11 Phosphorylation time course

To determine which signaling molecules acting upstream of calcium release might be involved in 2H9-mediated effects, sensitized BMMCs were either incubated or not with 2H9 antibody and activated for different time with TNP-BSA. Cells were then lysed in lysis buffer B supplemented with detergent (1% NP-40 and 1% lauryl maltoside) and an inhibitor of protein tyrosine phosphatases sodium orthovanadate. Samples were boiled in non-reducing sample buffer and resolved on 10% SDS-PAGE gel. After western blotting, tyrosine phosphorylation was detected by probing membrane with anti-phosphotyrosine antibody (PY20) and anti-phosphoPLCγ1 with combination. Immunostaining of actin was used as loading control.

Fig. 27 shows that many proteins including those with molecular weight of LAT, NTAL and PLCγ1 are phosphorylated in BMMCs pretreated with 2H9 at 0 min time point. In contrast, all these proteins are less phosphorylated at later time points. This however correlates with previously obtained results of degranulation and calcium release.

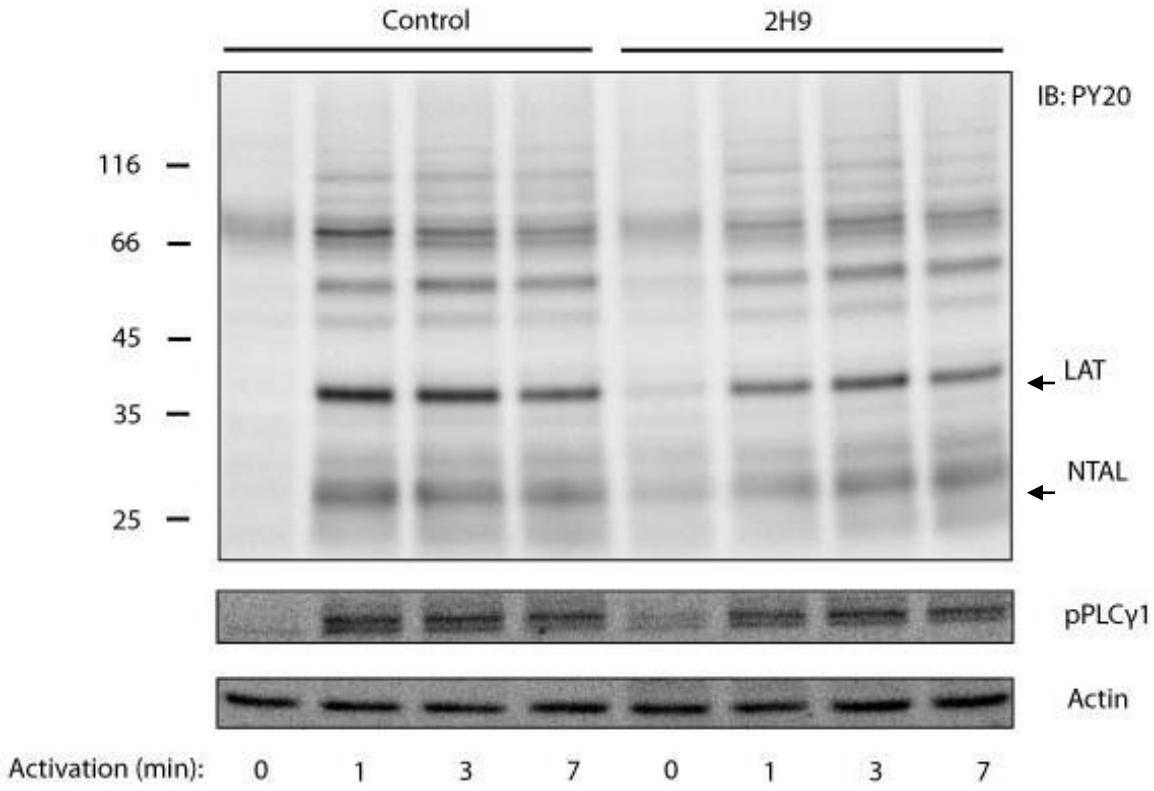

Fig. 27 – Differences in tyrosine phosphorylation in BMMCs triggered by antigen caused by 2H9 antibody pretreatment.

Sensitized BMMCs preincubated with 30 μg/ml of anti-CD9 antibody (2H9) were compared to cells without preincubation (control) at different time of activation by TNP-BSA (30 μg/ml).Whole tyrosine phosphorylation was detected by anti-phosphotyrosine (PY20) antibody (5000×). Arrows mark bands with molecular weight corresponding to LAT and NTAL proteins. Phosphorylation status of PLCγ1 (pPLCγ1) was detected by anti-phosphoPLCγ1 antibody (500×) in combination with anti-rabbit-IgG-HRP secondary antibody (10,000×). Actin, which served as loading control, was detected by anti-actin antibody (1000×) and anti-mouse-IgG-HRP (10,000×).

5.12 Analysis of cells with decreased or enhanced CD9 expression

5.12.1 Generation of CD9 knockdown and overexpressing cells

Technique of gene silencing is now commonly used method which enables to discover function of cellular proteins by analyzing phenotypes resulting from their lowered expression. It is also a powerful tool for verifying results obtained by different methods. We therefore proceeded to generation of BMMCs with altered levels of CD9 protein – either downregulated (CD9KD) or

upregulated (CD9OE). To do so, lentiviral system (Open biosystems) which provides easy and stable transfection of primary cells was used. This system is based on infection of cells with replication-deficient form of lentivirus carrying gene of interest or sequence for short hairpin ribonucleic acid (shRNA) under strong CMV promoter. Vector for CD9 overexpression (pCDH/CD9) was constructed by subcloning CD9 cDNA from pYX-Asc vector to lentiviral expression vector pCDH. For detailed procedure overview see 4.7 in materials and methods.

In order to verify effectiveness of overexpression and silencing, intact cells were probed with anti-CD9 antibody (2H9; 100×) and fluorescent secondary anti-rat-IgG-FITC antibody (300×) and analyzed on flow cytometer. Furthermore, to determine total protein level, cell lysates (lysis buffer B supplemented with 1% NP-40 and 1% Lauryl maltoside) were resolved on 12% polyacrylamide gel and blotted to nitrocellulose membranes. Membranes were then probed with 2H9 antibody (1000×) and anti-actin antibody (1000×), used as a loading control and then with secondary antibodies anti-rat-IgG-HRP (8000×) and anti-mouse-IgG-HRP (10,000×) respectively.

Fig. 28 shows that the lowest total CD9 expression is in cells infected with vector construct TRCN0000066393 (93) while expression in non-silencing control (non-siRNA) remains identical to non-infected (NI) cells. It also appears that level of CD9 protein is increased in cells infected with pCDH/CD9 vector (CD9OE). Again cells infected with empty pCDH vector (non-OE) contains comparable amount of CD9 as NI cells.

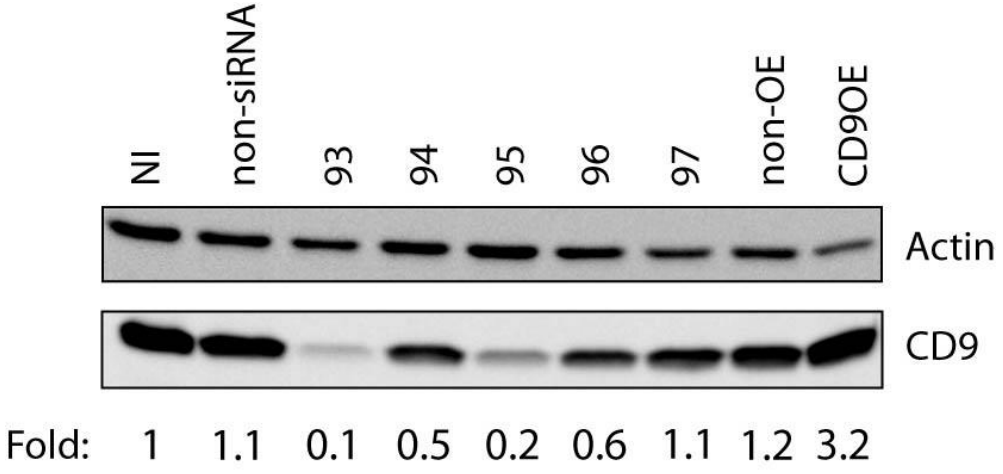

Fig. 28 – Expression of CD9 in CD9KD and CD9OE BMMCs.

BMMCs lysates were separated on 12% SDS-PAGE gel, western blotted and expression of CD9 was detected by 2H9 antibody and anti-rat-IgG-HRP secondary antibody. Actin was used as a loading control. Numbers indicate fold change of CD9 amount over non-infected (NI) control normalized to amount of Actin.

Considering these results, cells carrying construct 93 were choosen for surface expression analysis on flow cytometer. Results in Fig. 29 and Fig. 30 correspond to data shown in Fig.28 and thus 93 cells which had lowest CD9 level were selected for later experiments and later on termed as CD9KD.

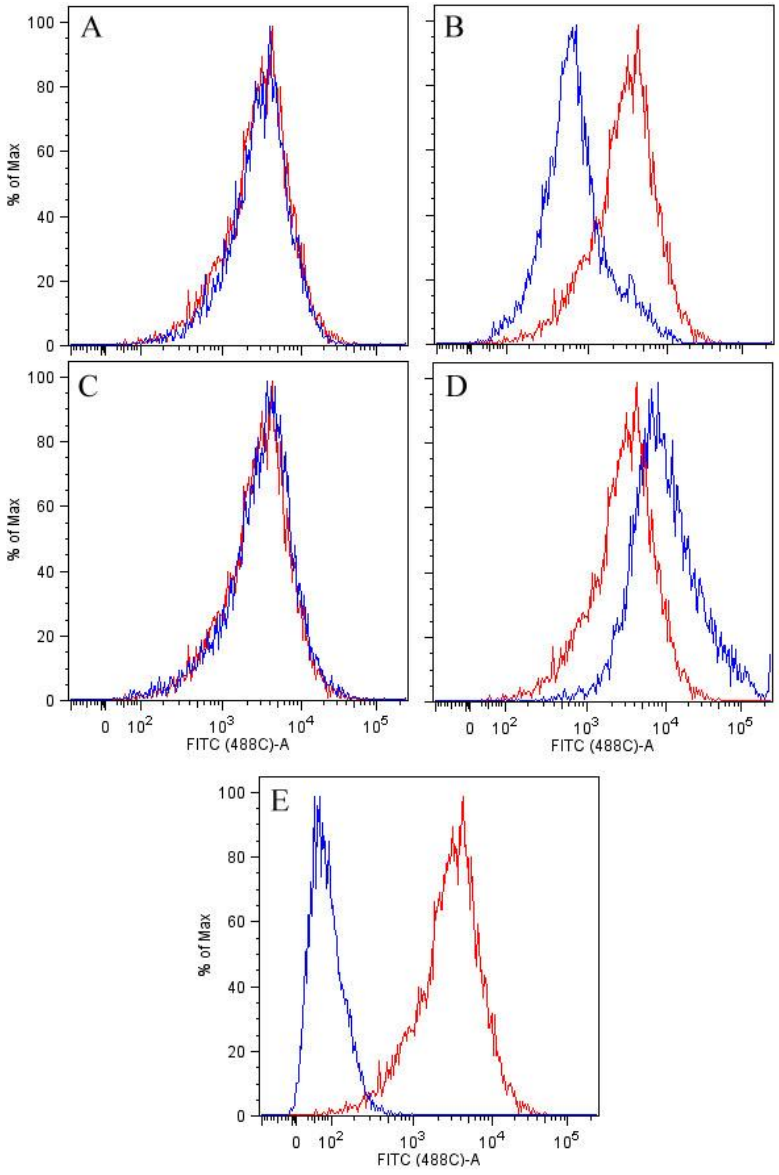

Fig. 29 – Expression of CD9 in CD9KD an CD9OE cells analyzed by flow cytometry.
BMMCs were incubated with 10 µg/ml of 2H9 antibody and then probed with 300× diluted secondary anti-rat-IgG-FITC antibody. Red line represents fluorescence of non-infected (NI) cells compared to non-siRNA control cells (A), CD9KD cells (B), non-OE cells (C), CD9OE cells (D) and background fluorescence of cells probed by secondary antibody only (E) represented by blue line.

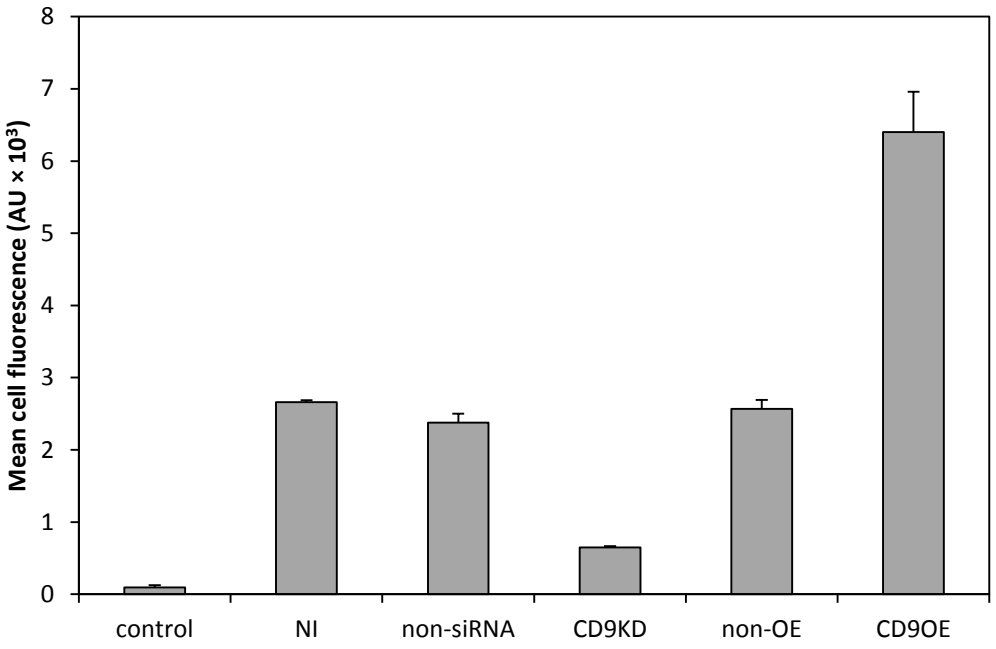

Fig. 30 – Calculated mean cell fluorescence from flow cytometry profile of CD9 expression. *Data represents average of geometric mean ± SD of experiments performed in triplicate. Background fluorescence (control), non-infected cells (NI), non-siRNA, CD9KD, non-OE and CD9OE cells.*

5.12.2 Degranulation of CD9KD and CD9OE cells pretreated with anti-CD9 antibody

Next step was to prove previously obtained results using CD9KD and CD9OE established cells. Again, cells were incubated or not with 2H9 antibody (30 µg/ml) and after 15 min activated by addition of TNP-BSA. Degranulation of 2H9-treated cells was calculated as percentage of degranulation of corresponding non-treated cells.

From Fig. 31 is evident that when CD9 expression is downregulated by shRNA (CD9KD), antibody-meditated inhibitory effect is significantly reduced. Importantly, in case of CD9OE cells, the inhibitory effect was even more pronounced than in WT cells.

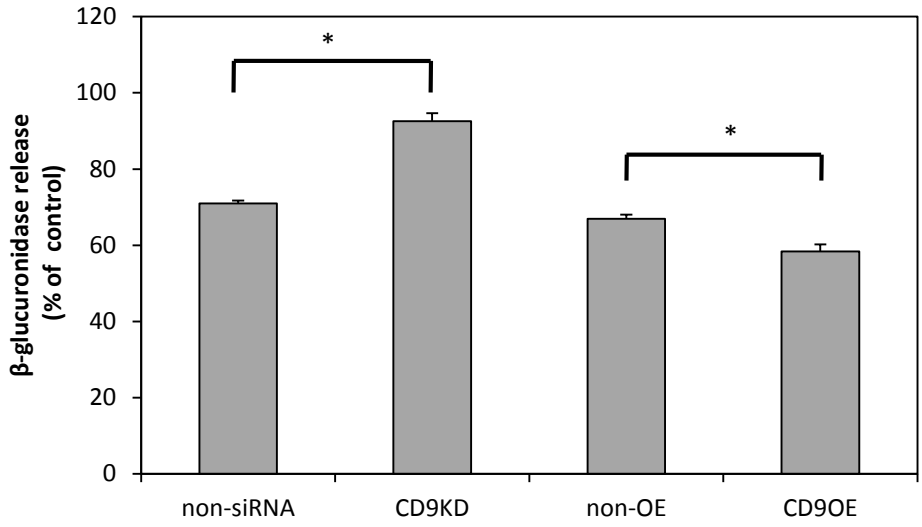

Fig. 31 – Effect of anti-CD9 antibody on antigen-mediated degranulation of CD9KD and CD9OE BMMCs.

Sensitized BMMCs were preincubated with 30 μg/ml of 2H9 antibody. Cells were then activated with 0.5 μg/ml of TNP-BSA. Extent of degranulation was estimated by amount of β-glucuronidase released to supernatant. Data are presented as percentage of 2H9-non-treated controls ± SD of two experiments performed in triplicate. Statistical significance was determined between CD9KD and CD9OE cells and their non-infected controls (non-siRNA, non-OE). (, P<0.05)*

5.12.3 CD9KD and calcium response

To support degranulation data, intracellular calcium levels were measured in CD9KD and non-siRNA control cells after triggering with 2H9 antibody followed by addition of TNP-BSA. Results from control experiment shown in Fig. 32 demonstrate that there is no difference in calcium response between CD9KD and non-siRNA cells. Surprisingly, this suggests that lowering CD9 expression does not have any effect on mast cell activation. However, when both these cells are triggered with antibody, CD9KD cells exhibit lower calcium response compared to non-siRNA control (Fig. 33). Moreover, when subsequently activated with TNP-BSA, CD9KD cells have higher response than non-siRNA cells and it almost reaches values observed in control experiment (compare Fig. 33 to Fig. 32).

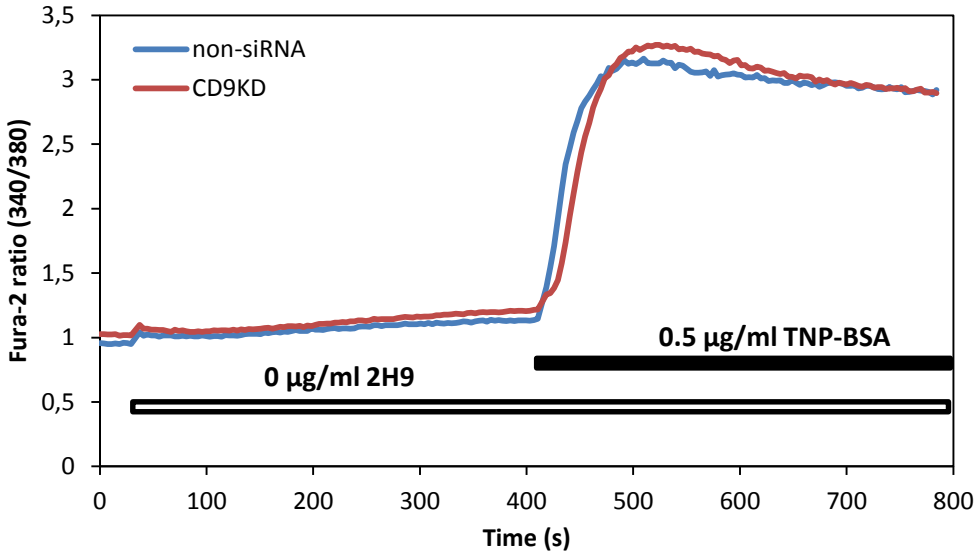

Fig. 32 – Control calcium experiment comparing CD9KD and non-siRNA cells.

Calcium mobilization of Fura-2 loaded cells was measured on Infinite 200M plate reader. Cells were first challenged with BSS-BSA instead 2H9 antibody followed by TNP-BSA triggering. Calcium level is expressed as ratio of emission with excitation at 340 nm and 380 nm. Curves represent mean of three experiments.

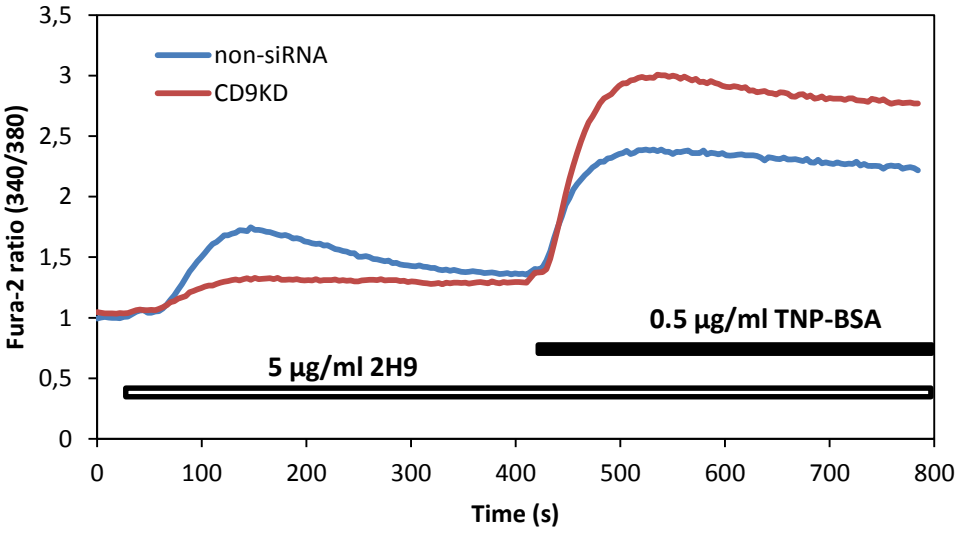

Fig. 33 – Calcium response after 2H9 and TNP-BSA triggering in CD9KD and non-siRNA cells.

Calcium mobilization of Fura-2 loaded cells was measured on Infinite 200M plate reader. Cells were first triggered by 2H9 antibody followed by TNP-BSA triggering. Calcium level is expressed as ratio of emission with excitation at 340 nm and 380 nm. Curves represent mean of three experiments.

5.12.4 CD9KD degranulation

Results in Fig. 34 surprisingly showed that there is almost no difference between CD9KD and control cells in calcium release initiated by TNP-BSA triggering. Therefore β-glucuronidase assay was performed to verify these results on level of degranulation. Result of this experiment confirmed previous one (Fig. 33) that CD9KD cells show no difference in degranulation compared to control non-siRNA cells.

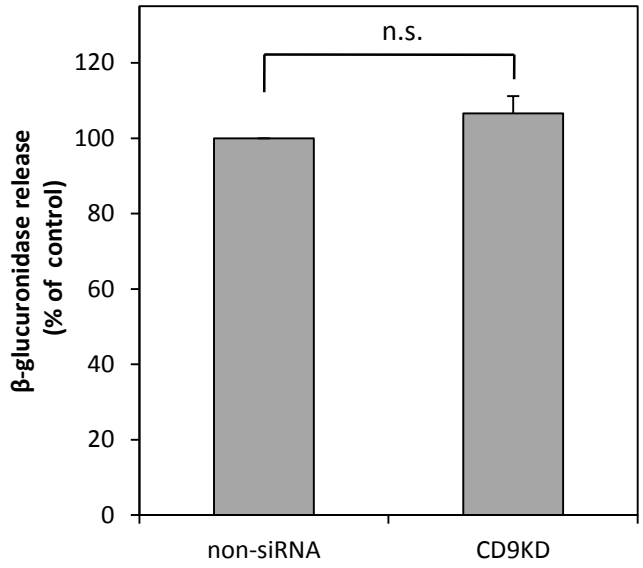

Fig. 34 – Comparison of CD9KD and non-siRNA cells antigen-mediated degranulation.
Sensitized BMMCs were activated with 0.5 μg/ml of TNP-BSA. Extent of degranulation was estimated by amount of β-glucuronidase released to supernatant. Data are presented as mean ± SD of three experiments performed in triplicate. Statistical significance was determined between CD9KD and non-siRNA control. (n.s., P>0.05; n=3)

6 Discussion

Mast cells are known effector cells of the immune system. They have been implicated in such important processes as host defense against bacteria, toxins or parasites. However, in some cases they can develop improper reaction against harmless environmental antigens and thus causing allergies. It is therefore essential to understand signaling events that lead to activation of these cells in order to develop new treatment strategies.

Monoclonal antibodies are unique tools that can be used either for curing allergies as in the case of Omalizumab (Winchester et al., 2006) or for identifying new molecules and characterization of various protein functions involved in mast cell signal transduction. Our laboratory already developed several monoclonal antibodies which were useful in further research of mast cell signaling (Hálová et al., 2001, 2002; Smrž et al., 2008). Initial aims of this diploma thesis were to characterize properties of an antibody raised against membrane structures of BMMCs which showed strong binding affinity to these cells. Next objective was to identify specificity of this antibody.

To this end we found that 2H9 antibody strongly reacts with its binding partner on the surface of BMMCs and can be used for detection of the antigen by flow cytometry, western blot immunodetection and immunoprecipitation. We therefore decided to proceed to identification of target protein. The most used strategies for identification of unknown proteins are Edman degradation and MS. However, classical method of Edman degradation holds many drawbacks such as necessity of high amount and purity of protein, low accuracy and problems with glycosylated proteins. On the other hand, modern method of MS analysis efficiently eliminates these problems by its higher sensitivity and thus low amount of protein is needed and glycosylations do not cause any problem. Taking all these considerations into account, we decided to isolate the antigen by immunoaffinity purification followed by MS analysis. Because binding of rat IgG_1 antibody isotype to protein A is limited, immobilized protein G was used instead and in order to eliminate contamination from similarly large Ig light chain, 2H9 antibody was covalently coupled to protein G by DMP. Using this optimized purification procedure, the target protein was successfully purified and identified by MS as CD9.

The antibody specificity was supported by other results which correspond to what is known about CD9. It was shown that CD9 is not a GPI-anchored protein but integral four times spanning membrane protein (Boucheix et al., 1991) and it has broad tissue distribution (Sincock et al., 1997). Final proof for CD9 identity came from cross-immunoprecipitation with 2H9 and commercial antibody KMC8.8.

Protein CD9 is one of the most studied members of tetraspanin superfamily. Its structure comprises of two short cytoplasmic tails, four transmembrane domains and small and large extracellular loops. LEL is known to contain two disulphide bridges which stabilize its conformation (Seigneuret et al., 2001). Decrease in detection efficiency of reduced CD9 by immunodetection with 2H9 antibody suggests that antibody probably recognizes conformational epitope on LEL which is destroyed after disulphide bond breakage. Research in past two decades revealed implication of CD9 in many processes such as cellular fusion, motility, adhesion and survival. Considerable amount of interest was dedicated to research of role of CD9 in hematopoietic cells. Anti-CD9 antibodies were shown to activate platelets (Ozaki et al., 1995), macrophages (Kaji et al., 2001) and eosinophils (Kim et al., 1997) even though these effects were Fc receptor dependent. Furthermore, antibodies against CD9 (Higginbottom et al., 2000b) and other tetraspanin proteins CD63 (Kraft et al., 2005) and CD81 (Fleming et al., 1997) were indispensable for uncovering roles of these tetraspanins in mast cell signaling and physiology. Previous study describing effects of anti-CD9 antibody on activation of mast cells was dealing only with effects on RBL cell line but no reports on mouse mast cells (e.g. BMMCs) were published up to now. This encouraged us to take closer look on function of this protein in BMMCs using our anti-CD9 antibody (2H9).

Initial experiments with BMMCs exposed to 2H9 antibody showed interesting results. Antibody alone stimulated degranulation of these cells, supporting the results of previous study with RBL cells (Higginbottom et al., 2000b).Subsequent activation of these cells via FcεRI triggering by TNP-BSA resulted in lower extent of degranulation which more resembled effects of antibodies against CD81 and CD63 (Fleming et al., 1997; Kraft et al., 2005). Moreover, these effects seem to be, consistently with previous studies, concentration dependent. These actions could be inflicted by various mechanisms such as masking interaction epitope for CD9 interaction partner molecule by 2H9 antibody or forced aggregation of CD9 proteins by molecule of immunoglobulin which might cause alterations in TEMs composition or organization. Results of experiment where CD9 was additionally crosslinked by anti-rat secondary antibody did not show any significant enhancement of 2H9-mediated inhibition of degranulation. This might be explained by the hypothesis that the effect is not caused by forced aggregation but rather by competing with endogenous interaction partner of CD9. However, another possibility still remains that 2H9-mediated dimerization of CD9 already present in dimers (Kovalenko et al., 2004) might be sufficient to disrupt TEMs composition.

Another possibility is that 2H9 antibody bound to CD9 could sterically block access of TNP-BSA to FcεRI receptor and thus cause cells to become less activated. Experiments with

fluorescently labeled TNP-BSA showed that its binding to IgE-primed Fc receptor is the same, regardless of 2H9 concentration used for BMMCs preincubation. This proves that steric blocking of antigen binding is not responsible for 2H9-mediated inhibition of degranulation. Previous study dealing with RBL cells activation by anti-CD9 antibody concluded that this effect was caused by crosslinking of CD9 with FcεRI receptor via anti-CD9 antibody itself (Higginbottom et al., 2000b). To test the possibility that 2H9 antibody interacts through its Fc portion with FcεRI and thus crosslinks it to CD9, sensitized and non-sensitized BMMCs were treated with 2H9 antibody and also cells were treated with mixture of 2H9 and high concentration IgE to compete for 2H9 binding to FcεRI receptor. In both cases 2H9-mediated activation and inhibition of degranulation respectively were preserved. Another possibility could be that 2H9 antibody acts through binding to Fcγ receptor as was described in case of platelets or macrophages (Griffith et al., 1991; Kaji et al., 2001). Mast cells were also shown to possess different Fcγ receptors on their surface which can provide either activatory or inhibitory signals and thus could be responsible for 2H9-mediated activities. However, experiments with cells preincubated with excess of normal rat serum IgG antibodies excluded this possibility. Thus it seems that none of these mechanisms are responsible for the observed 2H9-mediated activities.

As mentioned before, various anti-CD9 antibodies were reported to have either activatory or inhibitory effects on mast cell degranulation. Testing two different commercially available anti-CD9 antibodies KMC8.8 and N-19 showed that KMC8.8 has similar effect on mast cell activation as 2H9 antibody. Surprisingly, N-19 did not inflict any change in mast cell degranulation but test for binding ability showed that this antibody is not able to bind CD9 on surface of BMMCs. Control antibody, specific for CD48 protein, was able to bind to its target molecule but did not alter mast cell response. This means that 2H9 in not the only anti-CD9 antibody capable to interfere with activation of mast cells. In contrast, other antibodies of the same isotype but specific for other surface protein were inefficient.

Mast cell signaling pathways converge at release of Ca^{2+} from ER to cytosol. When ER stores are depleted, calcium sensor STIM1 clusters and moves to regions of ER which are close to plasma membrane where it activates calcium channels consisting of Orai1 subunits. This results in calcium influx and more increase of cytosolic calcium level (Vig and Kinet, 2009). Calcium is known to activate PKC and both together act as master regulators of mast cell secretory granules exocytosis (Gilfillan and Tkaczyk, 2006). Experiments showed that alterations in calcium response are responsible for both 2H9-mediated BMMCs activation and inhibition of degranulation via FcεRI aggregation. Binding of 2H9 antibody to BMMCs caused transient peak of intracellular calcium

level. When these cells were activated via TNP-BSA, the calcium response was generally lower than in cells which were not pretreated with 2H9 antibody. Similar mechanism was also observed for another anti-CD9 antibody, KMC8.8. These experiments mapped only overall change in cytosolic calcium. However, anti-CD9 antibodies might potentially act at two different points of this signaling event: (1) at the level of calcium release from ER and (2) at the level of extracellular calcium influx. Results revealed that BMMCs pretreated with 2H9 antibody exhibited slightly lower calcium release from ER, the initiation of which was also markedly shifted to the later time. Subsequent calcium influx was also impaired under these conditions. When BMMCs were activated via inhibitor of ER Ca^{2+} ATPases thapsigargin, which leads to accumulation of calcium in cytosol without activation of proximal signaling, 2H9-pretreated BMMCs degranulated with the same extent and their intracellular calcium level was identical to control cells non-treated with antibody. This suggests that 2H9 antibody does not interfere with calcium influx machinery (for example by blocking Orai1 channels) but rather acts upstream or at the level of calcium release from ER. Taking all these results together it is possible to propose hypothesis that the initial calcium release caused by 2H9 antibody binding is responsible for subsequent lower and delayed calcium release from ER and thus also impaired calcium influx.

To determine which signaling proteins acting upstream of calcium release are involved in anti-CD9-mediated processes, phosphorylation status of cellular proteins was examined. The results showed that the level of tyrosine phosphorylation of proteins with molecular weight of LAT, NTAL and PLCγ1, is increased in 2H9-activated BMMCs in the absence of antigen exposure. In contrast, pretreatment with 2H9 antibody decreased phosphorylation of all these proteins in cells activated by antigen. This correlates with the results on the effect of 2H9 on degranulation and calcium release. Mechanism of the observed 2H9-induced phosphorylation might involve activation of Scr family kinases Lyn or Fyn or as previously described activation of Syk kinase (Ozaki et al., 1995). However, in their case Syk kinase activation was coupled with CD9 and Fc receptor crosslinking and this scenario was excluded by our experiments. Final proof require performing experiments in which the cells will be activated with $F(ab)_2$ fragments of 2H9 antibody which lack Fc portion responsible for association with Fc receptors.

To verify effects of 2H9 antibody on BMMCs, stabile BMMC transfectants with decreased (CD9KD) or increased (CD9OE) levels of CD9 were generated using lentiviral transfection system. Experiments on these cells confirmed involvement of CD9 protein in before-mentioned effects of 2H9 antibody. CD9KD cells showed substantially less inhibition of degranulation and calcium release caused by 2H9 binding while inhibition of degranulation in case of CD9OE was more

prominent. Unexpectedly, degranulation of CD9KD triggered by TNP-BSA remained unchanged compared to WT cells. This might be explained by the fact that remaining endogenous CD9 (~10%, see Fig. 28) could be sufficient to maintain its activity. However this is most probably not the case because if remaining CD9 is sufficient for maintaining its activity, then 2H9 antibody would trigger same inhibition of antigen-mediated degranulation and calcium release as WT cells. More probable seems hypothesis that lack of CD9 in CD9KD cells is compensated by another tetraspanin localized in TEMs. One of possible tetraspanins responsible for this potential compensation might be CD81. Reasons for this are that CD81 is structurally similar to CD9 (Seigneuret et al., 2001), effects of anti-CD81 antibody were similar to those observed with 2H9 antibody (Fleming et al., 1997) and, importantly, CD81 KO mice were shown to have similar phenotype as CD9 KO mice and CD9 and CD81 double-KO mice have even more severe phenotype than single-KO mice (Kaji et al., 2002; Rubinstein et al., 2006; Takeda et al., 2008). It will be therefore advantageous to examine physiological aspects of mast cells generated from CD9 and CD81 double-KO mouse or produce cells with concurrently silenced expression of both CD9 and CD81 tetraspanins.

Monoclonal antibody 2H9 can be widely used for identification and characterization of mouse CD9. Its useful properties predict that the antibody can be used for commercial purposes. To this end, the antibody was transferred, based on Institutional agreement, to company Exbio, a.s.

7 Summary

Results of this diploma thesis led to these conclusions:

- Characterization of new rat monoclonal antibody 2H9, raised against BMMCs, showed that this antibody is of IgG_1 subtype and is suitable for use in flow cytometry, immunodetection by western blots and immunoprecipitation.
- Using of our optimized procedure for immunoaffine isolation combined with MS analysis led to identification of 2H9 antibody target protein as member of tetraspanin family CD9. This was also supported by comparison with commercially available anti-CD9 antibodies.
- Upon its binding to CD9 on the cell surface, 2H9 antibody was shown to initiate BMMCs degranulation and at the same time inhibited antigen-mediated degranulation of these cells. These effects were not caused by blocking access of antigen to FcεRI, coupling of CD9 to FcεRI by 2H9 antibody nor by acting through Fcγ receptors.
- Examining signaling steps leading to mast cell degranulation revealed that 2H9-induced degranulation and inhibition of antigen-mediated signaling reflected changes in calcium response. Moreover, anti-CD9 antibody acted upstream of calcium release from ER because thapsigargin-mediated activation remained unchanged and phosphorylation state of proteins playing role in FcεRI receptor proximal signaling (e.g. LAT, NTAL and PLCγ1) was altered in cells pretreated with 2H9 antibody.
- Newly generated cells with decreased (CD9KD) or increased (CD9OE) levels of CD9 showed, respectively less and more pronounced effects mediated by anti-CD9 antibody, supporting the role of CD9 in these processes. However, degranulation of CD9KD cells was comparable to wild-type cells which is probably the result of compensation by other tetraspanin family member.
- In summary, protein CD9 plays dual role in regulation of mast cell signalization. CD9 could act as a negative regulator of mast cell activation. However, this ability is compromised by binding of anti-CD9 antibody which probably competes with unknown interaction partner of CD9 or disrupts TEMs composition by aggregating CD9 molecules. This somehow leads to activation of protein tyrosine kinases and low-level degranulation. However, this might also activate negative feed-back mechanisms which then dampen signalization after antigen-mediated activation resulting in lower extent of degranulation.

8 References

1. Anzai, N., Lee, Y., Youn, B.S., Fukuda, S., Kim, Y.J., Mantel, C., Akashi, M., and Broxmeyer, H.E. (2002): C-kit associated with the transmembrane 4 superfamily proteins constitutes a functionally distinct subunit in human hematopoietic progenitors. Blood *99*, 4413-4421.

2. Asai, K., Kitaura, J., Kawakami, Y., Yamagata, N., Tsai, M., Carbone, D.P., Liu, F.T., Galli, S.J., and Kawakami, T. (2001): Regulation of mast cell survival by IgE. Immunity *14*, 791-800.

3. Berditchevski, F. (2001): Complexes of tetraspanins with integrins: more than meets the eye. JCell Sci *114*, 4143-4151.

4. Berditchevski, F., Gilbert, E., Griffiths, M.R., Fitter, S., Ashman, L., and Jenner, S.J. (2001): Analysis of the CD151-alpha3beta1 integrin and CD151-tetraspanin interactions by mutagenesis. J Biol Chem *276*, 41165-41174.

5. Berditchevski, F., Odintsova, E., Sawada, S., and Gilbert, E. (2002): Expression of the palmitoylation-deficient CD151 weakens the association of alpha 3 beta 1 integrin with the tetraspanin-enriched microdomains and affects integrin-dependent signaling. J Biol Chem *277*, 36991-37000.

6. Boucheix, C., Benoit, P., Frachet, P., Billard, M., Worthington, R.E., Gagnon, J., and Uzan, G. (1991): Molecular cloning of the CD9 antigen. A new family of cell surface proteins. JBiolChem *266*, 117-122.

7. Boucheix, C., and Rubinstein, E. (2001): Tetraspanins. Cell MolLife Sci *58*, 1189-1205.

8. Cannon, K.S., and Cresswell, P. (2001): Quality control of transmembrane domain assembly in the tetraspanin CD82. EMBO J *20*, 2443-2453.

9. Claas, C., Stipp, C.S., and Hemler, M.E. (2001): Evaluation of prototype transmembrane 4 superfamily protein complexes and their relation to lipid rafts. JBiolChem *276*, 7974-7984.

10. Dombrowicz, D., Lin, S., Flamand, V., Brini, A.T., Koller, B.H., and Kinet, J.P. (1998): Allergy-associated FcRbeta is a molecular amplifier of IgE- and IgG-mediated in vivo responses. Immunity *8*, 517-529.

11. Dráberová, L., and Dráber, P. (1993): Cross-linking of Thy-1 glycoproteins or high-affinity IgE receptors induces mast cell activation via different mechanisms. Immunology *80*, 103-109.

12. Drucker, L., Tohami, T., Tartakover-Matalon, S., Zismanov, V., Shapiro, H., Radnay, J., and Lishner, M. (2006): Promoter hypermethylation of tetraspanin members contributes to their silencing in myeloma cell lines. Carcinogenesis *27*, 197-204.

13. Field, K.A., Holowka, D., and Baird, B. (1999): Structural aspects of the association of FcepsilonRI with detergent-resistant membranes. J Biol Chem *274*, 1753-1758.

14. Fleming, T.J., Donnadieu, E., Song, C.H., Laethem, F.V., Galli, S.J., and Kinet, J.P. (1997): Negative regulation of Fc epsilon RI-mediated degranulation by CD81. J Exp Med *186*, 1307-1314.

15. Garcia-Espana, A., Chung, P.J., Sarkar, I.N., Stiner, E., Sun, T.T., and Desalle, R. (2008): Appearance of new tetraspanin genes during vertebrate evolution. Genomics *91*, 326-334.

16. Garman, S.C., Wurzburg, B.A., Tarchevskaya, S.S., Kinet, J.P., and Jardetzky, T.S. (2000): Structure of the Fc fragment of human IgE bound to its high-affinity receptor Fc epsilonRI alpha. Nature *406*, 259-266.

17. Gilfillan, A.M., Peavy, R.D., and Metcalfe, D.D. (2009): Amplification mechanisms for the enhancement of antigen-mediated mast cell activation. Immunol Res *43*, 15-24.

18. Gilfillan, A.M., and Tkaczyk, C. (2006): Integrated signalling pathways for mast-cell activation. Nat Rev Immunol *6*, 218-230.

19. Griffith, L., Slupsky, J., Seehafer, J., Boshkov, L., and Shaw, A.R. (1991): Platelet activation by immobilized monoclonal antibody: evidence for a CD9 proximal signal. Blood *78*, 1753-1759.

20. Grimbaldeston, M.A., Chen, C.C., Piliponsky, A.M., Tsai, M., Tam, S.Y., and Galli, S.J. (2005): Mast cell-deficient W-sash c-kit mutant Kit W-sh/W-sh mice as a model for investigating mast cell biology in vivo. Am J Pathol *167*, 835-848.

21. Hálová, I., Dráberová, L., and Dráber, P. (2001): New monoclonal antibodies to rat testicular antigen, TEC-21. Folia Biol (Praha) *47*, 180-182.

22. Hálová, I., Dráberová, L., and Dráber, P. (2002): A novel lipid raft-associated glycoprotein, TEC-21, activates rat basophilic leukemia cells independently of the type 1 Fc epsilon receptor. Int Immunol *14*, 213-223.

23. Hata, D., Kawakami, Y., Inagaki, N., Lantz, C.S., Kitamura, T., Khan, W.N., Maeda-Yamamoto, M., Miura, T., Han, W., Hartman, S.E*., et al.* (1998): Involvement of Bruton's tyrosine kinase in FcepsilonRI-dependent mast cell degranulation and cytokine production. J Exp Med *187*, 1235-1247.

24. He, Z.Y., Gupta, S., Myles, D., and Primakoff, P. (2008): Loss of surface EWI-2 on CD9 null oocytes. Mol Reprod Dev.

25. Hemler, M.E. (2001): Specific tetraspanin functions. JCell Biol *155*, 1103-1107.

26. Hemler, M.E. (2005): Tetraspanin functions and associated microdomains. NatRevMolCell Biol *6*, 801-811.

27. Hemler, M.E. (2008): Targeting of tetraspanin proteins--potential benefits and strategies. Nat Rev Drug Discov *7*, 747-758.

28. Higginbottom, A., Quinn, E.R., Kuo, C.C., Flint, M., Wilson, L.H., Bianchi, E., Nicosia, A., Monk, P.N., McKeating, J.A., and Levy, S. (2000a): Identification of amino acid residues in CD81 critical for interaction with hepatitis C virus envelope glycoprotein E2. J Virol *74*, 3642-3649.

29. Higginbottom, A., Wilkinson, I., McCullough, B., Lanza, F., Azorsa, D.O., Partridge, L.J., and Monk, P.N. (2000b): Antibody cross-linking of human CD9 and the high-affinity immunoglobulin E receptor stimulates secretion from transfected rat basophilic leukaemia cells. Immunology *99*, 546-552.

30. Hong, H., Kitaura, J., Xiao, W., Horejsi, V., Ra, C., Lowell, C.A., Kawakami, Y., and Kawakami, T. (2007): The Src family kinase Hck regulates mast cell activation by suppressing an inhibitory Src family kinase Lyn. Blood *110*, 2511-2519.

31. Hong, I.K., Kim, Y.M., Jeoung, D.I., Kim, K.C., and Lee, H. (2005): Tetraspanin CD9 induces MMP-2 expression by activating p38 MAPK, JNK and c-Jun pathways in human melanoma cells. ExpMolMed *37*, 230-239.

32. Huang, C.L., Liu, D., Masuya, D., Kameyama, K., Nakashima, T., Yokomise, H., Ueno, M., and Miyake, M. (2004): MRP-1/CD9 gene transduction downregulates Wnt signal pathways. Oncogene *23*, 7475-7483.

33. Huang, C.L., Ueno, M., Liu, D., Masuya, D., Nakano, J., Yokomise, H., Nakagawa, T., and Miyake, M. (2006): MRP-1/CD9 gene transduction regulates the actin cytoskeleton through the downregulation of WAVE2. Oncogene *25*, 6480-6488.

34. Huang, S., Yuan, S., Dong, M., Su, J., Yu, C., Shen, Y., Xie, X., Yu, Y., Yu, X., Chen, S.*, et al.* (2005): The phylogenetic analysis of tetraspanins projects the evolution of cell-cell interactions from unicellular to multicellular organisms. Genomics *86*, 674-684.

35. Charrin, S., Manie, S., Oualid, M., Billard, M., Boucheix, C., and Rubinstein, E. (2002): Differential stability of tetraspanin/tetraspanin interactions: role of palmitoylation. FEBS Lett *516*, 139-144.

36. Irani, A.M., Craig, S.S., DeBlois, G., Elson, C.O., Schechter, N.M., and Schwartz, L.B. (1987): Deficiency of the tryptase-positive, chymase-negative mast cell type in gastrointestinal mucosa of patients with defective T lymphocyte function. J Immunol *138*, 4381-4386.

37. Jabril-Cuenod, B., Zhang, C., Scharenberg, A.M., Paolini, R., Numerof, R., Beaven, M.A., and Kinet, J.P. (1996): Syk-dependent phosphorylation of Shc. A potential link between FcepsilonRI and the Ras/mitogen-activated protein kinase signaling pathway through SOS and Grb2. J Biol Chem *271*, 16268-16272.

38. Kaji, K., Oda, S., Miyazaki, S., and Kudo, A. (2002): Infertility of CD9-deficient mouse eggs is reversed by mouse CD9, human CD9, or mouse CD81; polyadenylated mRNA injection developed for molecular analysis of sperm-egg fusion. DevBiol *247*, 327-334.

39. Kaji, K., Oda, S., Shikano, T., Ohnuki, T., Uematsu, Y., Sakagami, J., Tada, N., Miyazaki, S., and Kudo, A. (2000): The gamete fusion process is defective in eggs of Cd9-deficient mice. NatGenet *24*, 279-282.

40. Kaji, K., Takeshita, S., Miyake, K., Takai, T., and Kudo, A. (2001): Functional association of CD9 with the Fc gamma receptors in macrophages. JImmunol *166*, 3256-3265.

41. Kalesnikoff, J., and Galli, S.J. (2008): New developments in mast cell biology. Nat Immunol *9*, 1215-1223.

42. Kazarov, A.R., Yang, X., Stipp, C.S., Sehgal, B., and Hemler, M.E. (2002): An extracellular site on tetraspanin CD151 determines alpha 3 and alpha 6 integrin-dependent cellular morphology. J Cell Biol *158*, 1299-1309.

43. Kersey, J.H., LeBien, T.W., Abramson, C.S., Newman, R., Sutherland, R., and Greaves, M. (1981): P-24: a human leukemia-associated and lymphohemopoietic progenitor cell surface structure identified with monoclonal antibody. J Exp Med *153*, 726-731.

44. Kim, J.T., Gleich, G.J., and Kita, H. (1997): Roles of CD9 molecules in survival and activation of human eosinophils. JImmunol *159*, 926-933.

45. Kimura, T., Kihara, H., Bhattacharyya, S., Sakamoto, H., Appella, E., and Siraganian, R.P. (1996): Downstream signaling molecules bind to different phosphorylated

immunoreceptor tyrosine-based activation motif (ITAM) peptides of the high affinity IgE receptor. J Biol Chem *271*, 27962-27968.

46. Kinet, J.P. (1999): The high-affinity IgE receptor (Fc epsilon RI): from physiology to pathology. Annu Rev Immunol *17*, 931-972.

47. Kirshenbaum, A.S., Goff, J.P., Semere, T., Foster, B., Scott, L.M., and Metcalfe, D.D. (1999): Demonstration that human mast cells arise from a progenitor cell population that is CD34(+), c-kit(+), and expresses aminopeptidase N (CD13). Blood *94*, 2333-2342.

48. Kitadokoro, K., Bordo, D., Galli, G., Petracca, R., Falugi, F., Abrignani, S., Grandi, G., and Bolognesi, M. (2001): CD81 extracellular domain 3D structure: insight into the tetraspanin superfamily structural motifs. EMBO J *20*, 12-18.

49. Kitadokoro, K., Ponassi, M., Galli, G., Petracca, R., Falugi, F., Grandi, G., and Bolognesi, M. (2002): Subunit association and conformational flexibility in the head subdomain of human CD81 large extracellular loop. BiolChem *383*, 1447-1452.

50. Kovalenko, O.V., Metcalf, D.G., DeGrado, W.F., and Hemler, M.E. (2005): Structural organization and interactions of transmembrane domains in tetraspanin proteins. BMCStructBiol *5*, 11.

51. Kovalenko, O.V., Yang, X., Kolesnikova, T.V., and Hemler, M.E. (2004): Evidence for specific tetraspanin homodimers: inhibition of palmitoylation makes cysteine residues available for cross-linking. BiochemJ *377*, 407-417.

52. Kovalenko, O.V., Yang, X.H., and Hemler, M.E. (2007): A novel cysteine crosslinking method reveals a direct association between claudin-1 and tetraspanin CD9. MolCell Proteomics.

53. Kraft, S., Fleming, T., Billingsley, J.M., Lin, S.Y., Jouvin, M.H., Storz, P., and Kinet, J.P. (2005): Anti-CD63 antibodies suppress IgE-dependent allergic reactions in vitro and in vivo. J Exp Med *201*, 385-396.

54. Kropshofer, H., Spindeldreher, S., Rohn, T.A., Platania, N., Grygar, C., Daniel, N., Wolpl, A., Langen, H., Horejsi, V., and Vogt, A.B. (2002): Tetraspan microdomains distinct from lipid rafts enrich select peptide-MHC class II complexes. Nat Immunol *3*, 61-68.

55. Kuehn, H.S., Beaven, M.A., Ma, H.T., Kim, M.S., Metcalfe, D.D., and Gilfillan, A.M. (2008): Synergistic activation of phospholipases Cgamma and Cbeta: a novel mechanism for PI3K-independent enhancement of FcepsilonRI-induced mast cell mediator release. Cell Signal *20*, 625-636.

56. Lam, V., Kalesnikoff, J., Lee, C.W., Hernandez-Hansen, V., Wilson, B.S., Oliver, J.M., and Krystal, G. (2003): IgE alone stimulates mast cell adhesion to fibronectin via pathways similar to those used by IgE + antigen but distinct from those used by Steel factor. Blood *102*, 1405-1413.

57. Lammerding, J., Kazarov, A.R., Huang, H., Lee, R.T., and Hemler, M.E. (2003): Tetraspanin CD151 regulates alpha6beta1 integrin adhesion strengthening. Proc Natl Acad Sci U S A *100*, 7616-7621.

58. Lanza, F., Wolf, D., Fox, C.F., Kieffer, N., Seyer, J.M., Fried, V.A., Coughlin, S.R., Phillips, D.R., and Jennings, L.K. (1991): cDNA cloning and expression of platelet p24/CD9. Evidence for a new family of multiple membrane-spanning proteins. J Biol Chem *266*, 10638-10645.

59. Le Naour, F., Rubinstein, E., Jasmin, C., Prenant, M., and Boucheix, C. (2000): Severely reduced female fertility in CD9-deficient mice. Science *287*, 319-321.

60. Letourneur, O., Sechi, S., Willette-Brown, J., Robertson, M.W., and Kinet, J.P. (1995): Glycosylation of human truncated Fc epsilon RI alpha chain is necessary for efficient folding in the endoplasmic reticulum. J Biol Chem *270*, 8249-8256.

61. Levy, S., and Shoham, T. (2005a): Protein-protein interactions in the tetraspanin web. Physiology(Bethesda) *20*, 218-224.

62. Levy, S., and Shoham, T. (2005b): The tetraspanin web modulates immune-signalling complexes. NatRevImmunol *5*, 136-148.

63. Lin, S., Cicala, C., Scharenberg, A.M., and Kinet, J.P. (1996): The Fc(epsilon)RIbeta subunit functions as an amplifier of Fc(epsilon)RIgamma-mediated cell activation signals. Cell *85*, 985-995.

64. Little, K.D., Hemler, M.E., and Stipp, C.S. (2004): Dynamic regulation of a GPCR-tetraspanin-G protein complex on intact cells: central role of CD81 in facilitating GPR56-Galpha q/11 association. Mol Biol Cell *15*, 2375-2387.

65. Longo, N., Yanez-Mo, M., Mittelbrunn, M., de la, R.G., Munoz, M.L., Sanchez-Madrid, F., and Sanchez-Mateos, P. (2001): Regulatory role of tetraspanin CD9 in tumor-endothelial cell interaction during transendothelial invasion of melanoma cells. Blood *98*, 3717-3726.

66. Marshall, J.S. (2004): Mast-cell responses to pathogens. Nat Rev Immunol *4*, 787-799.

67. Masciopinto, F., Campagnoli, S., Abrignani, S., Uematsu, Y., and Pileri, P. (2001): The small extracellular loop of CD81 is necessary for optimal surface expression of the large loop, a putative HCV receptor. Virus Res *80*, 1-10.

68. Metcalfe, D.D., Baram, D., and Mekori, Y.A. (1997): Mast cells. Physiol Rev *77*, 1033-1079.

69. Min, G., Wang, H., Sun, T.T., and Kong, X.P. (2006): Structural basis for tetraspanin functions as revealed by the cryo-EM structure of uroplakin complexes at 6-A resolution. JCell Biol *173*, 975-983.

70. Mitamura, T., Iwamoto, R., Umata, T., Yomo, T., Urabe, I., Tsuneoka, M., and Mekada, E. (1992): The 27-kD diphtheria toxin receptor-associated protein (DRAP27) from vero cells is the monkey homologue of human CD9 antigen: expression of DRAP27 elevates the number of diphtheria toxin receptors on toxin-sensitive cells. J Cell Biol *118*, 1389-1399.

71. Mitsuzuka, K., Handa, K., Satoh, M., Arai, Y., and Hakomori, S. (2005): A specific microdomain ("glycosynapse 3") controls phenotypic conversion and reversion of bladder cancer cells through GM3-mediated interaction of alpha3beta1 integrin with CD9. JBiolChem *280*, 35545-35553.

72. Miura, K., Schroeder, J.T., Hubbard, W.C., and MacGlashan, D.W., Jr. (1999): Extracellular signal-regulated kinases regulate leukotriene C4 generation, but not histamine release or IL-4 production from human basophils. J Immunol *162*, 4198-4206.

73. Miyado, K., Yamada, G., Yamada, S., Hasuwa, H., Nakamura, Y., Ryu, F., Suzuki, K., Kosai, K., Inoue, K., Ogura, A*., et al.* (2000): Requirement of CD9 on the egg plasma membrane for fertilization. Science *287*, 321-324.

74. Miyake, M., Inufusa, H., Adachi, M., Ishida, H., Hashida, H., Tokuhara, T., and Kakehi, Y. (2000): Suppression of pulmonary metastasis using adenovirally motility related protein-1 (MRP-1/CD9) gene delivery. Oncogene *19*, 5221-5226.

75. Moribe, H., Yochem, J., Yamada, H., Tabuse, Y., Fujimoto, T., and Mekada, E. (2004): Tetraspanin protein (TSP-15) is required for epidermal integrity in Caenorhabditis elegans. J Cell Sci *117*, 5209-5220.

76. Nakamura, K., Iwamoto, R., and Mekada, E. (1995): Membrane-anchored heparin-binding EGF-like growth factor (HB-EGF) and diphtheria toxin receptor-associated protein (DRAP27)/CD9 form a complex with integrin alpha 3 beta 1 at cell-cell contact sites. JCell Biol *129*, 1691-1705.

77. Odintsova, E., Voortman, J., Gilbert, E., and Berditchevski, F. (2003): Tetraspanin CD82 regulates compartmentalisation and ligand-induced dimerization of EGFR. J Cell Sci *116*, 4557-4566.

78. Ovalle, S., Gutierrez-Lopez, M.D., Olmo, N., Turnay, J., Lizarbe, M.A., Majano, P., Molina-Jimenez, F., Lopez-Cabrera, M., Yanez-Mo, M., Sanchez-Madrid, F*., et al.* (2007): The tetraspanin CD9 inhibits the proliferation and tumorigenicity of human colon carcinoma cells. IntJCancer.

79. Ozaki, Y., Satoh, K., Kuroda, K., Qi, R., Yatomi, Y., Yanagi, S., Sada, K., Yamamura, H., Yanabu, M., and Nomura, S. (1995): Anti-CD9 monoclonal antibody activates p72syk in human platelets. JBiolChem *270*, 15119-15124.

80. Parravicini, V., Gadina, M., Kovarova, M., Odom, S., Gonzalez-Espinosa, C., Furumoto, Y., Saitoh, S., Samelson, L.E., O'Shea, J.J., and Rivera, J. (2002): Fyn kinase initiates complementary signals required for IgE-dependent mast cell degranulation. Nat Immunol *3*, 741-748.

81. Pivniouk, V.I., Martin, T.R., Lu-Kuo, J.M., Katz, H.R., Oettgen, H.C., and Geha, R.S. (1999): SLP-76 deficiency impairs signaling via the high-affinity IgE receptor in mast cells. J Clin Invest *103*, 1737-1743.

82. Qi, J.C., Wang, J., Mandadi, S., Tanaka, K., Roufogalis, B.D., Madigan, M.C., Lai, K., Yan, F., Chong, B.H., Stevens, R.L*., et al.* (2006): Human and mouse mast cells use the tetraspanin CD9 as an alternate interleukin-16 receptor. Blood *107*, 135-142.

83. Qi, R., Ozaki, Y., Kuroda, K., Asazuma, N., Yatomi, Y., Satoh, K., Nomura, S., and Kume, S. (1996): Differential activation of human platelets induced by Fc gamma receptor II cross-linking and by anti-CD9 monoclonal antibody. JImmunol *157*, 5638-5645.

84. Rivera, J. (2005): NTAL/LAB and LAT: a balancing act in mast-cell activation and function. Trends Immunol *26*, 119-122.

85. Rous, B.A., Reaves, B.J., Ihrke, G., Briggs, J.A., Gray, S.R., Stephens, D.J., Banting, G., and Luzio, J.P. (2002): Role of adaptor complex AP-3 in targeting wild-type and mutated CD63 to lysosomes. Mol Biol Cell *13*, 1071-1082.

86. Rubinstein, E., Le Naour, F., Lagaudriere-Gesbert, C., Billard, M., Conjeaud, H., and Boucheix, C. (1996): CD9, CD63, CD81, and CD82 are components of a surface tetraspan network connected to HLA-DR and VLA integrins. EurJImmunol *26*, 2657-2665.

87. Rubinstein, E., Ziyyat, A., Prenant, M., Wrobel, E., Wolf, J.P., Levy, S., Le Naour, F., and Boucheix, C. (2006): Reduced fertility of female mice lacking CD81. Dev Biol *290*, 351-358.

88. Runge, K.E., Evans, J.E., He, Z.Y., Gupta, S., McDonald, K.L., Stahlberg, H., Primakoff, P., and Myles, D.G. (2007): Oocyte CD9 is enriched on the microvillar membrane and required for normal microvillar shape and distribution. Dev Biol *304*, 317-325.

89. Saito, Y., Tachibana, I., Takeda, Y., Yamane, H., He, P., Suzuki, M., Minami, S., Kijima, T., Yoshida, M., Kumagai, T.*, et al.* (2006): Absence of CD9 Enhances Adhesion-Dependent Morphologic Differentiation, Survival, and Matrix Metalloproteinase-2 Production in Small Cell Lung Cancer Cells. Cancer Res *66*, 9557-9565.

90. Sala-Valdes, M., Ursa, A., Charrin, S., Rubinstein, E., Hemler, M.E., Sanchez-Madrid, F., and Yanez-Mo, M. (2006): EWI-2 and EWI-F link the tetraspanin web to the actin cytoskeleton through their direct association with ezrin-radixin-moesin proteins. JBiolChem *281*, 19665-19675.

91. Sauer, G., Windisch, J., Kurzeder, C., Heilmann, V., Kreienberg, R., and Deissler, H. (2003): Progression of cervical carcinomas is associated with down-regulation of CD9 but strong local re-expression at sites of transendothelial invasion. ClinCancer Res *9*, 6426-6431.

92. Seigneuret, M., Delaguillaumie, A., Lagaudriere-Gesbert, C., and Conjeaud, H. (2001): Structure of the tetraspanin main extracellular domain. A partially conserved fold with a structurally variable domain insertion. JBiolChem *276*, 40055-40064.

93. Shi, W., Fan, H., Shum, L., and Derynck, R. (2000): The tetraspanin CD9 associates with transmembrane TGF-alpha and regulates TGF-alpha-induced EGF receptor activation and cell proliferation. J Cell Biol *148*, 591-602.

94. Sincock, P.M., Mayrhofer, G., and Ashman, L.K. (1997): Localization of the transmembrane 4 superfamily (TM4SF) member PETA-3 (CD151) in normal human tissues: comparison with CD9, CD63, and alpha5beta1 integrin. J Histochem Cytochem *45*, 515-525.

95. Singethan, K., Topfstedt, E., Schubert, S., Duprex, W.P., Rima, B.K., and Schneider-Schaulies, J. (2006): CD9-dependent regulation of Canine distemper virus-induced cell-cell fusion segregates with the extracellular domain of the haemagglutinin. J Gen Virol *87*, 1635-1642.

96. Smrž, D., Dráberová, L., and Dráber, P. (2007): Non-apoptotic phosphatidylserine externalization induced by engagement of glycosylphosphatidylinositol-anchored proteins. J Biol Chem *282*, 10487-10497.

97. Smrž, D., Lebduška, P., Dráberová, L., Korb, J., and Dráber, P. (2008): Engagement of phospholipid scramblase 1 in activated cells: implication for phosphatidylserine externalization and exocytosis. J Biol Chem *283*, 10904-10918.

98. Stevens, R.L., Friend, D.S., McNeil, H.P., Schiller, V., Ghildyal, N., and Austen, K.F. (1994): Strain-specific and tissue-specific expression of mouse mast cell secretory granule proteases. Proc Natl Acad Sci U S A *91*, 128-132.

99. Stipp, C.S., Kolesnikova, T.V., and Hemler, M.E. (2003a): EWI-2 regulates alpha3beta1 integrin-dependent cell functions on laminin-5. J Cell Biol *163*, 1167-1177.

100. Stipp, C.S., Kolesnikova, T.V., and Hemler, M.E. (2003b): Functional domains in tetraspanin proteins. Trends BiochemSci *28*, 106-112.

101. Suzuki, K., and Verma, I.M. (2008): Phosphorylation of SNAP-23 by IkappaB kinase 2 regulates mast cell degranulation. Cell *134*, 485-495.

102. Tachibana, I., and Hemler, M.E. (1999): Role of transmembrane 4 superfamily (TM4SF) proteins CD9 and CD81 in muscle cell fusion and myotube maintenance. JCell Biol *146*, 893-904.

103. Takeda, T., Hattori, N., Tokuhara, T., Nishimura, Y., Yokoyama, M., and Miyake, M. (2007): Adenoviral transduction of MRP-1/CD9 and KAI1/CD82 inhibits lymph node metastasis in orthotopic lung cancer model. Cancer Res *67*, 1744-1749.

104. Takeda, Y., He, P., Tachibana, I., Zhou, B., Miyado, K., Kaneko, H., Suzuki, M., Minami, S., Iwasaki, T., Goya, S.*, et al.* (2008): Double deficiency of tetraspanins CD9 and CD81 alters cell motility and protease production of macrophages and causes chronic obstructive pulmonary disease-like phenotype in mice. J Biol Chem *283*, 26089-26097.

105. Takeda, Y., Tachibana, I., Miyado, K., Kobayashi, M., Miyazaki, T., Funakoshi, T., Kimura, H., Yamane, H., Saito, Y., Goto, H.*, et al.* (2003): Tetraspanins CD9 and CD81 function to prevent the fusion of mononuclear phagocytes. J Cell Biol *161*, 945-956.

106. Tanio, Y., Yamazaki, H., Kunisada, T., Miyake, K., and Hayashi, S.I. (1999): CD9 molecule expressed on stromal cells is involved in osteoclastogenesis. Exp Hematol *27*, 853-859.

107. Tarrant, J.M., Robb, L., van Spriel, A.B., and Wright, M.D. (2003): Tetraspanins: molecular organisers of the leukocyte surface. Trends Immunol *24*, 610-617.

108. Tkaczyk, C., Okayama, Y., Metcalfe, D.D., and Gilfillan, A.M. (2004): Fcgamma receptors on mast cells: activatory and inhibitory regulation of mediator release. Int Arch Allergy Immunol *133*, 305-315.

109. Todres, E., Nardi, J.B., and Robertson, H.M. (2000): The tetraspanin superfamily in insects. Insect Mol Biol *9*, 581-590.

110. Tu, L., Sun, T.T., and Kreibich, G. (2002): Specific heterodimer formation is a prerequisite for uroplakins to exit from the endoplasmic reticulum. Mol Biol Cell *13*, 4221-4230.

111. Unternaehrer, J.J., Chow, A., Pypaert, M., Inaba, K., and Mellman, I. (2007): The tetraspanin CD9 mediates lateral association of MHC class II molecules on the dendritic cell surface. ProcNatlAcadSciUSA *104*, 234-239.

112. Vig, M., and Kinet, J.P. (2009): Calcium signaling in immune cells. Nat Immunol *10*, 21-27.

113. Volná, P., Lebduška, P., Dráberová, L., Šímová, S., Heneberg, P., Boubelík, M., Bugajev, V., Malissen, B., Wilson, B.S., Hořejší, V.*, et al.* (2004): Negative regulation of mast cell signaling and function by the adaptor LAB/NTAL. J Exp Med *200*, 1001-1013.

114. Vonakis, B.M., Haleem-Smith, H., Benjamin, P., and Metzger, H. (2001): Interaction between the unphosphorylated receptor with high affinity for IgE and Lyn kinase. J Biol Chem *276*, 1041-1050.

115. Williams, A.F., Galfre, G., and Milstein, C. (1977): Analysis of cell surfaces by xenogeneic myeloma-hybrid antibodies: differentiation antigens of rat lymphocytes. Cell *12*, 663-673.

116. Winchester, D.E., Jacob, A., and Murphy, T. (2006): Omalizumab for asthma. N Engl J Med *355*, 1281-1282.

117. Yamaguchi, M., Lantz, C.S., Oettgen, H.C., Katona, I.M., Fleming, T., Miyajima, I., Kinet, J.P., and Galli, S.J. (1997): IgE enhances mouse mast cell Fc(epsilon)RI expression in vitro and in vivo: evidence for a novel amplification mechanism in IgE-dependent reactions. J Exp Med *185*, 663-672.

118. Yang, X., Claas, C., Kraeft, S.K., Chen, L.B., Wang, Z., Kreidberg, J.A., and Hemler, M.E. (2002): Palmitoylation of tetraspanin proteins: modulation of CD151 lateral interactions, subcellular distribution, and integrin-dependent cell morphology. MolBiolCell *13*, 767-781.

119. Yashiro-Ohtani, Y., Zhou, X.Y., Toyo-Oka, K., Tai, X.G., Park, C.S., Hamaoka, T., Abe, R., Miyake, K., and Fujiwara, H. (2000): Non-CD28 costimulatory molecules present in T cell rafts induce T cell costimulation by enhancing the association of TCR with rafts. J Immunol *164*, 1251-1259.

120. Yauch, R.L., and Hemler, M.E. (2000): Specific interactions among transmembrane 4 superfamily (TM4SF) proteins and phosphoinositide 4-kinase. Biochem J *351 Pt 3*, 629-637.

121. Zhang, X.A., Bontrager, A.L., and Hemler, M.E. (2001): Transmembrane-4 superfamily proteins associate with activated protein kinase C (PKC) and link PKC to specific beta(1) integrins. JBiolChem *276*, 25005-25013.

122. Zhu, G.Z., Miller, B.J., Boucheix, C., Rubinstein, E., Liu, C.C., Hynes, R.O., Myles, D.G., and Primakoff, P. (2002): Residues SFQ (173-175) in the large extracellular loop of CD9 are required for gamete fusion. Development *129*, 1995-2002.

123. Zoller, M. (2009): Tetraspanins: push and pull in suppressing and promoting metastasis. Nat Rev Cancer *9*, 40-55.